4-15-2020

Temporal transport dynamics of the Amazon River Plume revealed using radium isotope analysis

Elana J. Ames
Coastal Carolina University

Temporal transport dynamics of the Amazon River Plume revealed using radium isotope analysis

By:

Elana J. Ames

Submitted in partial fulfillment of the requirements for the Degree of Master of Science in Coastal Marine and Wetland Studies in the School of the Coastal Environment

Gupta College of Science

Coastal Carolina University

April 2020

Dr. Richard Peterson	Dr. Joseph Montoya
Major Professor	Committee Member
Dr. Angelos Hannides	Dr. Ajit Subramaniam
Committee Member	Committee Member
Dr. Richard Viso	Dr. Michael Roberts
Chair, Department of Coastal and Marine Systems Science	Dean, Gupta College of Science

Acknowledgements

This work is the result of collaboration and guidance from many individuals. First and foremost, I would like to sincerely thank Dr. Rick Peterson, my major advisor. Without his unwavering support, patience, and expertise this thesis would not have been possible. I greatly appreciate having a role model to learn so much from, in both science and life.

My gratitude goes to my other committee members Dr. Joe Montoya, Dr. Ajit Subramaniam, and Dr. Angelos Hannides for their invaluable assistance and direction. Each of you has contributed significantly to my development as a scientist.

Many thanks to the National Science Foundation and CCU Department of Coastal and Marine Systems Science for funding the research discussed in this thesis.

I would also like to express my gratitude to my peers: Leigha Peterson, Matt Kurpiel, Charlotte Kollman, Christina Boyce, Alec Villafana, Jianna Wankle, Matt Stanek, Doug Pastore, Todd Rhodes, and Kaitlin Dick for their assistance and support throughout this project, both in and out of the field. An additional thank you to all the past and current faculty and students of Coastal Carolina University's School of the Coastal Environment. A special thanks to the officers and crew of the R/V Endeavor for making our science at sea possible.

Lastly, I would like to thank my family for their continued love, support, and encouragement during my time in graduate school and all my endeavors. Rachel and Claudia, thank you for being amazing role models since the day I was born. Mom and Dad, no number of pages could express my gratitude to you both.

Abstract

The Amazon River is the largest river by discharge in the world. It carries terrestrial nutrients into the Western Tropical North Atlantic via a buoyant freshwater plume, conveying water hundreds to thousands of kilometers away and driving critical biogeochemical cycles near the coast. Factors controlling the delivery of nutrients offshore by the plume are complicated and interconnected, yet these nutrients impact the foundation of phytoplankton community structures across the entire plume ecosystem. To better understand the temporal dynamics of this massive, highly influential region, we employ naturally occurring radium isotopes (^{223}Ra, ^{224}Ra, ^{226}Ra, and ^{228}Ra) to analyze mixing and transport behaviors through two separate research cruises to the Amazon River plume during high discharge seasons in 2018 and 2019. Radium is uniquely suited for this task because it displays elevated activities at the low end of a salinity gradient and decreases offshore as a function of dilution for all isotopes and radioactive decay for only the short-lived isotopes (^{223}Ra and ^{224}Ra). Known half-lives of these isotopes allow us to calculate apparent radium 'ages' to assess dissolved material transport scales and rates, and presumably also represent those of dissolved nutrients as well. Our results from ^{224}Ra/^{226}Ra apparent ages suggest that low salinity plume waters travel at a rate of 77 - 136 cm/s and are influenced by river discharge. Transport rates across the plume boundary were found to be significantly lower, ranging between 13 and 44 cm/s. Examining the horizontal mixing in this boundary region indicates that advection is the dominant process. An estimated eddy diffusion coefficient for the core of the plume mixing vertically with ambient waters was found to be $3.9 \times 10^{-4} \pm 1.5 \times 10^{-4}$ m^2/s, varying significantly with respect to salinity profiles. Determining the temporal scale of dissolved material (e.g., nutrients) movement across this region is a valuable first step in examining the foundation of planktonic food web dynamics of the Amazon River plume.

Table of Contents

List of Tables

List of Figures

1. **Introduction**

River discharge can have significant impacts on biogeochemical cycling in the oceans resulting from the addition of terrestrial sediments, nutrients, organisms, and even pollutants. Worldwide, rivers supply ~30% of the nitrogen and phosphorus input to the coastal oceans (37-66 Tg/yr and 4-11 Tg/yr for total N and total P respectively), with this relative contribution having increased recently due to rising contributions of anthropogenic nutrients (Gruber & Galloway, 2008; Seitzinger et al., 2010; Sevink et al., 2010; Sharples et al., 2017). The concentrations of N and P which make it to the open ocean vary with geographic location as a function of watershed nutrient loading rates and biogeochemical cycling processes on the shelf (Schlesinger & Bernhardt, 2013; Sharples et al., 2017). The time scales of such nutrient delivery to the oceans is thought to be highly influential to planktonic community structures, particularly in the Western Tropical North Atlantic (Montoya et al., 2002; Subramaniam et al., 2008; Weber et al., 2017).

The Amazon River has the largest drainage basin in the world, contributing ~15% of the total freshwater input to the oceans (Vorosmarty et al., 2000; Del Vecchio & Subramaniam, 2004). It has a mean annual discharge rate of 193,700 m^3/s (Hu et al., 2004) into the Western Tropical North Atlantic Ocean, where it creates a massive surface plume that reaches the Caribbean Sea. Hydrographic surveys indicate that the plume is generally 3-10 m thick and between 80 and >200 km wide across the continental shelf (Lentz & Limeburner, 1995; Del Vecchio & Subramaniam, 2004). The spatial extent and location of the plume varies seasonally with discharge: during high discharge in the summer and fall, the plume extends farther offshore, becoming entrained in the North Equatorial Counter Current (NECC) after flowing north along the eastern coast of South America (Hu et al., 2004); during periods of low discharge, the plume

flows within the North Brazil Current (NBC) to the northwest but with a reduced range and no retroflection to the east (Mascarenhas et al., 2016). As a result, the Amazon River plume is an expansive, highly dynamic system that creates unique environments for biota in the water column.

In particular, the magnitude of primary productivity within the Amazon River plume is globally significant, making it a region of interest to ocean scientists. Distinct differences in primary production rates and associated communities exist spatially across the plume. At least three communities of phytoplankton have been identified in the plume, with no single factor seemingly sufficient to explain their distribution in relation to plume core waters or the edges of the plume (Goes et al., 2014; Weber et al., 2017). Production near the mouth is limited by light availability as high loads of riverine suspended particles reduce solar transmittance through the water column (Goes et al., 2014). However, production throughout the majority of the plume is generally limited by nutrient availability (DeMaster et al., 1991; Gouveia et al., 2019). Beyond the mouth, studies have shown that nutrient concentrations are not consistently conservative with respect to salinity. For example, phosphate shows a preferential release within the plume as the water moves from the mouth and mixes with the ambient ocean (Loick-Wilde et al., 2016; Weber et al., 2017).

This behavior has significant implications for nutrient dynamics and primary producers. The ocean is generally nutrient limited, but this release of phosphate in offshore waters drives the system towards strong nitrogen limitation and creates a niche for phytoplankton that fix nitrogen, known as diazotrophs. Diazotrophs convert dissolved N_2 gas into bioavailable organic nitrogen, therefore exploiting an ecological niche where N:P ratios are generally too low for other primary producers to flourish (Montoya et al., 2002). Nitrogen fixers such as the cyanobacterium

Trichodesmium and diatom-diazotroph associations (DDAs) support high rates of primary production throughout the Amazon River plume (Carpenter et al., 1997; Carpenter et al., 1999; Subramaniam et al., 2008). Such low N:P ratios in these areas are thought to result from a delicate balance between transport, growth, and regeneration. Global rates of nitrogen fixation are understood to be vastly underestimated, making it essential to examine the characteristics of regions where they are known to thrive (Mohr et al., 2010).

While diazotrophy in the Amazon River is generally recognized to occur, it is seemingly governed by a time-dependent quality in which a requisite set of conditions (N:P availability) must be met. Nutrient concentrations within the plume vary in relation to salinity, time, and distance from the river mouth. Understanding the complex interplay among all these parameters is required to resolve the ecosystem scale influence of the Amazon River plume on the planktonic food webs.

Constraining timing mechanisms associated with mixing and transport of a river plume and associated solutes represents a critical step toward understanding coastal-ocean diazotrophy as well as the transport of material (e.g. sediments) and buoyancy. Radium isotopes are uniquely suited to provide this temporal context for analysis of the time scales of plume mixing. Four naturally-occurring isotopes of radium (^{226}Ra, ^{228}Ra, ^{223}Ra, and ^{224}Ra) with a wide range of half-lives (1600 years, 5.75 years, 11.4 days, and 3.6 days, respectively) serve as an ideal, biologically inactive tracer system of river plume mixing. In freshwater, radium is strongly particle-reactive and is therefore found mostly adsorbed to sediments (Swarzenski, 2007). As the particles enter higher salinity waters (~5-15) within a river estuary, some radium desorbs via ion-exchange and supplies dissolved radium to the aqueous phase in the water column (Moore et al., 1996; Moore, 2000a). The primary source of radium to the Amazon River plume is therefore

thought to be riverine discharge (Li et al., 1977; Moore & Edmond, 1984; Key et al., 1985; Moore et al., 1995). Another source of radium to this area may occur via regeneration and release from benthic sediments, but density stratification of the water column should prevent this source from contributing substantially to the surface plume (Moore et al., 1995, 1996). These properties make the suite of radium isotopes ideal for tracing interactions among distinct water masses on time scales ranging from days to months.

As radium-enriched plume waters move farther offshore, the short-lived isotopes ^{223}Ra and ^{224}Ra will undergo measurable decreases in activity due to both mixing (dilution) and radioactive decay. The long-lived isotopes, however, act as conservative tracers because they are only affected by mixing over these time scales. The inherent rate of decay specific to each isotope permits the use of the radium isotope suite as a geochronometer of plume mixing and transport dynamics. The differences in half-lives of the radium isotopes make it possible to examine the age of a water mass, termed the "apparent radium age" (Moore, 2000a). Additionally, Moore (2000b) shows that the relationship between a short-lived isotope and transport distance from the source can indicate the degree of mixing that has occurred between the plume and ambient waters surrounding the plume.

This project aims to use radium isotopes as a water mass tracer system to constrain mixing and transport dynamics of the Amazon River plume. Specifically, we characterize the history and longevity of distinct plume water masses by quantifying apparent radium ages. We also determine the horizontal mixing behavior of surface waters in and around the plume, as well as the vertical mixing behavior between the plume and underlying waters. By characterizing the rates of solute mixing between the plume and ambient waters, we can provide critical context that may ultimately enable the theoretical separation of the complementary effects of biological

uptake and dilutional mixing on changing nutrient concentrations along the plume transport pathway. Thus, this information may offer unique insight into the temporal conditions in which N:P ratios become most ideal for diazotrophy.

These efforts are designed to provide integral temporal context for investigators amid a larger research study seeking to characterize the impacts of diazotrophy on marine ecosystems. The Amazon River plume is one of many locations that supports dynamic populations of diazotrophic organisms. Since the Amazon River plume is a complex region to study, the standard methods of measuring nitrogen fixation and related biological significance may strongly benefit from additional temporal context for a better understanding of community structures. As such, a comprehensive effort is required to assess the time-dependent nature of biogeochemical cycling within the plume as it pertains to diazotrophy. Radium isotopic analysis is capable of delivering a temporal context for the plume, thus providing a missing piece required to understand this dynamic system.

2. **Methods**

2.1. Site Description

This study is based on data from two research cruises in the Western Tropical North Atlantic aboard the *R/V Endeavor* during the Amazon River high discharge season. Cruise EN614 sampled from May 6 – June 1, 2018 and EN640 sampled from June 13 – July 8, 2019. Sampling was organized to document mixing conditions within the plume as well as between the plume and oligotrophic waters outside the plume. Remote sensing was used in near real-time to guide the cruise track toward areas of interest.

2.2. Sample Collection and Data Processing

At each sampling station, a standard suite of basic hydrographic (T, S, ρ) measurements was collected through CTD profiles of the entire water column. These measurements were analyzed to determine the hydrographic context of the region. We selected several depths within the mixed layer of the plume as well as below the plume to collect water samples via Niskin bottles for analysis of radium isotope activities. A volume of at least 10 L was required for analysis. This volume is less than that routinely used to sample radium isotopes in the open ocean (often ~100-1000 L). However, experience with Niskin bottle collection and particle filtration suggests that 10-20 L sample volumes are adequate to analytically resolve most radium activities within continental shelf waters near major river plumes (Peterson et al., 2013). With counting times ranging from ~1 to 24 hours, these volumes consistently yield 1-σ measurement uncertainties for ^{224}Ra, ^{226}Ra, and ^{228}Ra on the order of 10%. Any sample below the minimum detectable activity (MDA) was excluded from further analysis.

In addition, samples were collected from the ship's clean seawater system. While in transit, 15-20 L water samples were quickly collected from the continuous flowing intake system. This sampling strategy allowed us to characterize surface gradients at higher resolution without sacrificing valuable ship time to stop and conduct a CTD cast. These samples were collected every 20 – 25 km along the cruise track between CTD stations. Areas near the mouth of the Amazon River were prioritized for this sampling approach to capture the most dynamic location of short-lived radium isotope decay.

After sample collection, suspended particles were removed from all samples via filtration through GF/F filters, and the filtrate was subsequently passed over 25 g of dry acrylic fibers impregnated with MnO_2 at a flow rate of ~1 L/min (Moore & Reid, 1973). These Mn fibers

quantitatively adsorb radium isotopes for subsequent analysis (Moore, 1976). Each Mn fiber was washed with radium-free freshwater to remove any salts, then dried to a moisture content between 0.3 – 1 g H_2O / g fiber (Sun & Torgersen, 1998) using a compressed air stream. The fibers were counted immediately on a Radium Delayed Coincidence Counter (RaDeCC; (Moore & Arnold, 1996) for an initial measurement of total ^{223}Ra and ^{224}Ra. The fibers were counted on the RaDeCC again 3 to 6 weeks after collection to quantify any ^{224}Ra supported by decay of its parent, ^{228}Th, that may be adsorbed to the fibers. Subtracting this activity from the initial ^{224}Ra activity provides a measure of the excess, or unsupported, ^{224}Ra, which is the tracer of interest for this study. To measure ^{226}Ra, the fibers were sealed in an air-tight cartridge to allow for ingrowth of the gaseous daughter isotope, ^{222}Rn, then analyzed on a radon extraction line (Peterson et al., 2013). Samples were counted again on the RaDeCC 9-12 months after collection for ^{228}Ra analysis. This time interval is necessary to allow sufficient ^{228}Th ingrowth from ^{228}Ra decay to be differentiated from any ^{228}Th originally in the sample (Moore, 2008).

Since the radium isotopes used in this study are sourced from riverine suspended particles, it is necessary to consider continued input of radium to the water column from particles entrained in the plume. Delayed release of radium from particles would introduce a secondary source to the water column in addition to the radium that entered solution in the estuary. It is unlikely that the magnitude of this addition would result in a measurable difference to the isotope activities of the water column, but it must be considered. To do this, pre-weighed GFF filters were used to extract suspended particles from surface waters. Filters were dried in an oven at 60 °C for 24 hours and counted for radium isotopes via the RaDeCC as described above. Upon returning to the lab, samples were weighed for dry mass. The mass difference and the volume of each water sample yield the total suspended solids (TSS) concentration in mg/L. All of these

TSS samples were collected with a corresponding water column sample so dissolved radium activities can be compared with those on the suspended particles.

2.3. Research Approach

2.3.1. Apparent Radium Ages

The differences in half-lives of the radium isotopes make it possible to examine the age of a water mass, termed the "apparent radium age" (Moore, 2000a). This age represents the amount of time that a water sample has decayed since it was subject to radium input in the estuary. As waters move offshore, the short-lived isotope activities should decrease due to both mixing and decay, while the longer-lived isotope activities will only change due to mixing. Thus, normalizing a short-lived isotope ('*SL*') activity to that of a longer-lived isotope ('*LL*') removes the effect of mixing, leaving only radioactive decay to explain the change in activity ratio (Moore, 2000a):

$$T = \ln\left[\frac{\left(\frac{Ra_{SL}}{Ra_{LL}}\right)_{obs}}{\left(\frac{Ra_{SL}}{Ra_{LL}}\right)_{i}}\right] \cdot \frac{1}{\lambda_{LL} - \lambda_{SL}} \quad (1)$$

where T is the apparent radium age of the water, $\left(\frac{Ra_{SL}}{Ra_{LL}}\right)_{obs}$ is the observed activity ratio of a short-lived (SL) to long-lived (LL) isotope observed at a specific sampling location, $\left(\frac{Ra_{SL}}{Ra_{LL}}\right)_{i}$ is

the initial isotope activity ratio at T = 0, and λ represents the decay constants of each considered isotope. Using different isotopes in the numerator will functionally provide age estimates up to 3 weeks (^{224}Ra) or up to roughly 2 months (^{223}Ra) (Peterson et al., 2008). The initial activity ratio ($\left(\frac{Ra_{SL}}{Ra_{LL}}\right)_i$) is taken from the location closest to where radium first desorbs from particles (i.e., the lowest salinity sample) and signifies T = 0. The apparent ages of all other samples are calculated relative to this point.

2.3.2. Mixing Rates

The relationship between short-lived radium isotope activity and distance from the source (i.e., river estuary) can also indicate the degree of mixing that has occurred during transit (Moore, 2000b). From this relationship, eddy diffusion rates between a plume and ambient waters surrounding the plume can be calculated. The mixing rate is calculated on the basis that activity of the short-lived radium isotopes (^{223}Ra and ^{224}Ra) decreases as a function of distance offshore. Since these isotopes are also undergoing radioactive decay, plotting the natural logarithm of the activities as a function of distance offshore should yield a linear relationship with slope *m*. The following equation (Moore, 2000b) is then used to derive the eddy diffusion rate (K_h):

$$m = \sqrt{\frac{\lambda}{K_h}} \tag{2}$$

where λ is the decay constant of the isotope (0.189 day^{-1} for ^{224}Ra and 0.060 day^{-1} for ^{223}Ra) and K_h is the eddy diffusion coefficient, with units of square distance per time.

This approach is used to determine the horizontal mixing of the Amazon River plume using data from both the CTD and underway sampling. This mixing assessment is applied on a multidirectional scale to assess the interplume mixing as well as mixing between the plume and surrounding waters. This same mixing rate analysis is used to constrain vertical mixing within the surface waters of the plume using sampling depth as the distance scale and the radium isotope signature at the surface as the source.

Several assumptions must hold for the proposed models to be accurately applied to the plume system. First, we assume no additional input or removal of radium with respect to the process of interest (mixing/transport). A likely process that may violate this assumption would be continued interactions (scavenging and/or desorption) with suspended particles. Moore and Dymond (1991) report the residence time of radium in surface waters with respect to particle scavenging is on the order 500 years. Therefore, no measurable removal of radium via scavenging is expected over relevant timescales of plume mixing. Also, Moore (2015) demonstrates that radium isotopes desorb nearly quantitatively from suspended particles in the salinity range of 5-15, which is far lower than any waters we were able to sample. Further, this assumption implies that the only input of radium to the system should be that from the riverine discharge. Strong vertical stratification between the plume and ambient waters below it should be sufficient to prevent radium released from bottom sediments from mixing into the plume. Temperature and salinity measurements from the CTD are used to construct a density profile of the area and only samples with a statistically significant difference in ρ from surface to bottom were considered for analysis. Radium isotope signatures in bottom water were also measured to assess whether any contribution of bottom water into surface waters may have occurred, indicated by elevated radium activities at depth.

A second assumption is that the system must be in steady-state over at least the short-lived isotope lifetime (i.e., 3 weeks for ^{224}Ra). Repeat visits to two stations during each cruise provide data to test for variability in isotope activities as an indication of any deviation from steady-state. It is anticipated that any variability is minimal with respect to associated measurement uncertainty (Moore, 2015).

The role of advection within the system must also be considered as the radium mixing model (Eq. 2) assumes negligible advection (Moore, 2000b). To confirm that the dominant mixing process is eddy diffusion, the distribution of long-lived radium isotope activities must be examined with respect to distance from the estuary (Moore, 2000b; 2015). If the long-lived isotopes (^{226}Ra and ^{228}Ra) indicate a linear relationship between activity and distance, the system can reasonably be assumed to be relatively uninfluenced by advection (Moore, 2000b).

In contrast to the apparent age analysis, this method assumes that advective transport behaviors are negligible. Thus, comparing results from both the mixing rate analysis and the apparent age estimates can yield a first-order assessment of the different transport processes (advection vs. eddy diffusivity) that may impact the Amazon River plume.

3. **Results & Discussion**

3.1. Hydrographic Summary

The first cruise aboard the R/V Endeavor (EN614) encompassed an area of roughly 410,000 km^2 from 4°53'N to 16°35'N and from 50°27'W to 57°12'W. This area included international waters as well as territorial waters of Guyana, Suriname, and French Guiana. A total of 87 underway surface samples and 153 water column samples from 45 CTD casts were

collected for radium isotopic analysis (Figure 1A; Appendix A1). During the cruise, we sampled waters in low salinity (<30), mesohaline (30-35), and oceanic conditions (>35): a grouping convention defined by Subramaniam et al. 2008.

The second cruise, EN640, had a sampling area of 445,000 km^2, extending from 4˚53'N to 16˚00'N and from 50˚23'W to 60˚00'W. This area included international waters as well as territorial waters of Barbados, Suriname, and French Guiana. A total of 255 underway surface samples, 240 water column samples from 44 CTD casts, and 23 suspended particle samples were collected for radium isotopic analysis (Figure 1B; Appendix A2).

Sea surface salinity (Figures 1A and 1B) demonstrates that the Amazon River plume was more widespread during EN640 than the EN614 cruise period. Any inter-annual variability of the plume observed during these cruises was most likely due to the small difference in season between our sampling efforts (May versus June/July). A primary environmental factor differing between these cruises was discharge rate, which we accessed from the Environmental Research Observatory on the Rivers of the Amazon, Congo and Orinoco River Basins (HYBAM: www.ore-hybam.org). We mined data from a station ~650 km upstream of the Amazon River mouth (Obidos station ID: 17050001) which measures approximately 90% of the discharge that reaches the ocean (Geyer et al., 1996). We estimate that discharge rates from the Obidos monitoring station would not be reflected in our sampling region until approximately 30 days after measurement. In 2018, the maximum discharge (245,400 m^3/s) was recorded on June 26-27, 25 days after the end of EN614, indicating that our sampling took place preceding peak flow conditions. Average discharge for the 30 days prior to EN614 was 212,620 ± 8,000 m^3/s (Figure 2). For comparison, the 30-day average discharge prior to EN640 was 244,940 ± 2,000 m^3/s, over 13% higher than that preceding EN614. In 2019, the maximum discharge (253,600 m^3/s)

was recorded at Obidos during EN640 on July 1-3 (Figure 2), indicating that sampling once again took place before peak flow conditions in our study region. Overall, EN640 experienced higher discharge rates both during and prior to the cruise than EN614 which may help explain the larger area of fresh/mesohaline waters observed during EN640. The relationship between discharge and salinity is not surprising, and has been well documented for the Amazon River (Del Vecchio & Subramaniam, 2004).

3.2. Radium Activities

All four of the naturally-occurring radium isotopes have been measured for EN614 samples, whereas only three isotopes (^{223}Ra, ^{224}Ra, and ^{226}Ra) have been analyzed to date from EN640 (Appendix B). Activities are reported in dpm/100L with ± the 1-σ analytical uncertainty.

Of the 731 total samples measured, 43% of the ^{223}Ra values fall below our MDA and were consequently eliminated from consideration (only 4.5% of ^{224}Ra and 7% of ^{226}Ra samples fall below their associated MDA values). Higher precision counting systems would be necessary to consistently resolve low level environmental concentrations of ^{223}Ra (Moore & Arnold, 1996; Moore, 2008). From the remaining data, ^{223}Ra surface values range from 0.03 – 6.09 dpm/100L with an average of 0.74 ± 0.20 and 0.50 ± 0.14 dpm/100L for EN614 and EN640, respectively (Table 1). Although we do not consider ^{223}Ra in our analyses due to the relatively high analytical uncertainty, observing its behavior lends valuable insight to the isotopic context of our data set. For example, the average ^{223}Ra activity was higher during EN614 but the maximum activity of 6.09 ±1.44 dpm/100L was recorded during EN640. This trend agrees with similar findings for ^{224}Ra and ^{226}Ra: higher average activities during the first cruise, but a higher maximum measured during the second (Table 1).

From the isotope activity data, we examine the spatial distribution of surface activities to interpret the potential river plume signature. Highest activities are generally found closest to the mouth, presumably supplied by riverine suspended particles (Li et al., 1977; Moore & Edmond, 1984; Key et al., 1985). Our sampling efforts did not reach the mouth of the estuary; however, elevated surface radium activities are observed for every isotope near the coast at our southernmost stations (Figure 3).

Radium-224 activities differ between the cruises, averaging 5.70 ± 0.50 and 3.30 ± 0.29 dpm/100L for EN614 and EN640, respectively (Table 1). Similar studies have found ^{224}Ra activities ranging from 0.4 – 67 dpm/100L in the Amazon plume (Moore et al., 1995); 25 – 200 dpm/100L in the Yellow River estuary (Peterson et al., 2008); and 0.57 – 21.2 dpm/100L in the Taiwan Strait (Men et al., 2016). We can confidently state that our ^{224}Ra activities ranging from 0.01 – 43.10 dpm/100L are credible (Table 1). Further validity of our measurements is supported by the spatial distribution of ^{224}Ra which clearly demonstrates elevated activities nearest the mouth and to the northwest up the coast (Figure 3B).

The spatial distribution of ^{226}Ra may appear more arbitrary than the other isotopes (Figure 3C). This apparent lack of a spatial relationship to the river mouth is due to ^{226}Ra having an oceanic background concentration above zero (~2 dpm/100L) and a long half-life ($t_{1/2}$ = 1600 yr) allowing it to retain a relatively high background activity throughout the oceans (Moore & Edmond, 1984; Key et al., 1985; Moore & Dymond, 1991). Average ^{226}Ra values for EN614 and EN640 are functionally identical (18.25 ± 1.25 and 17.86 ± 1.38 dpm/100L, respectively; Table 1) and the range of 10.17 – 28.42 dpm/100L falls within the experimental error of other published data for this region: 5 - 22 dpm/100L (Key et al., 1985) and 5 – 30 dpm/100L (Moore & Dymond, 1991).

The other long-lived isotope, ^{228}Ra, displays elevated activates near the mouth as well in the northern reaches of our sampling (Figure 3D). The average activity (12.62 ± 0.10 dpm/100L) and range (0.02 – 52.80 dpm/100L) is on the same order as literature values for this area, which range from 1.4 – 51 dpm/100L for coastal waters and 3 – 74 dpm/100L for off-shore sampling as reported by Key et al. (1985) and Moore et al. (1995), respectively.

Higher radium activities are generally associated with lower salinity waters during EN614 (Figure 4). Short-lived isotopes (^{223}Ra and ^{224}Ra) show an inverse relationship with salinity while the long-lived isotopes (^{226}Ra and ^{228}Ra) are somewhat more equally distributed across the salinity spectrum (Figure 4).

The sampling regime for EN640 was largely focused on the northern mesohaline region as well as waters nearest the mouth (Figure 5). Of the surface samples collected on EN640, 75% were from mesohaline waters causing the sample distribution to be skewed to these higher salinities (Figure 6). There is a wide spread for ^{224}Ra within low salinities up to ~25 (Figure 6A), which correlates with the high activity southern trend shown in Figure 5A. Radium-226 however, shows the opposite pattern: higher variability corresponds to salinities above ~25 and an evenly distributed spatial map indicate that there is less influence from the river plume (Figures 5B and 6B).

3.3. Apparent Radium Ages

We use these data to explore the temporal context of the spatial characteristics within the Amazon River plume. One approach is to compute the 'apparent radium ages' for all surface samples (collected via both the underway sampling and from CTD casts) (Moore, 2000a: Eq. 1). Considering the relatively high analytical uncertainty associated with ^{223}Ra, we ignore data from

that isotope. Additionally, as ^{228}Ra has not yet been analyzed from EN640, we only consider the ^{224}Ra/^{226}Ra activity ratio to allow direct comparison between EN614 and EN640. As is often the case when computing apparent radium ages within river plumes, choosing the initial activity ratio represents a source of uncertainty in this analysis (Moore, 2000a; Moore et al., 1995). We have selected our initial activity ratio as the sample with the highest measured activity ratio (AR) in low salinity waters (Moore & Krest, 2004; Burnett et al., 2006; Peterson et al., 2008). For EN614, this sample was collected from underway station 018.09 at 5° 8' 14.64"N and 52° 1' 3.72"W. With a salinity of 24.2, that sample does not represent the freshest water sampled of 15.9, but this sample falls within plume salinity ranges and exhibits the highest ^{224}Ra / ^{226}Ra AR (1.2). For EN640, our initial AR of 3.0 is derived from a sample collected at 4° 52' 36.12"N and 51° 42' 9.72"W. This sample was derived from a CTD sample at station 006.01, with a measured salinity of 15.7 (lowest EN640 salinity = 12.6). These two T = 0 locations are less than 50 km apart, and ~560 km from the approximate mouth of the Amazon River. All apparent radium ages for each cruise are calculated relative to these positions, not the actual river estuary. Also, given the 3.66 day half-life of ^{224}Ra, its functional lifetime is ~ 6 half-lives, so apparent ages calculated to be greater than 21 days have been excluded from consideration.

Samples collected during EN614 nearest the mouth and in the core of the plume generally exhibit younger ages (Figure 7). The shape of the plume can be observed in the lower ages extending northwest inside the 34 isohaline. A sharp gradient in age around ~10 days along the eastern boundary of the plume corresponds to a horizontal halocline between plume and ambient waters (Figure 7).

In order to more closely investigate the aging behavior of plume waters, apparent radium ages are grouped into three salinity sets: low salinity (<30), mesohaline (30-35), and oceanic

(>35). The average age of EN614 samples in the low salinity group is 5.98 ± 3.92 days (n=41), in the mesohaline group is 11.55 ± 4.47 (n=64), and in the oceanic group is 13.63 ± 2.58 days (n=23). Examining the EN614 distribution of age with these salinity groups shows a positive relationship, with age increasing gradually until salinities reach ~28, followed by a more pronounced increase over the mesohaline and oceanic waters (Figure 8). A similar relationship is demonstrated by the $^{224}Ra/^{228}Ra$ apparent ages in the Yellow River estuary suggesting that the rapid increase in ages with salinity is due to a decrease in mixing at higher salinities (Moore & Krest, 2004; Peterson et al., 2008; Schiller & Kourafalou, 2010).

Apparent radium ages from the EN640 cruise were similarly calculated and further demonstrate that youngest ages are found nearest the mouth, consistent with age distributions from EN614 (Figure 9). In contrast to EN614, the salinity data for EN640 suggest the horizontal halocline is present closer to shore, just inside the 30 isohaline (Figures 7 and 9). Significantly fewer samples were observed with ages below ~10 days for EN640.

Again, apparent radium age is generally positively correlated with salinity as demonstrated in Figure 10, but with a distinct cluster in the mesohaline group due to higher sampling density in that salinity regime. The average age of EN640 samples in the low salinity group is 11.03 ± 6.31 days (n=49), in the mesohaline group is 17.27 ± 2.01 (n=177), and in the oceanic group is 17.56 ± 1.47 days (n=10). The gradual increase of age with salinity as was observed for EN614 is not found during EN640, instead there is large variability of age in the samples below salinities of ~25.

3.4. Transport Rates

Examining the distribution of apparent radium ages over distance can provide an estimated rate of transport of those waters and associated solutes (Moore, 2000a; Peterson et al., 2008). By plotting the relationship between age and distance across samples (e.g., Figure 11), we can estimate an apparent radium transport rate as the reciprocal of the regression slope. An important distinction is that these values are not the same as a real time water velocity. These transport rates only estimate apparent motion from discrete samples, serving as an observation of net displacement. Another limitation is the directionality of measurement: the plume does not travel consistently in one direction. Therefore, two samples both 100 km from our T = 0 can be representative of oceanic waters or the core of the plume depending on the directionality. Subsequently, distance alone (and therefore transport rates) does not offer a good indication of behavior unless examined in conjunction with another parameter such as salinity.

Although the total surface age versus distance does not support a high R^2 value (0.26), the high number of samples (128) grants a statistically strong linear relationship (p-value < 0.01) that can be used to calculate a transport rate (Figure 11). For EN614, we observe an increasing apparent radium age as a function of distance from the sample representing our initial (T=0) AR, as well as evidence pointing to several locations where there may be a linear fit.

Within this broader data set, we observe a number of interesting subsets of results that warrant a more intense examination (transects of these subsets are shown on Figure 12 with their calculated transport rate in cm/s). The slopes and correlation coefficients (R^2 values, p-values) of the best-fit linear lines for the results presented in Figure 12 are summarized in Table 2. No oceanic transects were analyzed because the open ocean environment is not responsive to the

plume's radium signature, and therefore assumptions inherent to the apparent radium age model do not hold.

Further analysis suggests that transport in the core of the plume (low salinity group) is an order of magnitude higher than plume boundary transects. This transport estimate may indicate the influence of the North Brazil Current moving up the coast (Hu et al., 2004). Comparison of the station 4 transect with the transect between stations 11-12, 17 shows a very similar transport rate despite the fact that station 4 is well-mixed mesohaline water and the Stn 11-12, 17 transect crosses a distinct salinity gradient and assumed plume boundary (Figure 12). It is important to note that this region experiences both along-shelf and cross-shelf advection at rates up to 10-20 cm/s and 55 cm/s respectively, (Geyer et al. 1996). The multi-directional measurement of transport from these subsets does not provide a specific 'cross-shelf' or 'along-shelf' comparison, but the range of transport estimates 15.79 – 44.31 cm/s (excluding the low salinity group) is consistent with literature rates (Geyer et al. 1996).

Such interesting inter-annual variability so far leads us to compare the EN614 and EN640 transport data. Examining the overall relationship between distance and apparent age draws attention to the higher proportion of mesohaline samples collected 1000 – 1400 km from T=0 (Figure 13). This cluster of measurements from mesohaline waters changes the general shape of the plot when compared to the EN614 counterpart (Figure 11.) It suggests that splitting the data into two groups defined by the respective total transport slopes may be necessary for analysis. However, this grouping yields inappropriate transport rates due to the multi-directional spatial distribution. Yet, the overall fit-statistics for EN640 are remarkably similar to those of EN614. Total transport for EN614 is estimated at 144 ± 25 cm/s and for EN640 is 188 ± 17 cm/s (Figures

11 and 13). This difference represents a roughly 27% increase from 2018 to 2019. The subset transects from EN640 also compare favorably to those measured during EN614 (Figure 14).

Similar studies examining the transport of Amazon River discharge provide a comparison to our findings. Hu et al. (2004) found an average plume translation speed of 35 cm/s from satellite data and lagrangian floats while Limeburner et al. (1995) measured the transport from shelf to retroflection with a drifter to be between 32-167 cm/s. Using radioisotopes in this region is not novel, as Moore et al. (1996) estimated the transport from shelf to retroflection must be >80 cm/s.

This radiotracer method has also been utilized in other river systems. Moore and Krest (2004) found that the Mississippi River attained transport rates from 2.3 – 17 cm/s on a spatial scale of ~80 km. The average discharge of the Mississippi River during their sampling periods was 11,200 m^3/s and 14,500 m^3/s. For comparison, the Amazon River discharge measured during EN640 was ~244,900 m^3/s, over 16 times higher than that of the Mississippi. Peterson et al. (2008) reported transport rates of the Yellow River plume to be 1.4-1.6 cm/s over 20 km. However, discharge of the Yellow River is over three orders of magnitude lower than that of the Amazon River.

3.5. Horizontal Mixing

In addition to examining apparent radium ages, we can also gain insight into the temporal context of spatial plume behaviors by assessing horizontal and vertical mixing rates. Using the Moore (2000b) model and Eq. 2, mixing rates are calculated on the basis that short-lived isotope activities decrease exponentially with distance from the source due to both radioactive decay and

mixing with ambient waters. Long-lived isotopes may operate as conservative tracers because no significant decay will occur over time frames of plume mixing.

We have selected a variety of transects from EN614 over which to compute mixing rates both within plume and across plume boundaries. For each transect, a relative distance was calculated between each sample location and that with the highest activity, since this analysis is independent of the T=0 location. A linear regression was then evaluated between distance and the natural log of ^{224}Ra activity, as well as between distance and the ^{226}Ra activity (Table 4). Both of these relationships should be linear under diffusive mixing conditions. Deviation from a linear trend can indicate a violation of assumptions behind the model that mixing is dominated by eddy diffusivity (Moore 2000b). The results of these regression tests are presented in Table 4 along with the calculated eddy diffusion coefficients (K_h) and an approximate spatial scale for context. A spatial distribution of the selected transects and mixing rates is shown in Figure 15. Positive slopes for the long-lived ^{226}Ra do not meet the necessary assumptions of the model and therefore should not be considered, however, when the short-lived isotope displayed a strong linear correlation, a K_h estimate was calculated. These K_h values are not indicative of the actual system behavior.

The transect defined by stations 6-10 exhibits the highest mixing rate, as well as the weakest salinity gradient (Figure 15). Salinity on transect 19 increases consistently but does not reach the oceanic range. Not fully crossing the plume boundary may be a valid explanation for the lower mixing rate observed as the stark difference in salinity across the boundary may significantly hamper plume mixing with ambient waters (Geyer et al., 1996). Transect 11-12, 17 crosses the strongest salinity gradient, going from 15.9 – 35.5 in just 250 km but shows a moderate diffusion coefficient.

Relatively high R^2 values for the short-lived compared to the long-lived distributions imply that there may be additional factors besides diurnal tidal energy controlling eddy diffusion and that advection may be playing a significant role(Geyer et al., 1996; Moore, 2000b). The calculated eddy diffusion coefficients are 1-2 orders of magnitude higher than values measured on the South Atlantic Bight (Moore 2000b), however, the spatial scale covered here is also an order of magnitude greater. Such variability could be minimized by time and distance averaging of the transect; due to sparse sampling density, this was not an ideal option for our analysis.

3.6. Vertical Mixing

To evaluate vertical mixing behaviors of the plume, the same analysis for horizontal mixing is used except depth below the air-sea interface is used for the spatial component instead of lateral distance. This analysis also assumes that the surface radium isotope signature is the source. Six stations from EN614 were selected for analysis by their salinity profiles and location in relation to the plume. For instance, station 17 presents a clear plume signature: higher radium activities at the surface that decrease with depth and a low surface salinity increasing with depth to ~10 m (Figure 16). These isotope activity profiles for each station were used to identify the depth at which an oceanic endmember was present since many of the profiles extend much deeper into the water column and we are only concerned with surface-mixed layer trends. A linear regression was evaluated for the natural log of ^{224}Ra activity and ^{226}Ra activity with respect to the limited depth and used to calculate a vertical eddy diffusion coefficient (Eq. 2; Table 5).

Stations 6, 8, and 33 did not show a significant p-value (<0.05) due to the low sample number (n) but were still included in the analysis because of the relatively high R^2 values (Table

5). The spatial distribution of these profiles in relation to the plume provides vital insight into the mixing dynamics (Figure 17). K_h values for stations 33, 8 and 17 show a general trend of higher eddy diffusion rates farther away from the river mouth. The highest K_h value ($3.6 \times 10^{-3} \pm 1.1 \times 10^{-3}$ m^2/s) is found at station 33, farthest north and in nearly oceanic waters (Figure 17.) This suggests that increased mixing is driven by weaker stratification, in other words, vertical mixing is slower with a strong salinity gradient. Station 6 is the exception to this trend, farther from the mouth than stations 8 and 17 but showing a lower K_h value (Figure 17).

3.7. Synthesis

Identifying the apparent radium ages and associated transport rates may characterize the history and longevity of distinct plume water masses. Examining specific subcategories within the salinity gradient provides an indication of which areas are primarily influenced by advective processes as opposed to diffusive mixing. Transects that fit assumptions for both transport and mixing analysis (EN614: stations 6-10, stations 11-12, 17, and station 19) reveal that neither process dominates the other on the reported spatial scales, but rather there is a combination of the two (Figures 12 and 15). This balance of forces may be a contributing factor to the complexity of diazotroph communities in the outer reaches of the plume. Illustrating the rates of solute mixing between the plume and ambient waters provides context for isolating the effects of biological uptake and dilutional mixing on changing nutrient concentrations. Faster vertical mixing on the periphery of the plume and higher transport rates within it may be a contributing factor to the temporal conditions required to produce ideal N:P ratios for diazotrophy.

3.8. Assumption Verifications

3.8.1. Bottom Water

To validate the assumption that the only input of radium to the system is from riverine discharge, the possible influence of radium released from bottom sediments must be considered. In particular, sampling stations located on the shelf are at risk due to the shallow depth of the water column. Radium isotopic profiles were constructed for each of these stations. If an enrichment was present at depth, the hydrographic data were consulted and an ANOVA analysis was performed on the density profile data to determine if a statistically significant pycnocline existed. Strong vertical stratification is generally sufficient to prevent mixing radium signatures from bottom to surface waters (Moore, 2015). All sampling stations agreed with the assumption of no bottom water radium input to surface waters.

3.8.2. Suspended Particles

In order to assess the unlikely, yet possible influence of a delayed or continual release of radium from particles in the water column, quantitative Total Suspended Solids (TSS) were measured on various samples from EN640. Analyses indicate that there is no relationship between TSS concentration and dissolved radium activity (p-value > 0.5), suggesting that the suspended particles are likely not introducing a secondary source of radium to the water column (Figure 18).

3.8.3. Underway/Surface Comparison

The shipboard underway seawater system intake was located at ~5 m depth, possibly lower than the surface plume thickness in some regions. In order to determine if these samples

are still representative of the genuine surface conditions, several underway sample activities were compared to surface CTD measurements taken at the same station, within 8 hours or less. This comparison was evaluated for both cruises and the ^{224}Ra activities agreed (p-value <0.01). This analysis ensures that the underway samples can be considered "surface" for the purpose of this study (Figure 19).

3.8.4. Transport Validation

We attempt an independent validation of our apparent radium age estimates using data from the shipboard Acoustic Doppler Current Profilers (ADCPs). The average along-stream current velocity of the plume and distance from the mouth should roughly agree with the relative water mass ages found using radium analysis. Current direction and velocity were measured continuously from two hull-mounted ADCPs over the duration of both cruises. Unfortunately, the ADCPs are mounted too low to resolve surface currents above 10 m, and therefore did not capture the currents relevant to plume transport.

4. **Conclusions**

Longevity of the plume water mass estimated by apparent radium ages appears to be roughly 10-15 days. Low salinity plume waters are found to travel at a rate of 77 - 136 cm/s and are likely influenced by freshwater discharge rates as evidenced by higher transport during EN640 (higher discharge). Considering the implications for solutes traveling within this water mass, discharge may be a significant factor in nutrient delivery. Relatively slower transport rates across plume boundaries ranging from 13 - 44 cm/s, well within other reported values for the

area, indicate a less dynamic environment that may be uniquely suited to the diazotroph communities common in the Amazon Plume region.

Horizontal mixing analysis for subsets in this region indicates that advection is generally the dominant process on spatial scales large enough for our sampling efforts to resolve. Transects that fit assumptions for both transport and mixing analysis (EN614: stations 6-10, stations 11-12, 17, and station 19) represent a balance of advective transport and diffusive mixing (Figures 12 and 15). Predictability of this balance would greatly depend on tidal forcing and riverine discharge, subjects that are generally approached from physical oceanography methods (Lentz & Limeburner, 1995; Geyer et al., 1996; Hu et al., 2004). Additionally, we find some degree of predictability in the vertical mixing behaviors in relation to spatial distribution within the plume. An estimated eddy diffusion coefficient for the core of the plume mixing vertically with ambient waters was found to be $3.9 \times 10^{-4} \pm 1.5 \times 10^{-4}$ m^2/s. Evidence to suggest vertical mixing is faster with less stratification (i.e. strong plume haloclines) can be interpreted from the Kh values in Figure 17, additional investigation is required to determine if the relationship holds true over a different salinity regime (e.g., EN640).

Nonetheless, this study provides a temporal context for understanding the transport and mixing dynamics of the Amazon River plume and surrounding waters. When applied to dissolved material (e.g., nutrients), these findings represent a valuable step in examining the foundation of planktonic food web dynamics of the Amazon River plume that will be explored further by collaborators amid a larger research study.

References

Burnett, W. C., Aggarwal, P. K., Aureli, A., Bokuniewicz, H., Cable, J. E., Charette, M. A., et al. (2006). Quantifying submarine groundwater discharge in the coastal zone via multiple methods. *Science of The Total Environment*, *367*, 498–543. https://doi.org/10.1016/j.scitotenv.2006.05.009

Carpenter, E., Montoya, J., Burns, J., Mulholland, M., Subramaniam, A., & Capone, D. (1999). Extensive bloom of a N_2-fixing diatom/cyanobacterial association in the tropical Atlantic Ocean. *Marine Ecology Progress Series*, *185*, 273–283. https://doi.org/10.3354/meps185273

Carpenter, E. J., Harvey, H. R., Fry, B., & Capone, D. G. (1997). Biogeochemical tracers of the marine cyanobacterium Trichodesmium. *Deep Sea Research Part I: Oceanographic Research Papers*, *44*, 27–38. https://doi.org/10.1016/S0967-0637(96)00091-X

Del Vecchio, R., & Subramaniam, A. (2004). Influence of the Amazon River on the surface optical properties of the western tropical North Atlantic Ocean. *Journal of Geophysical Research: Oceans*, *109*, C11001. https://doi.org/10.1029/2004JC002503

DeMaster, D., McKee, B., Moore, W., Nelson, D., Showers, W., & Smith, W. (1991). Geochemical Processes Occurring in the Waters at the Amazon River/Ocean Boundary. *Oceanography*, *4*, 15–20. https://doi.org/10.5670/oceanog.1991.16

Geyer, R. W., Beardsley, R. C., Candela, J., Limeburner, R., Johns, W. E., Castro, B. M., & Dias Soares, I. (1996). Physical oceanography of the Amazon shelf. *Continental Shelf Research*, *16*, 575–616. https://doi.org/10.1016/0278-4343(95)00051-8

Goes, J. I., Gomes, H. do R., Chekalyuk, A. M., Carpenter, E. J., Montoya, J. P., Coles, V. J., et al. (2014). Influence of the Amazon River discharge on the biogeography of phytoplankton communities in the western tropical north Atlantic. *Progress in Oceanography*, *120*, 29–40. https://doi.org/10.1016/j.pocean.2013.07.010

Gouveia, N. A., Gherardi, D. F. M., Wagner, F. H., Paes, E. T., Coles, V. J., & Aragão, L. E. O. C. (2019). The Salinity Structure of the Amazon River Plume Drives Spatiotemporal Variation of Oceanic Primary Productivity. *Journal of Geophysical Research: Biogeosciences*, *124*, 147–165. https://doi.org/10.1029/2018JG004665

Gruber, N., & Galloway, J. N. (2008). An Earth-system perspective of the global nitrogen cycle. *Nature*, *451*, 293–296. https://doi.org/10.1038/nature06592

Hu, C., Montgomery, E. T., Schmitt, R. W., & Muller-Karger, F. E. (2004). The dispersal of the Amazon and Orinoco River water in the tropical Atlantic and Caribbean Sea: Observation from space and S-PALACE floats. *Deep Sea Research Part II: Topical Studies in Oceanography*, *51*, 1151–1171. https://doi.org/10.1016/j.dsr2.2004.04.001

HYBAM. Environmental Research Observatory on the Rivers of the Amazon, Congo and Orinoco River Basins, Obidos Station ID: 17050001, discharge (2019). https://www.ore-hybam.org)

Key, R. M., Stallard, R. F., Moore, W. S., & Sarmiento, J. L. (1985). Distribution and flux of ^{226}Ra and ^{228}Ra in the Amazon River estuary. *Journal of Geophysical Research: Oceans, 90*, 6995–7004. https://doi.org/10.1029/JC090iC04p06995

Lentz, S. J., & Limeburner, R. (1995). The Amazon River Plume during AMASSEDS: Spatial characteristics and salinity variability. *Journal of Geophysical Research: Oceans, 100*, 2355–2375. https://doi.org/10.1029/94JC01411

Li, Y. H., Mathieu, G., Biscaye, P., & Simpson, H. J. (1977). The flux of ^{226}Ra from estuarine and continental shelf sediments. *Earth Planet. Sci. Lett., 37*, 237–241.

Loick-Wilde, N., Weber, S. C., Conroy, B. J., Capone, D. G., Coles, V. J., Medeiros, P. M., et al. (2016). Nitrogen sources and net growth efficiency of zooplankton in three Amazon River plume food webs. *Limnology and Oceanography, 61*, 460–481. https://doi.org/10.1002/lno.10227

Mascarenhas, A. C. C. 1, Gomes, G. S. 1, Lima, A. P. Y. 1, da Silva, H. K. N. 1, Santana, L. S. 1, Rosário, R. P. 2, & Rollnic, M., 2. (2016). Seasonal Variations of the Amazon River Plume with Focus on the Eastern Sector. *Journal of Coastal Research, 75*, 532–536. https://doi.org/10.2112/SI75-107.1

Men, W., Jiang, Y., Liu, G., Wang, F., & Zhang, Y. (2016). Study of water mixing in the coastal waters of the western Taiwan Strait based on radium isotopes. *Journal of Environmental Radioactivity, 152*, 16–22. https://doi.org/10.1016/j.jenvrad.2015.11.003

Mohr, W., LaRoche, J., Grosskopf, T., Wallace, D. W. R., & Wiebke Mohr. (2010). Methodological Underestimation of Oceanic Nitrogen Fixation Rates. *PLOS ONE, 5*.

Montoya, J. P., Carpenter, E. J., & Capone, D. G. (2002). Nitrogen fixation and nitrogen isotope abundances in zooplankton of the oligotrophic North Atlantic. *Limnology and Oceanography, 47*, 1617–1628. https://doi.org/10.4319/lo.2002.47.6.1617

Moore, W. S. (1976). Sampling ^{228}Ra in the deep ocean. *Deep-Sea Research, 23*, 647–651.

Moore, W. S. (2000a). Ages of continental shelf waters determined from ^{223}Ra and ^{224}Ra. *Journal of Geophysical Research: Oceans, 105*, 22117–22122. https://doi.org/10.1029/1999JC000289

Moore, W. S. (2000b). Determining coastal mixing rates using radium isotopes. *Continental Shelf Research, 20*, 1993–2007.

Moore, W. S. (2008). Fifteen years experience in measuring ^{224}Ra and ^{223}Ra by delayed-coincidence counting. *Marine Chemistry, 109*, 188–197. https://doi.org/10.1016/j.marchem.2007.06.015

Moore, W. S. (2015). Inappropriate attempts to use distributions of ^{228}Ra and ^{226}Ra in coastal waters to model mixing and advection rates. *Continental Shelf Research*, *105*, 95–100.

Moore, W. S., & Arnold, R. (1996). Measurement of ^{223}Ra and ^{224}Ra in coastal waters using a delayed coincidence counter. *Journal of Geophysical Research: Oceans*, *101*, 1321–1329. https://doi.org/10.1029/95JC03139

Moore, W. S., & Dymond, J. (1991). Fluxes of ^{226}Ra and barium in the Pacific Ocean: The importance of boundary processes. *Earth and Planetary Science Letters*, *107*, 55–68. https://doi.org/10.1016/0012-821X(91)90043-H

Moore, W. S., & Edmond, J. M. (1984). Radium and barium in the Amazon River system. *Journal of Geophysical Research: Oceans*, *89*, 2061–2065. https://doi.org/10.1029/JC089iC02p02061

Moore, W. S., & Krest, J. (2004). Distribution of ^{223}Ra and ^{224}Ra in the plumes of the Mississippi and Atchafalaya Rivers and the Gulf of Mexico. *Marine Chemistry*, *86*, 105–119. https://doi.org/10.1016/j.marchem.2003.10.001

Moore, W. S., & Reid, D. F. (1973). Extraction of radium from Natural Waters Using Manganese-Impregnated Acrylic Fibers. *Journal of Geophysical Research*, *78*, 8880–8886.

Moore, W. S., Astwood, H., & Lindstrom, C. (1995). Radium isotopes in coastal waters on the Amazon shelf. *Geochimica et Cosmochimica Acta*, *59*, 4285–4298. https://doi.org/10.1016/0016-7037(95)00242-R

Moore, W. S., DeMaster, D. J., Smoak, J. M., McKee, B. A., & Swarzenski, P. W. (1996). Radionuclide tracers of sediment-water interactions on the Amazon shelf. *Continental Shelf Research*, *16*, 645–665. https://doi.org/10.1016/0278-4343(95)00049-6

NOAA Coast Watch / Ocean Watch. MIRAS Sea surface salinity. (2019). https://www.coastwatch.noaa.gov

Peterson, R. N., Burnett, W. C., Taniguchi, M., Chen, J., Santos, I. R., & Misra, S. (2008). Determination of transport rates in the Yellow River–Bohai Sea mixing zone via natural geochemical tracers. *Continental Shelf Research*, *28*, 2700–2707. https://doi.org/10.1016/j.csr.2008.09.002

Peterson, R. N., Burnett, W. C., Opsahl, S. P., Santos, I. R., Misra, S., & Froelich, P. N. (2013). Tracking suspended particle transport via radium isotopes (^{226}Ra and ^{228}Ra) through the Apalachicola–Chattahoochee–Flint River system. *Journal of Environmental Radioactivity*, *116*, 65–75. https://doi.org/10.1016/j.jenvrad.2012.09.001

Schiller, R. V., & Kourafalou, V. H. (2010). Modeling river plume dynamics with the HYbrid Coordinate Ocean Model. *Ocean Modelling*, *33*, 101–117. https://doi.org/10.1016/j.ocemod.2009.12.005

Schlesinger, W., & Bernhardt, E. (2013). Inland Waters. In *Biogeochemistry: An Analysis of Global Change* (3rd ed., pp. 275–340). Elsevier.

Seitzinger, S. P., Mayorga, E., Bouwman, A. F., Kroeze, C., Beusen, A. H. W., Billen, G., et al. (2010). Global river nutrient export: A scenario analysis of past and future trends. *Global Biogeochemical Cycles*, *24*. https://doi.org/10.1029/2009GB003587

Sevink, J., Kooijman, A., & Sparrius, L. (2010). Nutrient cycling. *KNNV Publishing*. (pp. 333–351).

Sharples, J., Middelburg, J. J., Fennel, K., & Jickells, T. D. (2017). What proportion of riverine nutrients reaches the open ocean? *Global Biogeochemical Cycles*, *31*, 39–58. https://doi.org/10.1002/2016GB005483

Subramaniam, A., Yager, P. L., Carpenter, E. J., Mahaffey, C., Bjorkman, K., Cooley, S., et al. (2008). Amazon River enhances diazotrophy and carbon sequestration in the tropical North Atlantic Ocean. *Proceedings of the National Academy of Sciences*, *105*, 10460–10465. https://doi.org/10.1073/pnas.0710279105

Sun, Y., & Torgersen, T. (1998). The effects of water content and Mn-fiber surface conditions on ^{224}Ra measurement by ^{220}Rn emanation. *Marine Chemistry*, *62*, 299–306. https://doi.org/10.1016/S0304-4203(98)00019-X

Swarzenski, P. W. (2007). U/Th Series Radionuclides as Coastal Groundwater Tracers. *Chemical Reviews*, *107*, 663–674. https://doi.org/10.1021/cr0503761

Vorosmarty, C. J., Tian, H., Melillo, J. M., Kicklighter, D. W., McGuire, A. D., Helfrich, J., & Moore, B. (2000). Climatic and Biotic Controls on Annual Carbon Storage in Amazonian Ecosystems. *Global Ecology and Biogeography*, *9*, 315–335.

Weber, S. C., Carpenter, E. J., Coles, V. J., Yager, P. L., Goes, J., & Montoya, J. P. (2017). Amazon River influence on nitrogen fixation and export production in the western tropical North Atlantic. *Limnology and Oceanography*, *62*, 618–631. https://doi.org/10.1002/lno.10448

Tables

Table 1: Summary of surface activities for radium isotopes from both cruises: 2018 (EN614) and 2019 (EN640). Mean activities are shown with ± 1-σ average error.

Isotope	Cruise	Mean Activity (dpm/100L)	Range (dpm/100L)
^{223}Ra	EN614	0.74 ± 0.20	0.03 – 3.90
	EN640	0.50 ± 0.14	0.05 – 6.09
^{224}Ra	EN614	5.70 ± 0.50	0.01– 29.90
	EN640	3.30 ± 0.29	0.08 – 43.10
^{226}Ra	EN614	18.25 ± 1.25	10.36 – 24.85
	EN640	17.86 ± 1.38	10.17 – 28.42
^{228}Ra	EN614	12.62 ± 0.10	0.02 – 52.80
	EN640	n/a	n/a

Table 2: Summary of the EN614 linear regression results from apparent radium age versus transect distance to calculate transport rates shown in Figure 12.

Transect	Best-fit line slope (day / km)	R^2 value	p value	n	Transport rate (cm/s)	Approx. distance range (km)
Station 4	0.040 ± 0.004	0.86	< 0.01	16	28.74 ± 3.49	200
Stations 6-10	0.034 ± 0.005	0.62	< 0.01	35	34.34 ± 5.36	350
Stations 11-12, 17	0.062 ± 0.011	0.80	< 0.01	10	18.72 ± 4.04	250
Station 19	0.073 ± 0.009	0.84	< 0.01	14	15.79 ± 2.26	200
Stations 25-27	0.026 ± 0.006	0.68	< 0.01	10	44.31 ± 14.33	175
Low Salinity	0.009 ± 0.002	0.31	< 0.01	41	135.57 ± 42.34	800
Mesohaline*	0.012 ± 0.002	0.50	< 0.01	64	94.98 ± 13.82	1100
Total*	0.008 ± 0.001	0.26	< 0.01	128	143.81 ± 25.40	1400

*Not included in figure.

Table 3: Summary of the EN640 linear regression results from apparent radium age versus transect distance to calculate transport rates shown in Figure 14.

Transect	Best-fit line slope (day / km)	R^2 value	p value	n	Transport rate (cm/s)	Approx. distance range (km)
Station 1	0.014 ± 0.005	0.39	< 0.05	14	83.70 ± 47.37	200
Stations 4-7	0.091 ± 0.009	0.86	< 0.01	19	12.72 ± 1.35	250
Station 8	0.062 ± 0.008	0.84	< 0.01	13	18.71 ± 2.89	250
Stations 9-11*	0.032 ± 0.026	0.18	> 0.05	9	36.15 ± 154.48	120
Stations 19-20*	0.010 ± 0.008	0.15	> 0.05	11	110.52 ± 406.56	120
Low Salinity	0.015 ± 0.001	0.79	< 0.01	49	77.25 ± 6.24	1200
Mesohaline*	0.002 ± 0.001	0.08	< 0.01	177	652.18 ± 222.01	1200
Total*	0.006 ± 0.001	0.39	< 0.01	243	188.24 ± 16.54	1400

*Not included in figure.

Table 4: Summary of the EN614 linear regression results from ln^{224}Ra and ^{226}Ra activities versus relative transect distance shown in Figure 15. Horizontal eddy diffusion coefficients (K_h) are shown with ± 1-σ propagated error.

Transect	Isotope	Best-fit line slope (activity / km)	R^2 value	p value	n	K_h (m^2/s)	Approx. distance range (km)
Station 4*	ln ^{224}Ra	-0.007 ± 0.001	0.82	< 0.01	16	$4.1 \times 10^4 \pm 8.5 \times 10^3$	175
	^{226}Ra	0.005 ± 0.009	0.02	>0.05			
Stations 6-10	ln ^{224}Ra	-0.007 ± 0.001	0.69	< 0.01	35	$4.0 \times 10^4 \pm 7.9 \times 10^3$	375
	^{226}Ra	-0.019 ± 0.003	0.56	< 0.01			
Stations 11-12, 17	ln ^{224}Ra	-0.013 ± 0.002	0.82	< 0.01	10	$1.3 \times 10^4 \pm 3.4 \times 10^3$	250
	^{226}Ra	-0.027 ± 0.010	0.45	<0.05			
Station 19	ln ^{224}Ra	-0.015 ± 0.002	0.88	< 0.01	14	$9.5 \times 10^3 \pm 1.7 \times 10^3$	200
	^{226}Ra	-0.027 ± 0.010	0.40	<0.05			
Stations 25-27*	ln ^{224}Ra	-0.004 ± 0.003	0.16	>0.05	11	n/a	175
	^{226}Ra	0.012 ± 0.014	0.08	>0.05			
Low Salinity*	ln ^{224}Ra	-0.002 ± 0.001	0.30	< 0.01	41	$9.0 \times 10^5 \pm 3.2 \times 10^5$	800
	^{226}Ra	0.001 ± 0.001	0.01	>0.05			
Mesohaline*	ln ^{224}Ra	-0.003 ± 0.001	0.50	< 0.01	69	$2.2 \times 10^5 \pm 4.5 \times 10^4$	1200
	^{226}Ra	-0.001 ± 0.001	0.02	>0.05			

*Not included in figure.

Table 5: Summary of the EN614 linear regression results from ln^{224}Ra and ^{226}Ra activities versus depth for profiles shown spatially distributed in Figure 17. Vertical eddy diffusion coefficients (K_h) are shown with ± 1-σ propagated error.

Transect	Isotope	Best-fit line slope (activity / m)	R^2 value	p value	n	K_h (m^2/s)	Approx. depth range (m)
Station 3*	ln ^{224}Ra	-0.014 ± 0.003	0.89	>0.05	4	n/a	50
	^{226}Ra	-0.001 ± 0.001	0.21				
Station 6	ln ^{224}Ra	-0.110 ± 0.042	0.87	>0.05	3	$1.8 \times 10^{-4} \pm 8.6 \times 10^{-5}$	30
	^{226}Ra	-0.002 ± 0.001	0.89				
Station 8	ln ^{224}Ra	-0.048 ± 0.045	0.53	>0.05	3	$9.4 \times 10^{-4} \pm 6.9 \times 10^{-4}$	30
	^{226}Ra	-0.0004 ± 0.0001	0.93				
Station 17^	ln ^{224}Ra	-0.075 ± 0.019	0.75	<0.05	7	$3.9 \times 10^{-4} \pm 1.5 \times 10^{-4}$	20
	^{226}Ra	-0.004 ± 0.001	0.69				
Station 24*	ln ^{224}Ra	-0.017 ± 0.018	0.31	>0.05	4	n/a	35
	^{226}Ra	-0.001 ± 0.001	0.20				
Station 33	ln ^{224}Ra	-0.025 ± 0.005	0.96	>0.05	3	$3.6 \times 10^{-3} \pm 1.1 \times 10^{-3}$	25
	^{226}Ra	-0.001 ± 0.0001	0.98				

*Not calculated due to poor linear regression statistics.

^Detailed activity profile shown in Figure 16.

Figures

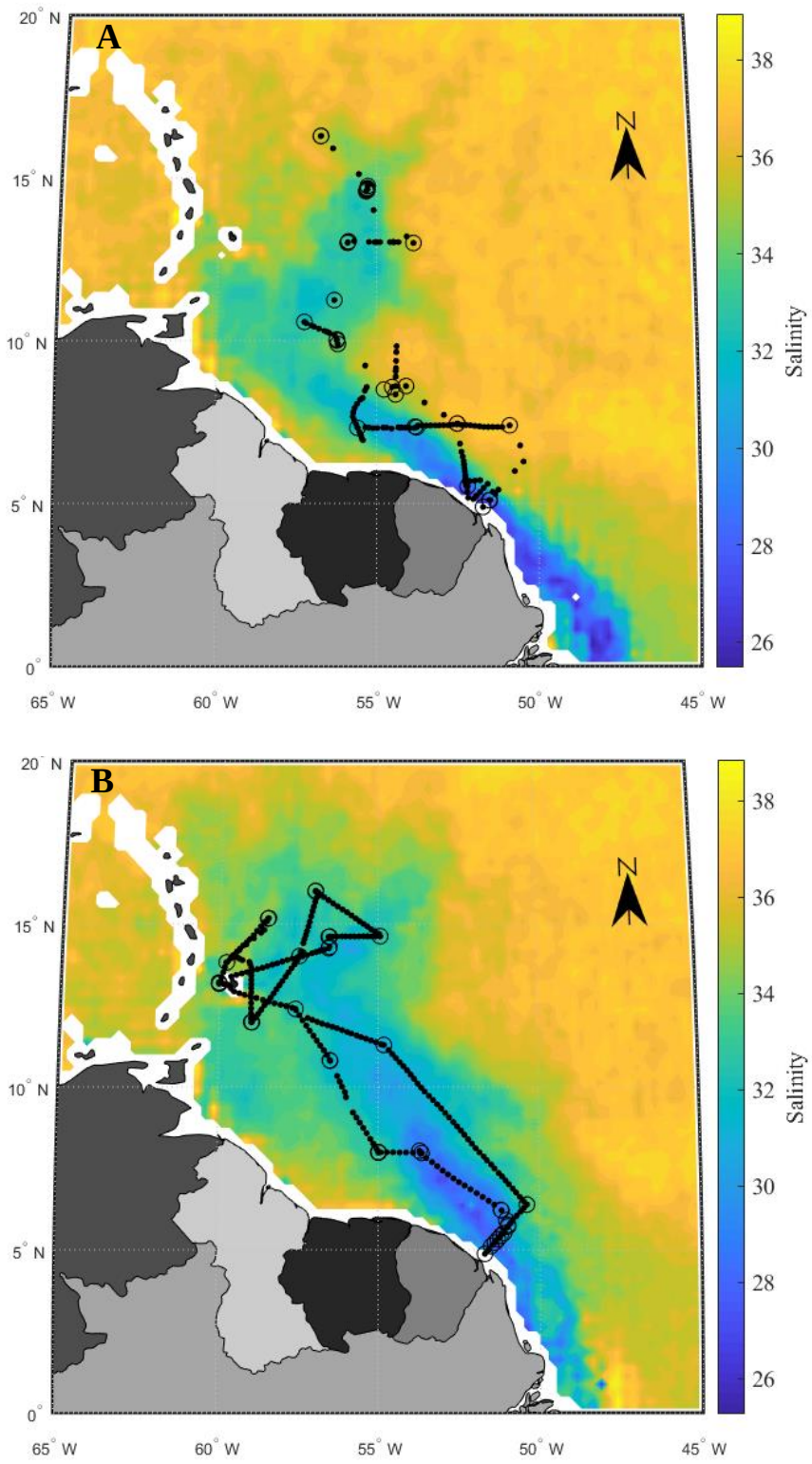

Figure 1. Sampling locations shown in and around the Amazon River plume (**A**: EN614; **B**: EN640) with CTD casts marked by open circles and underway sampling sites marked with small black circles. These locations are superimposed on the spatial distribution of sea surface salinity (data from www.coastwatch.noaa.gov) averaged over the duration of each cruise.

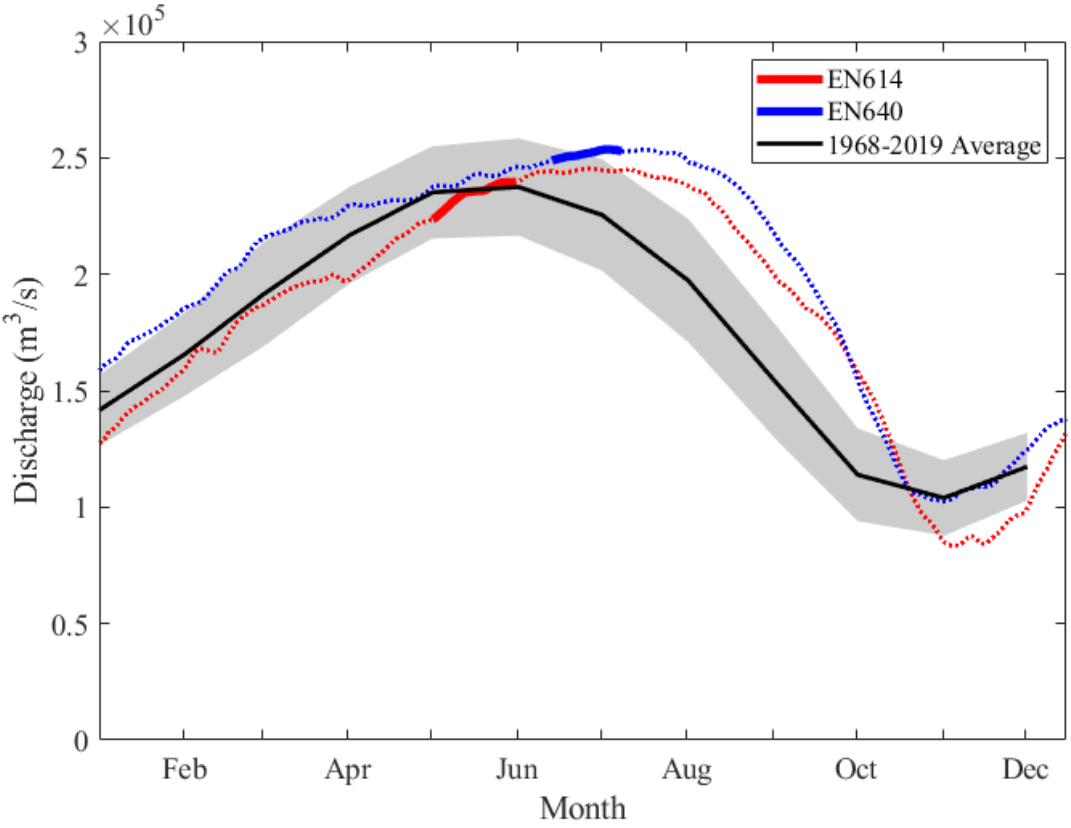

Figure 2. Amazon River discharge obtained from Obidos monitoring station (HYBAM: www.ore-hybam.org). For 2018 and 2019, (red and blue dotted lines, respectively) daily average discharge rates are plotted over the entire year with sampling periods highlighted as solid red and blue lines. The black line represents monthly discharge values averaged from 1968 to 2019 with one standard deviation shaded.

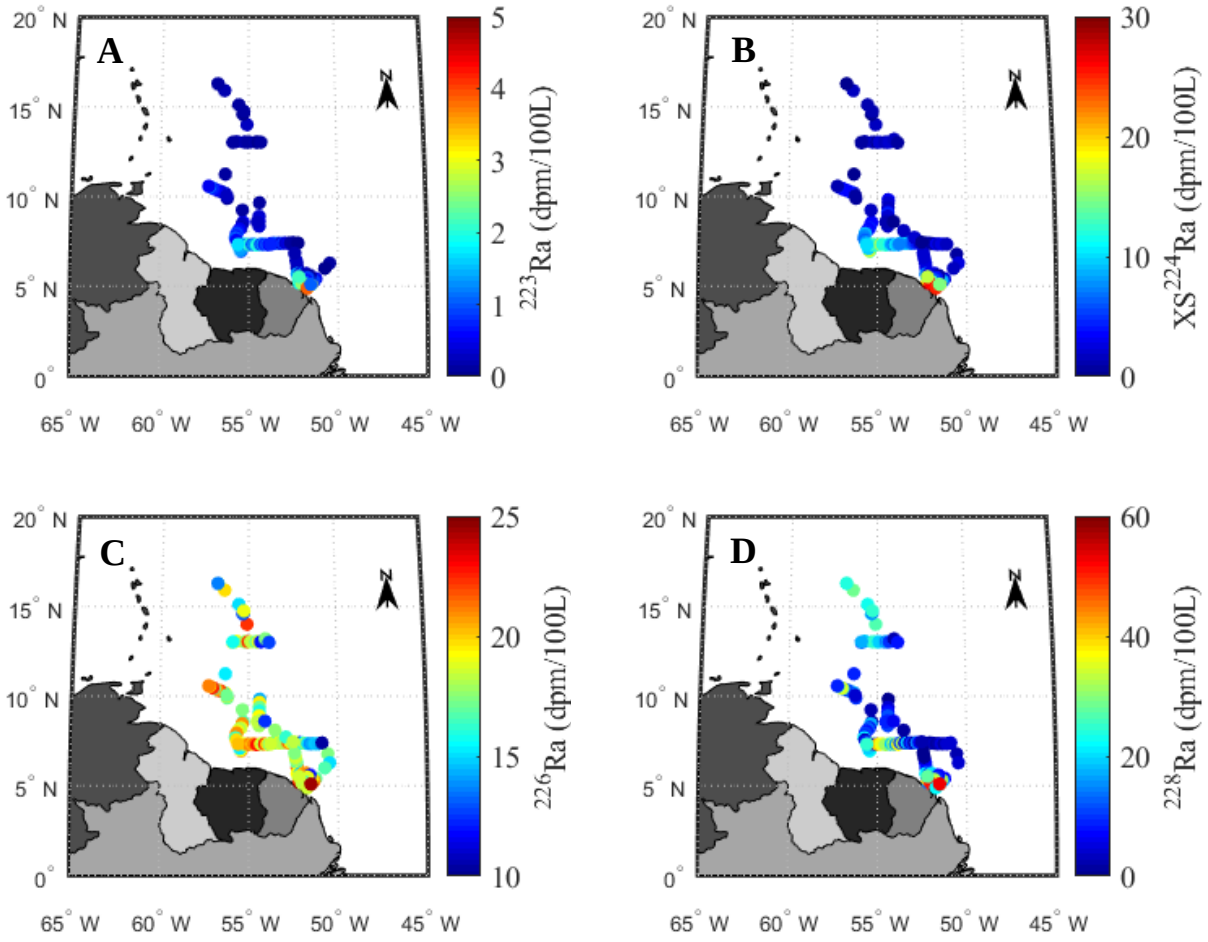

Figure 3. Spatial distribution of isotope activities for ^{223}Ra (**A**), excess ^{224}Ra (**B**), ^{226}Ra (**C**), and ^{228}Ra (**D**) as measured on EN614. Raw data with 1-σ analytical uncertainties are reported in Appendix B1.

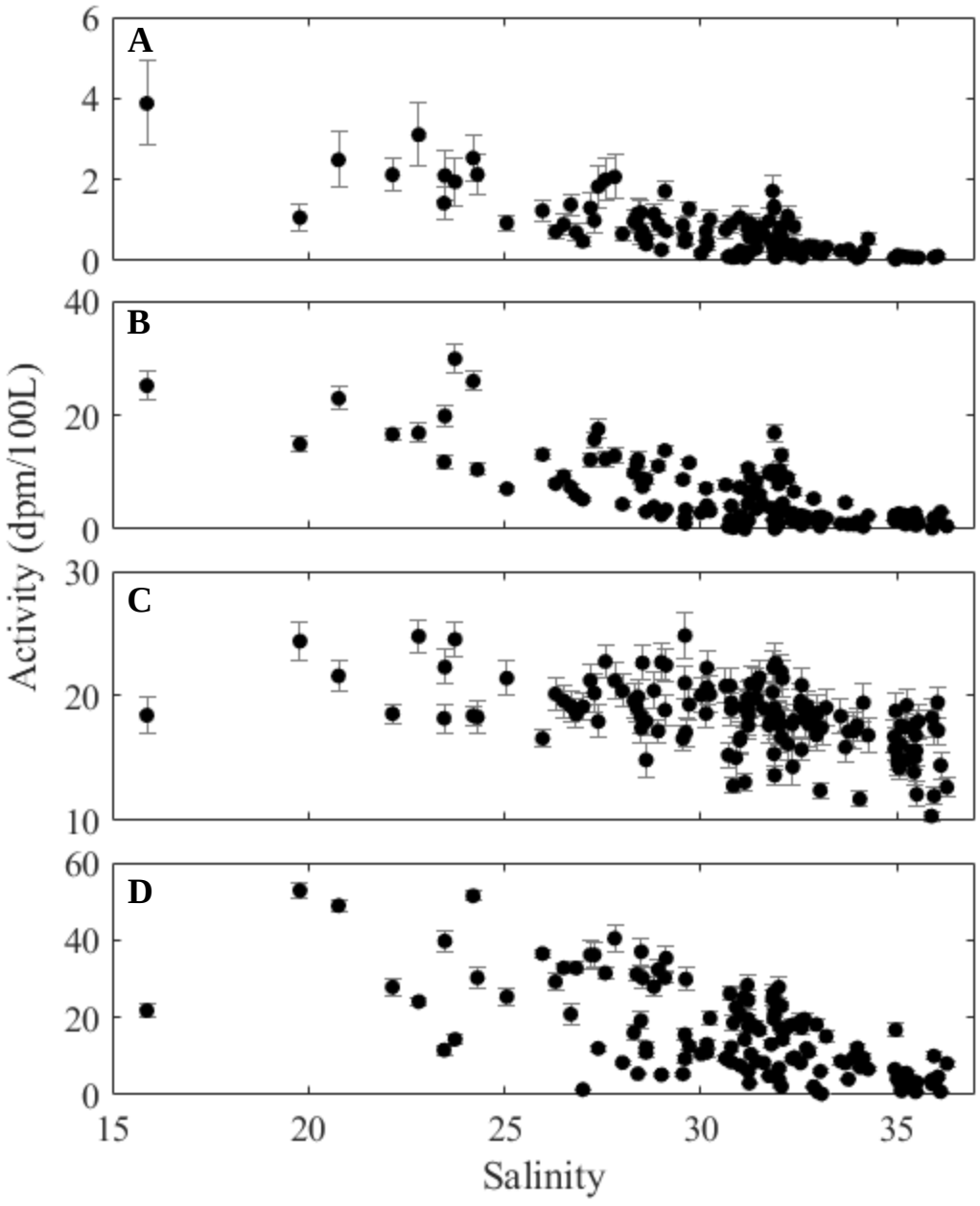

Figure 4. Distribution of ^{223}Ra (**A**), excess ^{224}Ra (**B**), ^{226}Ra (**C**), and ^{228}Ra (**D**) activities relative to measured salinity for EN614. Error bars represent 1-σ analytical uncertainties.

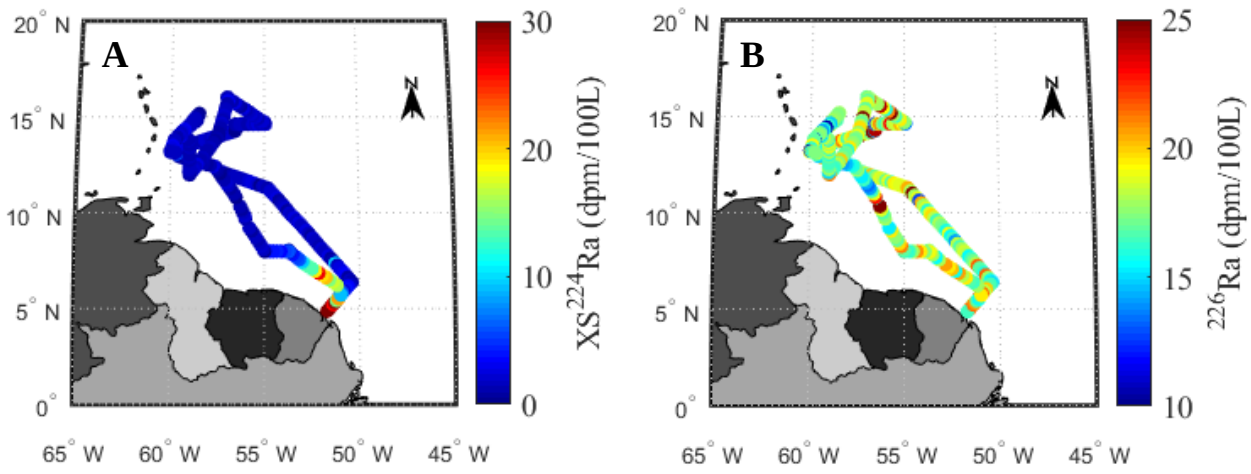

Figure 5. Spatial distribution of isotope activities for excess ^{224}Ra (**A**), ^{226}Ra (**B**) as measured on EN640. Raw data with 1-σ analytical uncertainties are reported in Appendix B2.

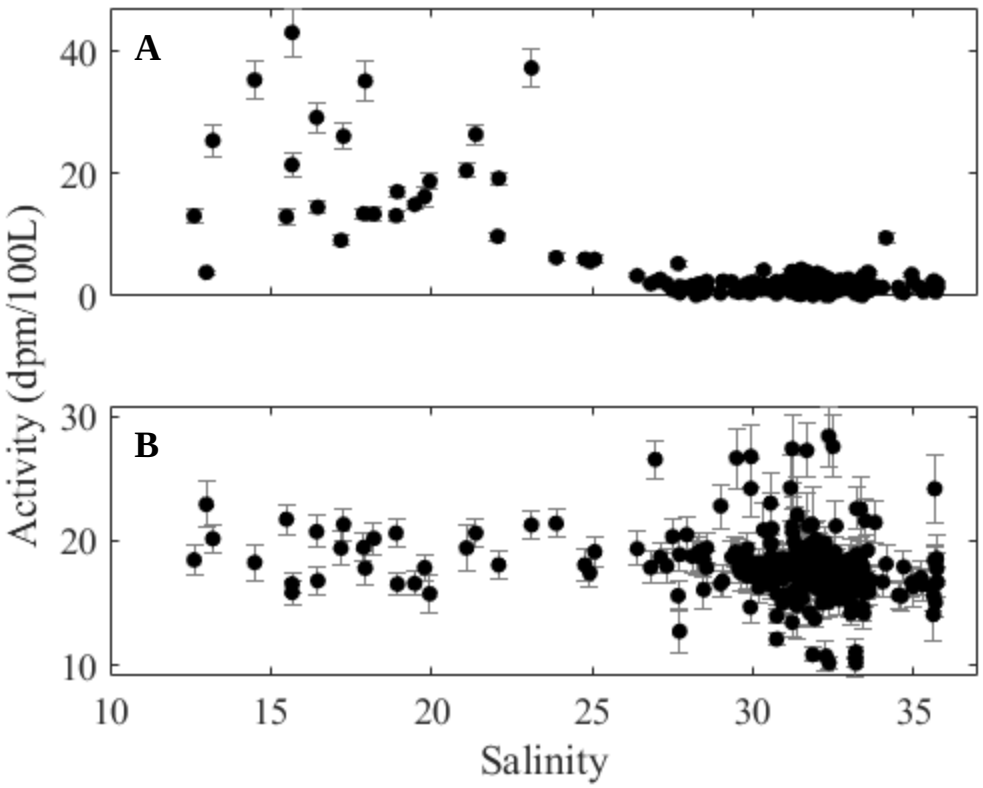

Figure 6. Distribution of excess ^{224}Ra (**A**) and ^{226}Ra (**B**) activities relative to measured salinity for EN640. Error bars represent 1-σ analytical uncertainties.

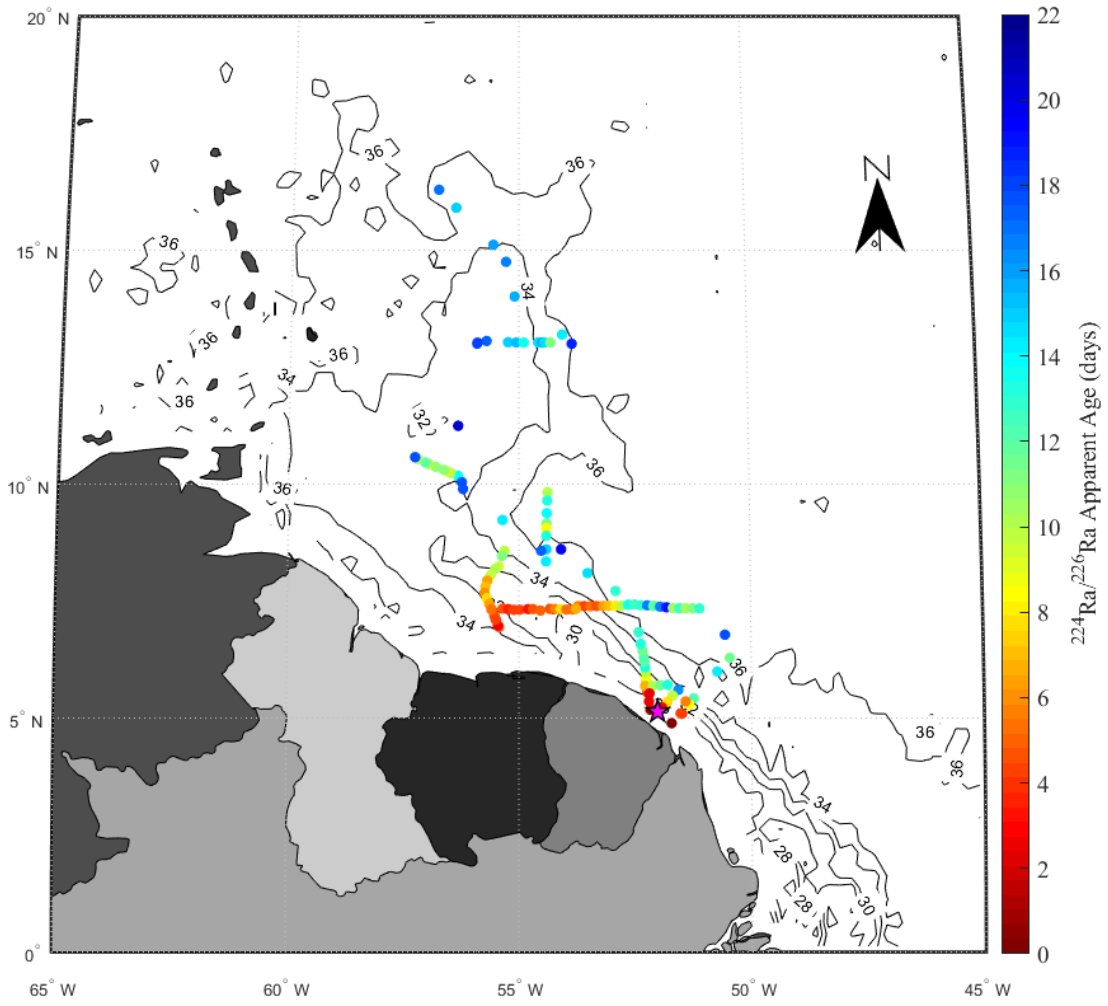

Figure 7. EN614 spatial distribution of apparent radium ages calculated from $^{224}Ra/^{226}Ra$ activity ratios. The determined T = 0 point is marked by pink star. Black contour lines indicate the NOAA Coast Watch sea surface salinity.

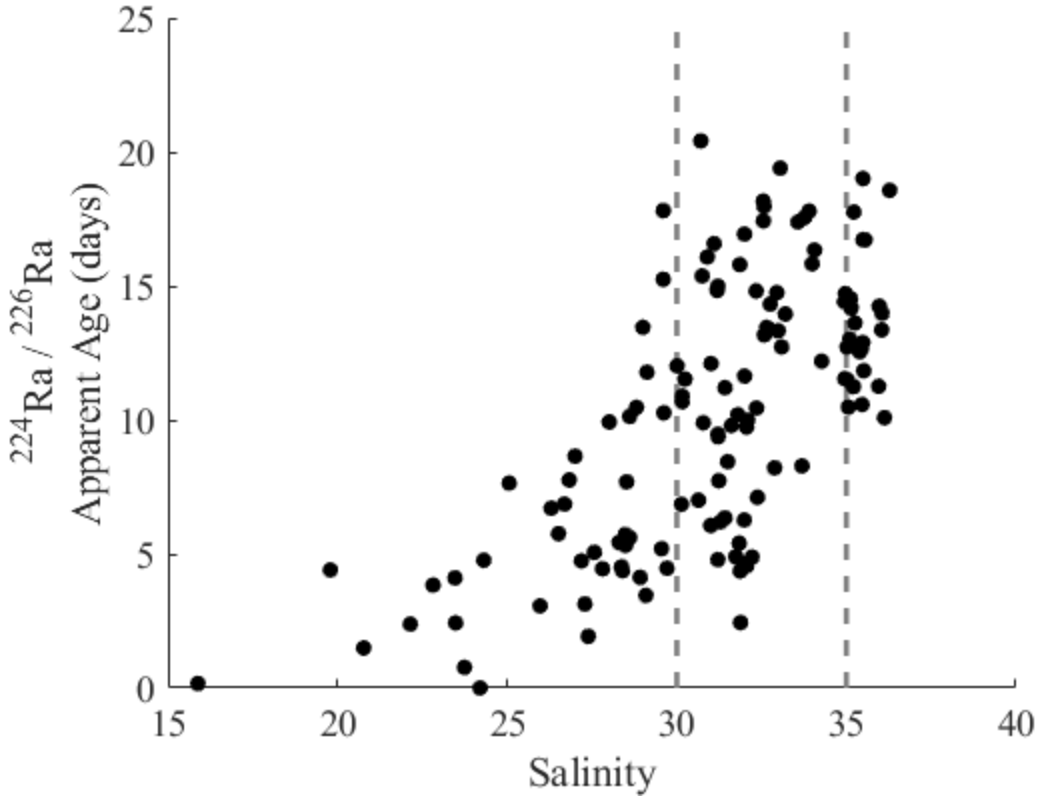

Figure 8. Apparent radium ages calculated from $^{224}Ra/^{226}Ra$ activity ratios relative to measured salinity from EN614. Vertical dashed lines separate the low salinity, mesohaline, and oceanic salinity regions as defined by Subramaniam et al. 2008.

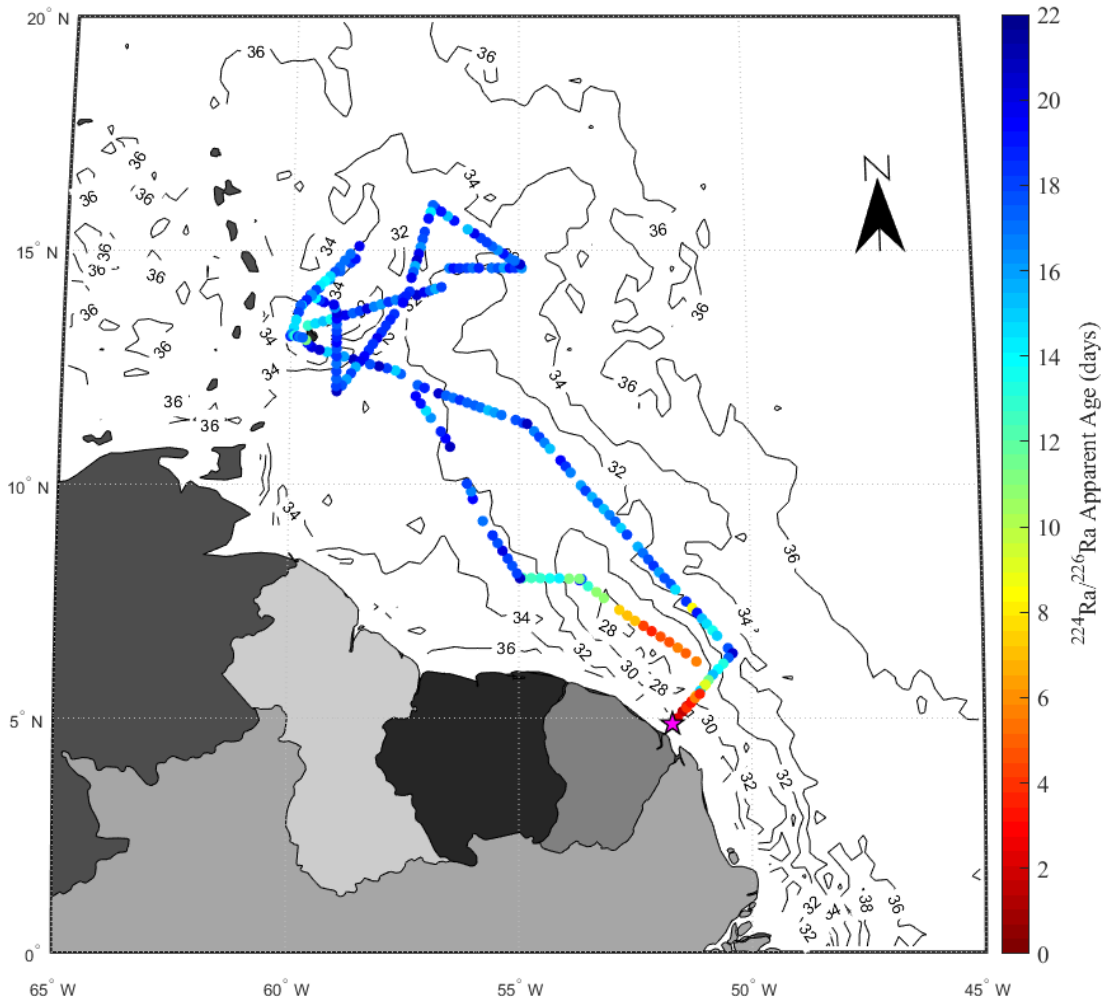

Figure 9. EN640 spatial distribution of apparent radium ages calculated from $^{224}Ra/^{226}Ra$ activity ratios. The determined T = 0 point is marked by pink star. Black contour lines indicate the NOAA Coast Watch sea surface salinity.

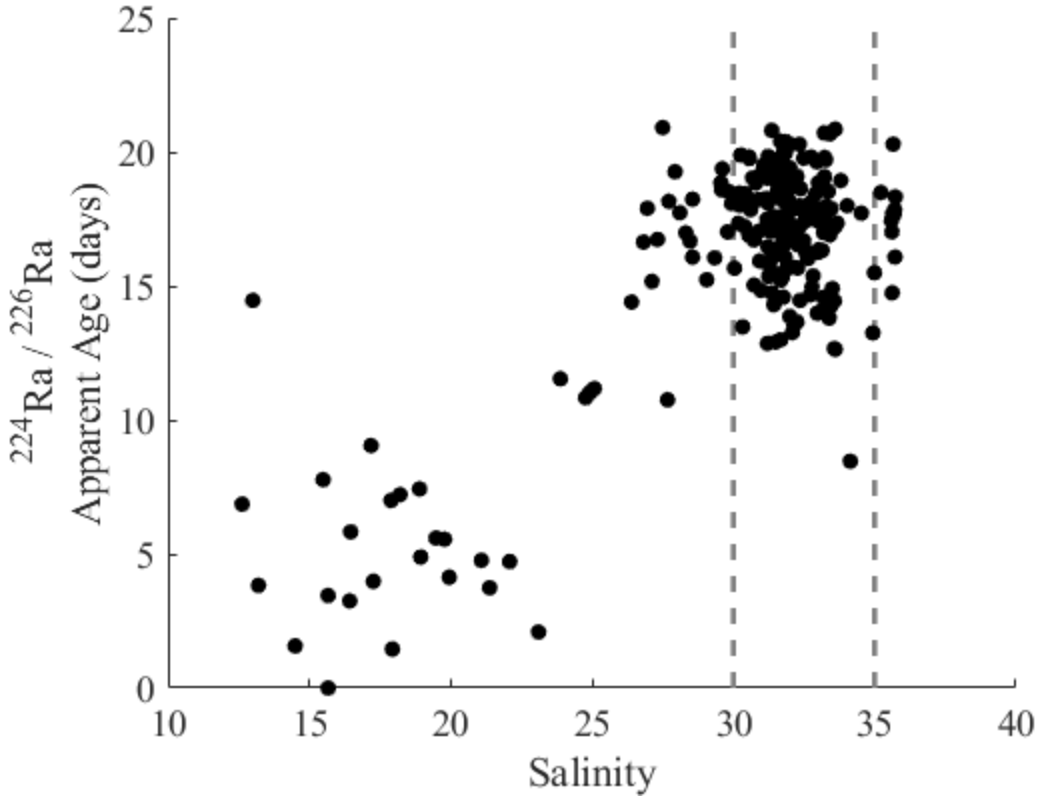

Figure 10. Apparent radium ages calculated from ^{224}Ra/^{226}Ra activity ratios relative to measured salinity from EN640. Vertical dashed lines separate the low salinity, mesohaline, and oceanic salinity regions as defined by Subramaniam et al. 2008.

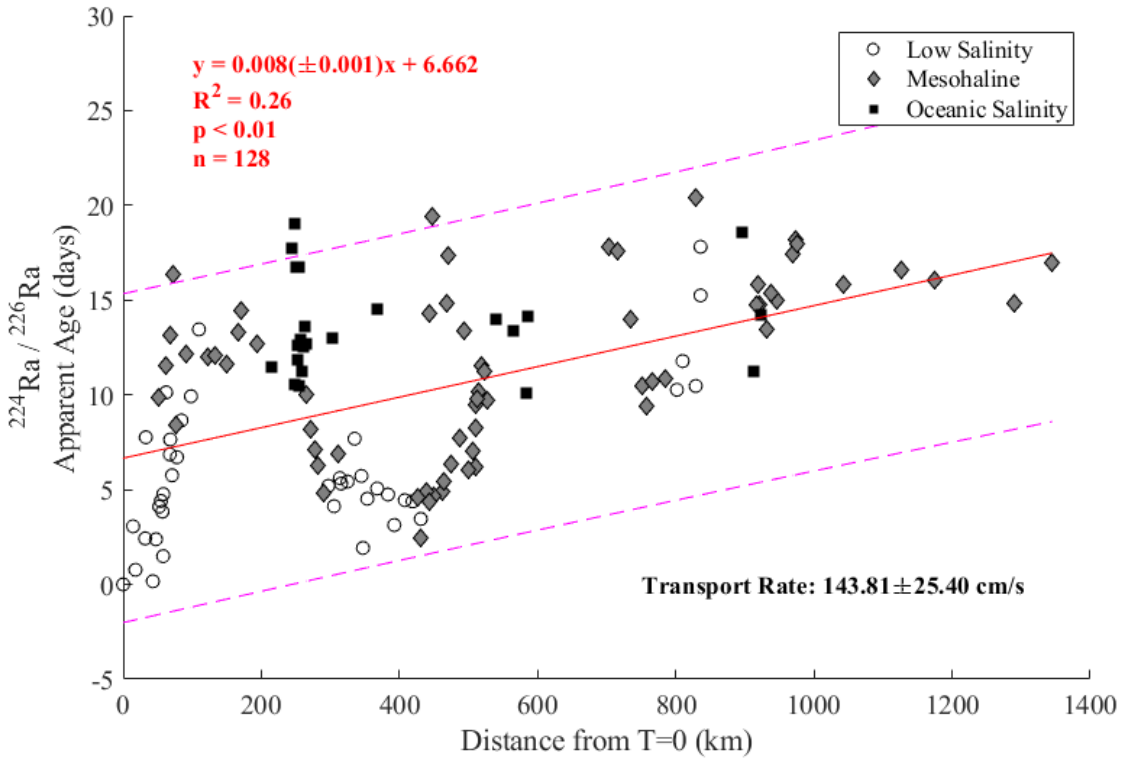

Figure 11. Apparent radium ages calculated from $^{224}Ra/^{226}Ra$ activity ratios for each salinity group plotted against their distance from the T = 0 sample for EN614. Best-fit line is shown in red with its 95% prediction interval. The transport rate shown is calculated as the reciprocal of the slope of the best-fit line.

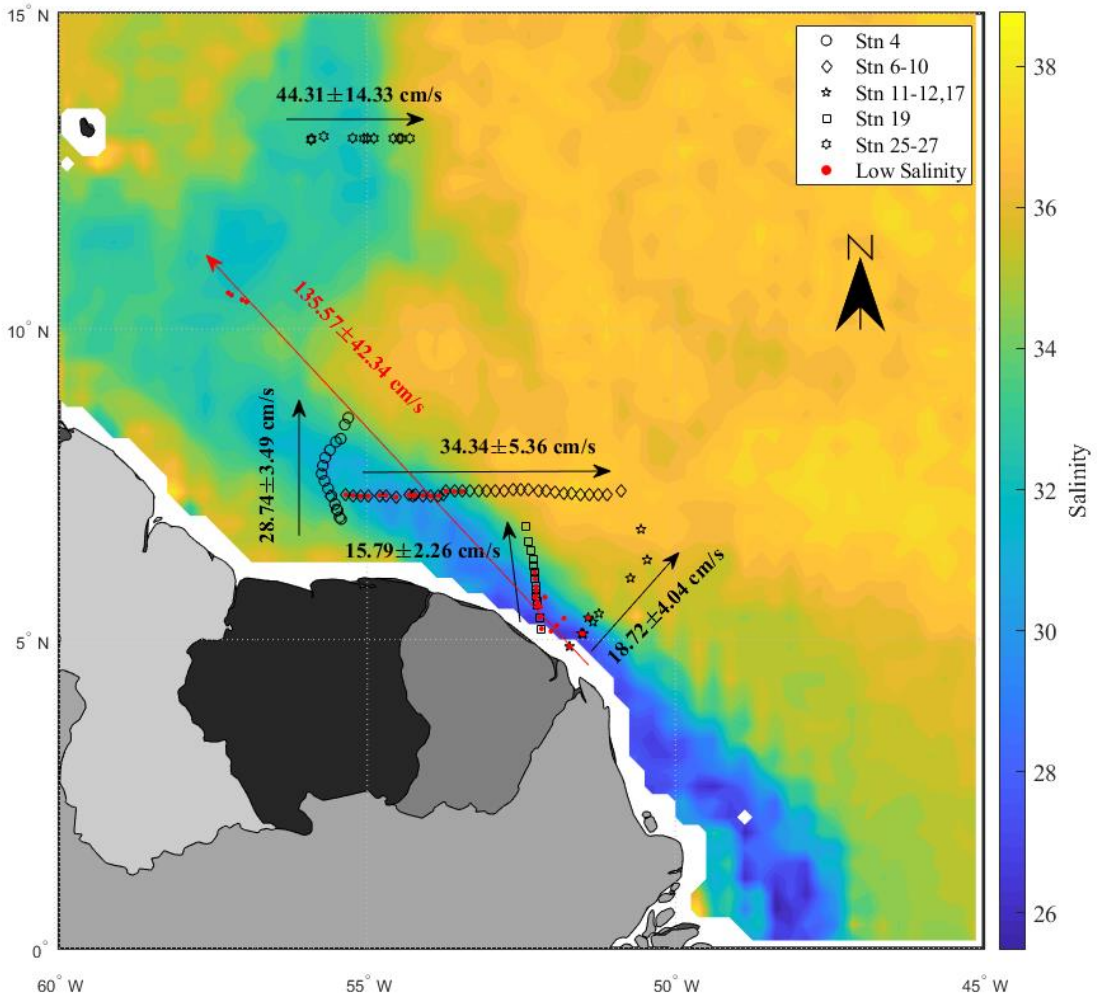

Figure 12. Transport rate vectors for EN614 transects shown spatially with their respective sample locations. Transport rates are calculated from best-fit linear regressions of the $^{224}Ra/^{226}Ra$ apparent age model (Table 2). Average sea surface salinity for the duration of the cruise is shown to depict the plume region.

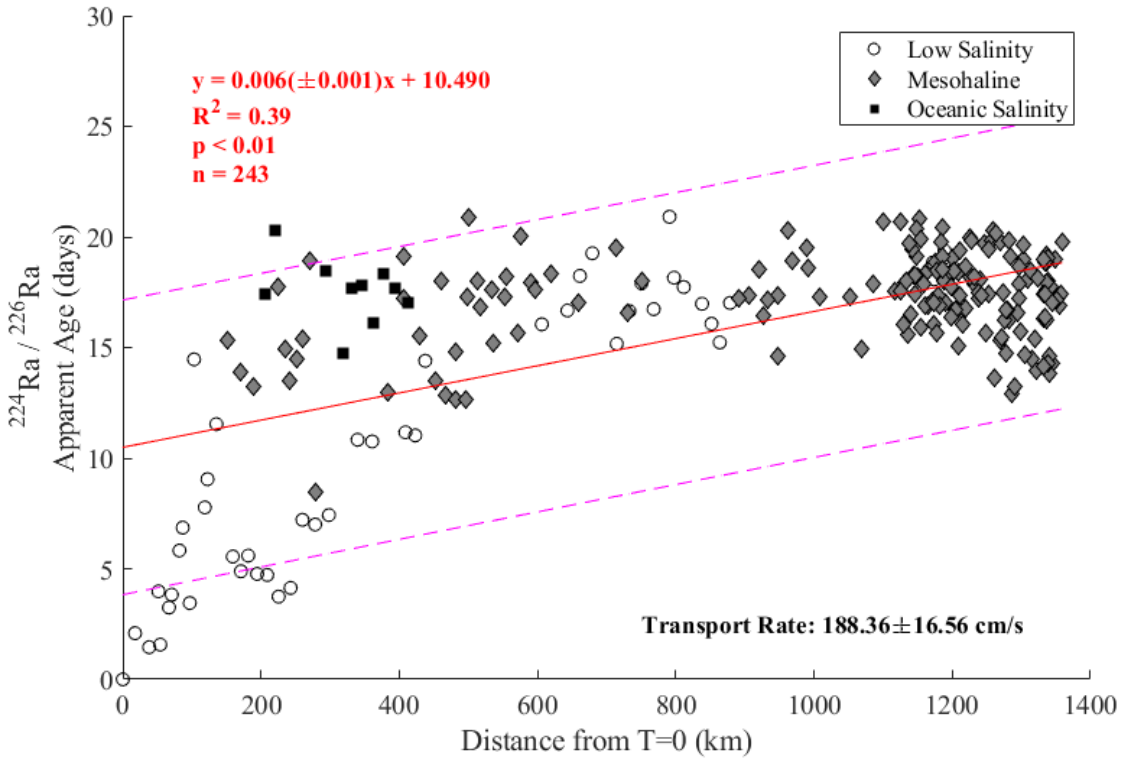

Figure 13. Apparent radium ages calculated from $^{224}Ra/^{226}Ra$ activity ratios for each salinity group plotted against their distance from the T = 0 sample for EN640. Best-fit line is shown in red with its 95% prediction interval. The transport rate shown is calculated as the reciprocal of the slope of the best-fit line.

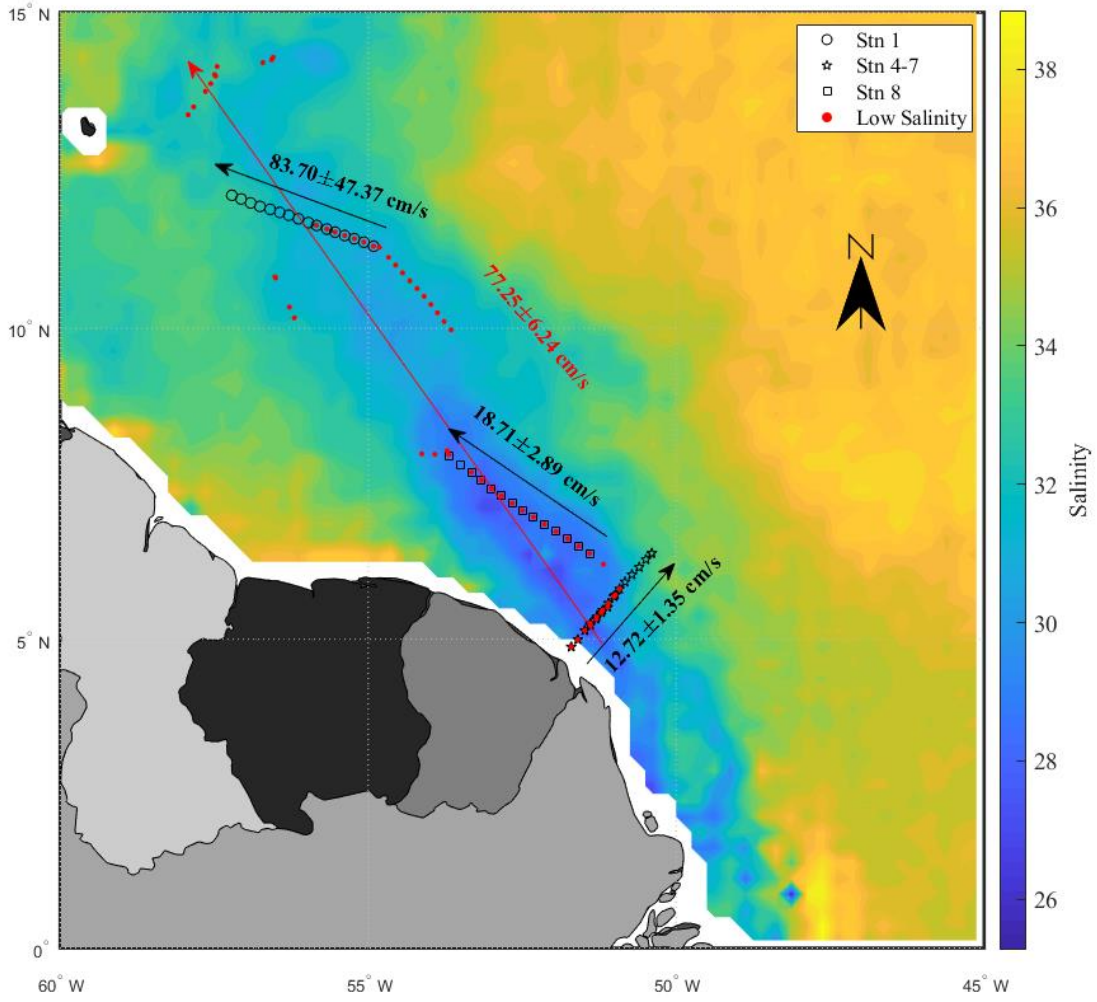

Figure 14. Transport rate vectors for EN640 transects shown spatially with their respective sample locations. Transport rates are calculated from best-fit linear regressions of the $^{224}Ra/^{226}Ra$ apparent age model (Table 3). Average sea surface salinity for the duration of the cruise is shown to depict the plume region.

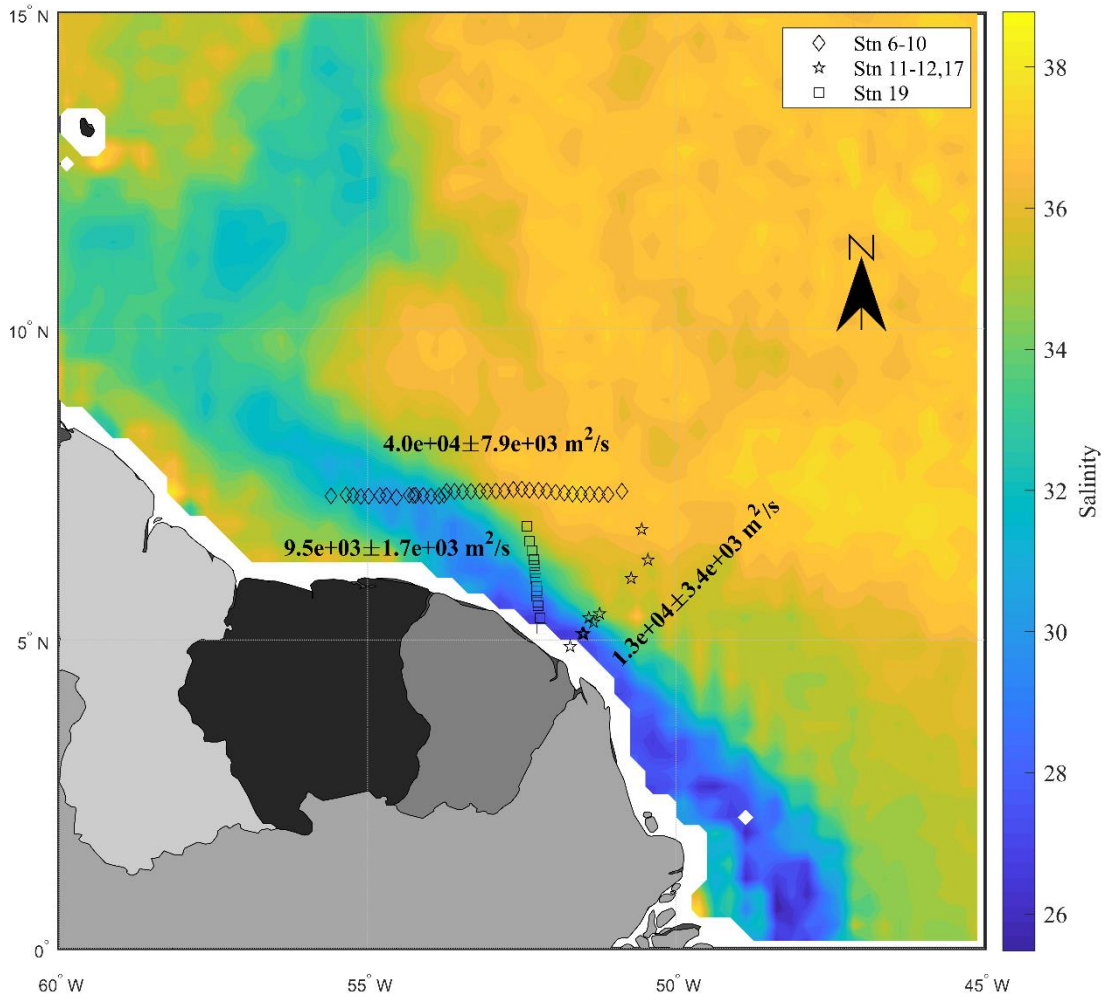

Figure 15. Eddy diffusion coefficients (K_h) shown spatially for three transects from EN614. (Results shown in Table 4). K_h is not shown for profiles that failed to meet the criteria necessary for the model to hold. Average sea surface salinity for the duration of the cruise is shown to depict the plume region.

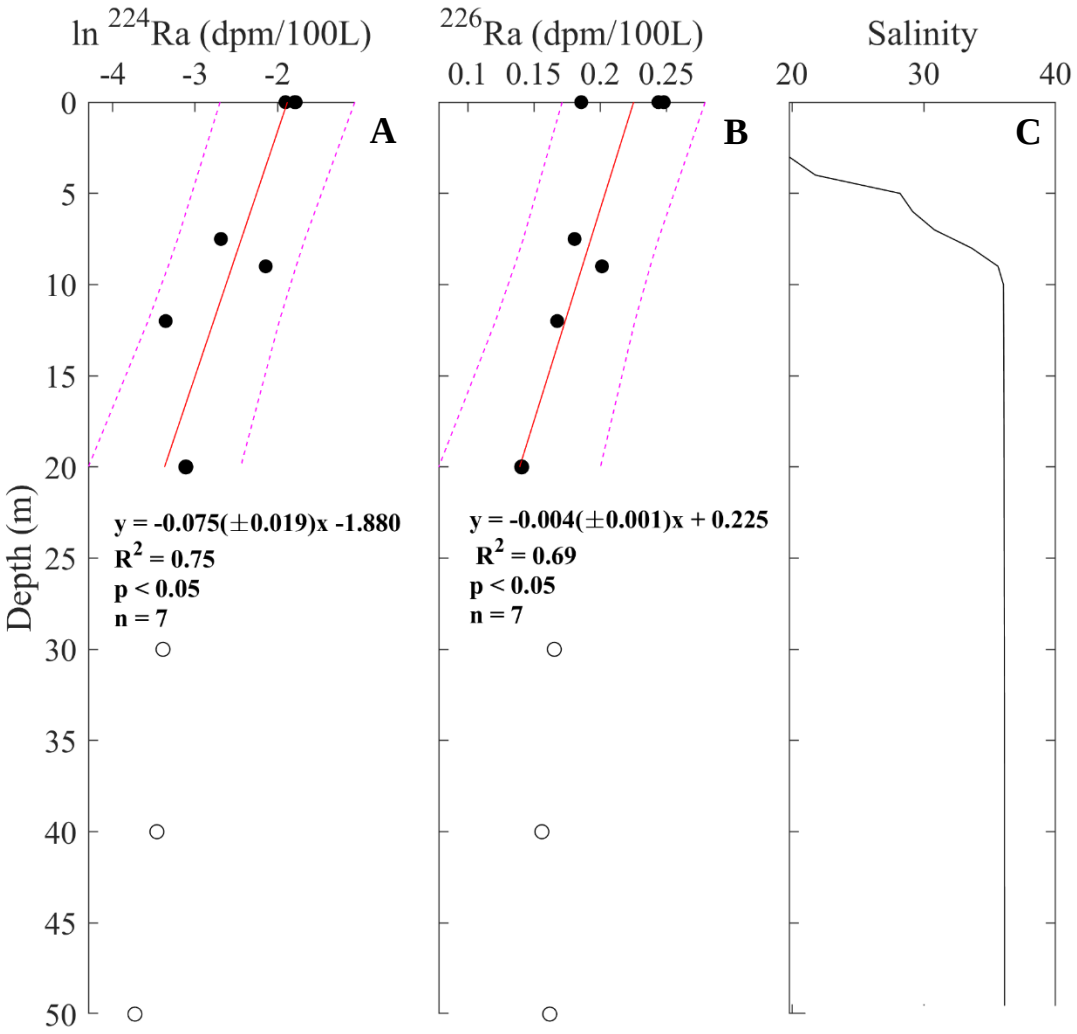

Figure 16. Depth profiles for EN614 station 17, casts 1, 3 and 9 combined. **A.)** $\ln^{224}Ra$ activity depth profile with best-fit line is shown in red with its 95% prediction interval. Black circles indicate the measurements that were used in the mixing analysis while open black circles are measurements were excluded. **B.)** Ra-226 activity depth profile with best-fit line is shown in red with its 95% prediction interval to validate the conservative mixing assumption. **C.)** Average salinity profile of the three casts measured via CTD. A summary of fit statistics for K_h values is shown in Table 5,

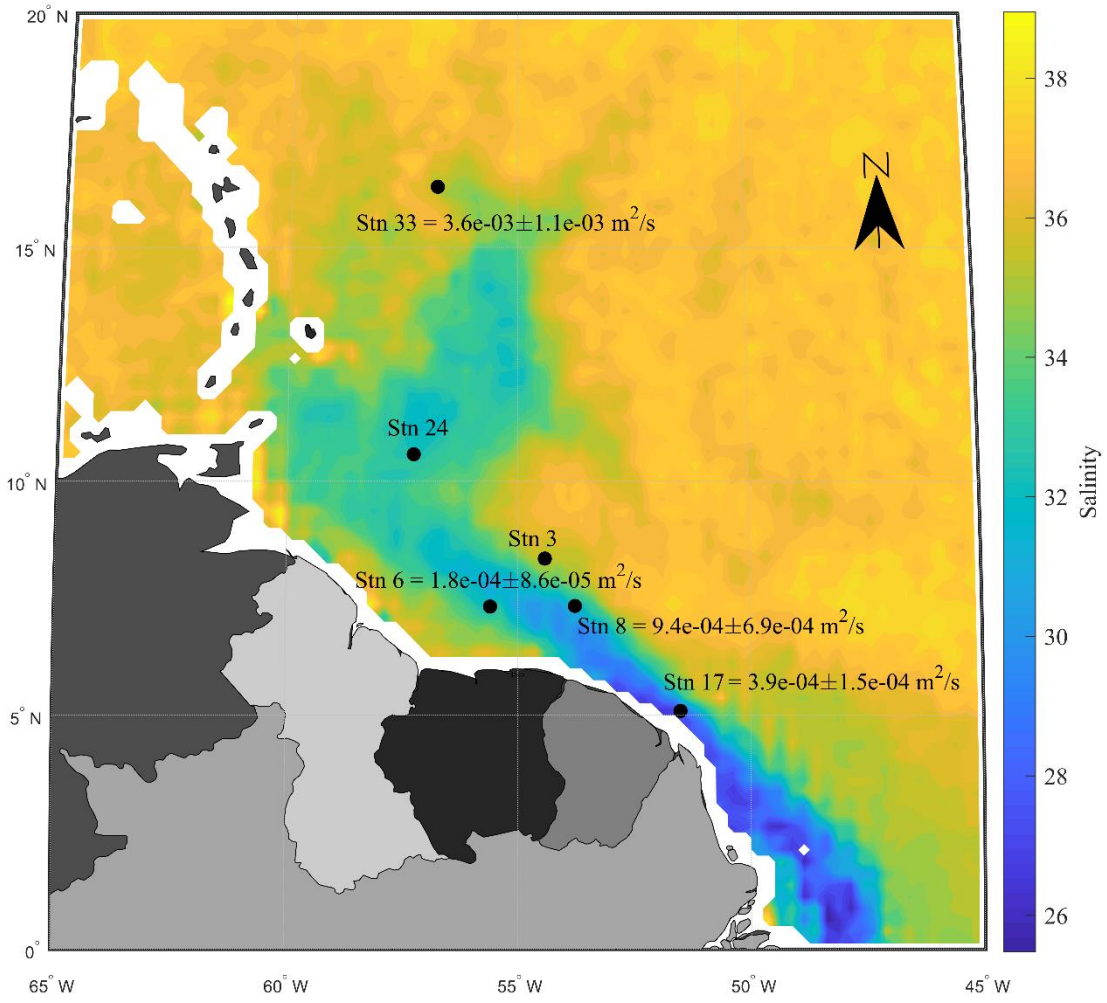

Figure 17. Eddy diffusion coefficients (K_h) shown spatially for EN614 vertical mixing profiles (Results shown in Table 5). K_h is not shown for profiles that failed to meet the criteria necessary for the model to hold. Sea surface salinity for the duration of the cruise is shown to depict the plume region. A summary of fit-statistics for K_h values is shown in Table 5.

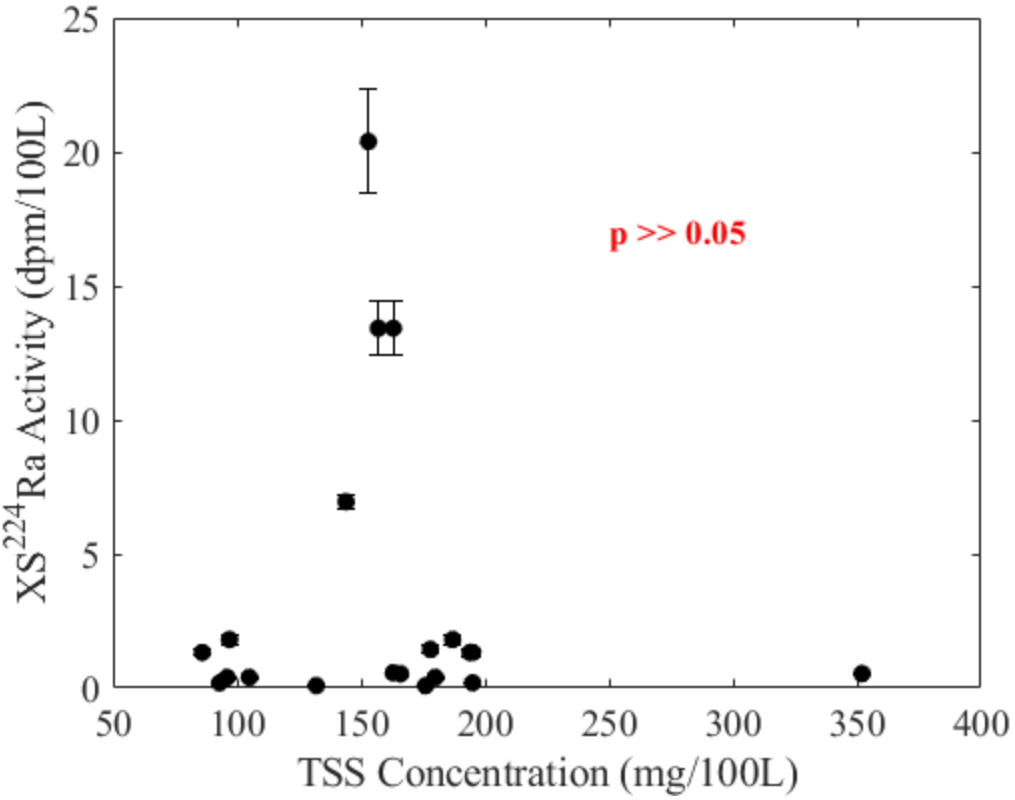

Figure 18. Total Suspended Solids (TSS) concentration plotted with the excess ^{224}Ra activity of the corresponding water sample. P-value > 0.05 indicates no significant relationship.

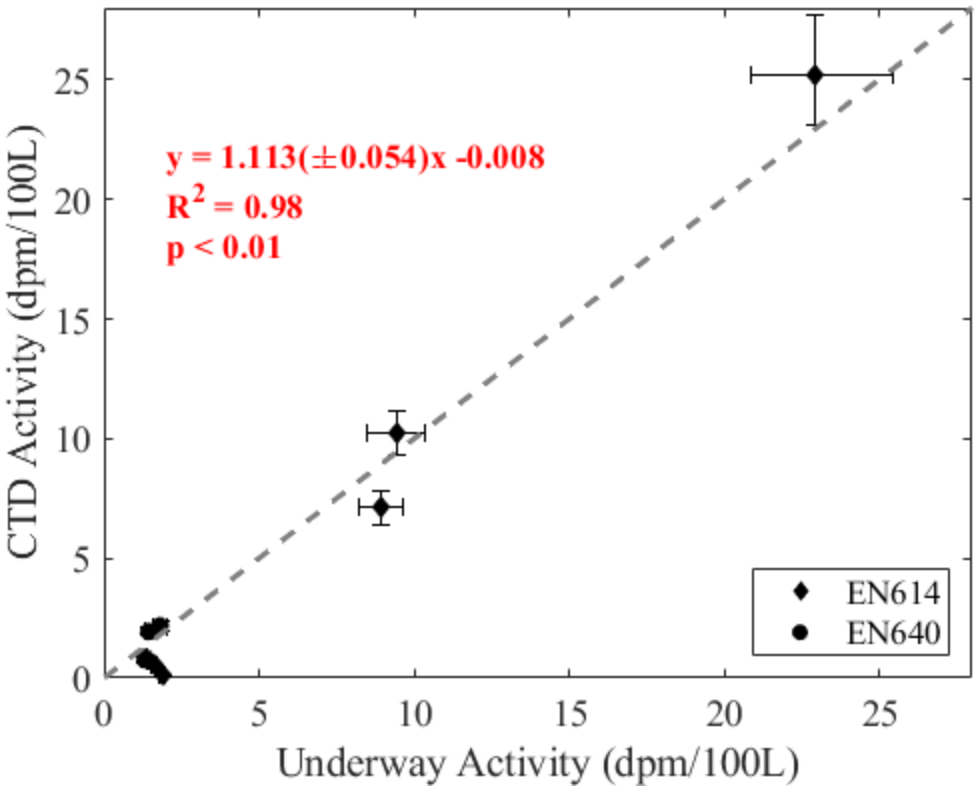

Figure 19. Excess ^{224}Ra activity comparison between the underway seawater system and the CTD samples taken at the same station, within 8 hours or less from both cruises. Relationship statistics calculated by the best-fit dashed gray line. P-value <0.01 indicates no significant difference.

Appendices

Appendix A: Metadata. Sample collection metadata for EN614 (**A1**) and EN640 (**A2**). U or C identifies the sample collection method; 'U' for the shipboard underway system or 'C' for CTD water column samples (*indicates sample was collected via bucket from the sea surface). Event code represents the station number and cast for each sample, the naming convention is used for all data types collected on these cruises. NaN values indicate missing data.

Appendix A1: EN614 Metadata.

U/C	Event Code	Collection Date Time	Latitude	Longitude	Depth	Salinity	Volume
		EST	decimal	decimal	m		L
C	001.01	5/6/18 13:45	11.247150	-56.323600	250	35.42	18.52
C	001.01	5/6/18 13:45	11.247150	-56.323600	200	36.01	17.09
C	001.01	5/6/18 13:45	11.247150	-56.323600	150	36.54	18.16
C	001.01	5/6/18 13:45	11.247150	-56.323600	98	36.94	17.45
C	001.01	5/6/18 13:45	11.247150	-56.323600	75	36.02	18.16
C	001.01	5/6/18 13:45	11.247150	-56.323600	50	35.99	18.16
C	001.01	5/6/18 13:45	11.247150	-56.323600	20	31.34	18.87
C	001.01	5/6/18 13:45	11.247150	-56.323600	10	30.71	17.80
C*	001.01	5/6/18 13:45	11.247150	-56.323600	0	30.71	17.09
U	002.01	5/7/18 8:37	9.830200	-54.378317	0	36.12	17.62
U	002.02	5/7/18 9:20	9.649050	-54.385067	0	36.04	16.56
U	002.04	5/7/18 11:02	9.379483	-54.394550	0	36.05	17.80
U	002.06	5/7/18 12:27	9.156267	-54.400067	0	34.95	17.62
U	002.08	5/7/18 13:07	9.065167	-54.406017	0	33.69	17.45
U	002.09	5/7/18 14:13	8.895300	-54.405200	0	32.70	17.98
U	002.10	5/7/18 16:06	8.607467	-54.406917	0	32.34	17.80
C	003.03	5/8/18 19:44	8.347633	-54.411533	250	35.17	17.80
C	003.03	5/8/18 19:44	8.347633	-54.411533	200	35.76	17.62
C	003.03	5/8/18 19:44	8.347633	-54.411533	75	36.27	17.62
C	003.03	5/8/18 19:44	8.347633	-54.411533	100	36.28	17.27
C	003.03	5/8/18 19:44	8.347633	-54.411533	75	36.27	18.52
C	003.03	5/8/18 19:44	8.347633	-54.411533	50	36.18	17.98
C	003.03	5/8/18 19:44	8.347633	-54.411533	25	32.79	17.80
C	003.03	5/8/18 19:44	8.347633	-54.411533	10	32.76	13.53
C	003.03	5/8/18 19:44	8.347633	-54.411533	0	32.75	12.99

C	003.07	5/9/18 9:10	8.575150	-54.518067	75	36.26	17.09
C	003.07	5/9/18 9:10	8.575150	-54.518067	50	36.19	13.17
C	003.07	5/9/18 9:10	8.575150	-54.518067	33	35.83	11.39
C	003.07	5/9/18 9:10	8.575150	-54.518067	10	33.57	13.71
C	003.07	5/9/18 9:10	8.575150	-54.518067	0	33.57	14.95
C	003.09	5/9/18 19:31	8.499050	-54.772400	28	35.15	18.52
C	003.09	5/9/18 19:31	8.499050	-54.772400	10	32.63	18.52
C	003.13	5/10/18 10:02	8.605317	-54.086167	110	36.27	15.31
C	003.13	5/10/18 10:02	8.605317	-54.086167	29	35.06	16.20
C	003.13	5/10/18 10:02	8.605317	-54.086167	0	33.05	32.58
U	004.01	5/9/18 20:28	8.575617	-55.310500	0	32.06	17.80
U	004.02	5/9/18 20:40	8.464300	-55.365517	0	31.42	17.80
U	004.03	5/9/18 21:06	8.239100	-55.431833	0	31.21	17.80
U	004.04	5/9/18 22:03	8.188850	-55.509433	0	31.80	17.62
U	004.05	5/9/18 23:04	8.056833	-55.607083	0	31.61	17.09
U	004.06	5/10/18 0:06	7.935517	-55.682533	0	31.28	17.45
U	004.07	5/10/18 1:05	7.806867	-55.721567	0	30.64	17.45
U	004.08	5/10/18 2:05	7.674967	-55.741133	0	31.00	18.16
U	004.09	5/10/18 3:07	7.560650	-55.694683	0	31.24	17.62
U	004.10	5/10/18 4:05	7.439550	-55.638083	0	31.42	18.34
U	004.11	5/10/18 5:06	7.319783	-55.582950	0	31.74	17.09
U	004.12	5/10/18 6:11	7.188217	-55.525800	0	32.02	18.16
U	004.13	5/10/18 7:01	7.082900	-55.481850	0	32.22	17.45
U	004.14	5/10/18 8:06	6.946900	-55.426750	0	32.06	17.27
U	004.15	5/10/18 9:08	6.978850	-55.451317	0	31.88	17.45
U	004.16	5/10/18 10:07	7.101750	-55.498150	0	31.87	17.27
C	006.01	5/11/18 11:37	7.322983	-55.592933	110	36.58	15.84
C	006.01	5/11/18 11:37	7.322983	-55.592933	85	36.41	17.80
C	006.01	5/11/18 11:37	7.322983	-55.592933	50	36.22	14.24
C	006.01	5/11/18 11:37	7.322983	-55.592933	27	36.08	15.31
C	006.01	5/11/18 11:37	7.322983	-55.592933	10	32.14	13.53
C	006.01	5/11/18 11:37	7.322983	-55.592933	0	31.84	17.09
U	007.01	5/10/18 20:08	7.339367	-55.350050	0	29.71	18.14
U	007.02	5/10/18 21:40	7.328350	-55.233117	0	29.09	17.62
U	007.03	5/10/18 21:59	7.313000	-55.111633	0	28.40	17.25
U	007.04	5/10/18 22:58	7.316350	-54.984950	0	27.81	17.27
U	007.05	5/11/18 0:05	7.326917	-54.257217	0	27.39	16.89
U	007.06	5/11/18 0:21	7.328083	-54.801600	0	27.29	16.89
U	007.07	5/11/18 1:17	7.329633	-54.695783	0	27.19	18.52
U	007.08	5/11/18 2:47	7.298583	-54.535417	0	27.57	17.78
U	007.09	5/11/18 4:25	7.335250	-54.327450	0	28.37	17.62
U	007.10	5/11/18 5:11	7.331983	-54.222433	0	28.48	16.89
U	007.11	5/11/18 6:10	7.327917	-54.098433	0	28.52	17.45

U	007.12	5/11/18 7:09	7.319250	-53.973483	0	28.30	17.25
U	007.13	5/11/18 8:06	7.320317	-53.841767	0	28.49	17.45
C	008.01	5/12/18 10:07	7.335400	-53.764317	100	36.46	18.52
C	008.01	5/12/18 10:07	7.335400	-53.764317	70	36.45	17.98
C	008.01	5/12/18 10:07	7.335400	-53.764317	45	36.16	14.24
C	008.01	5/12/18 10:07	7.335400	-53.764317	19	34.69	10.86
C	008.01	5/12/18 10:07	7.335400	-53.764317	10	30.14	13.88
C	008.01	5/12/18 10:07	7.335400	-53.764317	0	30.14	16.02
C	008.02	5/12/18 12:24	7.361633	-53.810600	203	35.60	17.40
C	008.02	5/12/18 12:24	7.361633	-53.810600	193	35.62	17.04
C	008.02	5/12/18 12:24	7.361633	-53.810600	150	35.83	17.75
C	008.02	5/12/18 12:24	7.361633	-53.810600	125	36.16	17.22
U	009.01	5/11/18 15:59	7.394817	-53.720017	0	28.61	17.42
U	009.02	5/11/18 17:09	7.392350	-53.591983	0	28.92	17.09
U	009.03	5/11/18 18:12	7.391983	-53.460533	0	29.55	17.25
U	009.04	5/11/18 19:04	7.393733	-53.324883	0	31.21	16.91
U	009.05	5/11/18 20:15	7.395550	-53.182750	0	31.99	17.42
U	009.06	5/11/18 21:01	7.398150	-53.063883	0	32.38	16.73
U	009.07	5/11/18 22:05	7.399717	-52.921200	0	32.88	17.07
U	009.08	5/11/18 23:01	7.401583	-52.782283	0	32.09	17.45
U	009.09	5/11/18 23:55	7.425367	-52.637983	0	35.25	17.07
U	009.10	5/12/18 1:00	7.428483	-52.504717	0	35.39	17.80
U	009.11	5/12/18 2:00	7.413783	-52.376583	0	35.48	17.62
U	009.12	5/12/18 3:20	7.409950	-52.230133	0	35.55	17.27
U	009.13	5/12/18 4:13	7.399217	-52.098067	0	35.51	17.62
U	009.14	5/12/18 5:13	7.381783	-51.952333	0	35.49	17.09
U	009.15	5/12/18 6:12	7.367600	-51.815700	0	35.49	17.80
U	009.16	5/12/18 7:07	7.352117	-51.678833	0	35.46	17.45
U	009.17	5/12/18 8:04	7.349317	-51.540017	0	35.44	17.09
U	009.18	5/12/18 9:07	7.347550	-51.400600	0	35.06	17.42
U	009.19	5/12/18 10:07	7.346117	-51.254483	0	35.21	17.45
U	009.20	5/12/18 11:05	7.345150	-51.106800	0	35.02	17.27
C	010.04	5/13/18 18:25	7.397017	-50.880400	77	36.13	47.89
C	010.04	5/13/18 18:25	7.397017	-50.880400	0	35.89	54.48
U	011.01	5/12/18 12:03	6.781750	-50.559167	0	35.22	18.52
U	011.02	5/12/18 15:45	6.288883	-50.459317	0	35.03	17.80
U	011.03	5/12/18 18:14	5.994033	-50.730533	0	34.94	16.73
U	011.06	5/12/18 22:32	5.421817	-51.241800	0	34.27	17.62
U	011.07	5/12/18 23:29	5.285467	-51.338433	0	31.50	17.80
U	011.08	5/13/18 12:15	5.355483	-51.416683	0	26.51	17.98
U	011.09	5/13/18 1:10	5.097117	-51.496400	0	20.77	17.98
C	012.01	5/14/18 14:50	4.890333	-51.718867	35	36.12	15.67
C	012.01	5/14/18 14:50	4.890333	-51.718867	20	36.12	17.62

C	012.01	5/14/18 14:50	4.890333	-51.718867	7	26.71	17.45
C	012.01	5/14/18 14:50	4.890333	-51.718867	0	15.88	17.80
C	017.01	5/15/18 5:55	5.093117	-51.505817	12	35.92	18.34
C	017.01	5/15/18 5:55	5.093117	-51.505817	0	22.81	17.27
C	017.03	5/15/18 9:22	5.100817	-51.525350	50	36.13	18.16
C	017.03	5/15/18 9:22	5.100817	-51.525350	30	36.12	17.27
C	017.03	5/15/18 9:22	5.100817	-51.525350	9	35.64	17.80
C	017.03	5/15/18 9:22	5.100817	-51.525350	0	19.79	14.95
C	017.90	5/16/18 9:38	5.527867	-52.191600	40	36.13	16.38
C	017.90	5/16/18 9:38	5.527867	-52.191600	20	36.12	30.80
C	017.90	5/16/18 9:38	5.527867	-52.191600	7.5	31.44	28.66
C	017.90	5/16/18 9:38	5.527867	-52.191600	0	22.15	34.54
U	018.01	5/15/18 19:58	5.684967	-52.283133	0	26.69	17.45
U	018.02	5/15/18 22:08	5.687967	-52.118217	0	28.61	17.80
U	018.03	5/16/18 0:24	5.699167	-51.958800	0	30.24	17.45
U	018.04	5/16/18 2:25	5.713400	-51.799567	0	32.58	17.27
U	018.05	5/16/18 5:03	5.602483	-51.572500	0	34.06	36.85
U	018.06	5/16/18 6:47	5.479850	-51.696650	0	30.78	17.80
U	018.07	5/16/18 8:31	5.346267	-51.808817	0	26.83	18.52
U	018.08	5/16/18 10:04	5.230550	-51.927433	0	25.97	36.67
U	018.09	5/16/18 12:34	5.137400	-52.017700	0	24.20	34.36
U	019.01	5/17/18 17:00	5.176750	-52.173617	0	23.74	17.96
U	019.02	5/17/18 18:04	5.356383	-52.203367	0	23.48	16.71
U	019.03	5/17/18 19:07	5.552550	-52.238350	0	23.46	17.42
U	019.04	5/17/18 19:24	5.610183	-52.243517	0	24.31	17.42
U	019.05	5/17/18 19:52	5.700317	-52.260217	0	25.06	17.42
U	019.06	5/17/18 20:22	5.796500	-52.256317	0	26.30	17.96
U	019.07	5/17/18 20:43	5.857583	-52.259783	0	27.00	17.96
U	019.08	5/17/18 21:18	5.982933	-52.273383	0	28.01	16.89
U	019.09	5/17/18 21:49	6.087267	-52.285200	0	29.00	17.60
U	019.10	5/17/18 22:24	6.199967	-52.297467	0	30.01	17.42
U	019.11	5/17/18 22:55	6.296150	-52.309500	0	31.01	17.60
U	019.12	5/17/18 23:46	6.437650	-52.337633	0	32.00	17.60
U	019.13	5/18/18 0:35	6.588967	-52.377133	0	32.99	17.42
U	019.15	5/18/18 2:09	6.835567	-52.420283	0	33.09	17.25
C	020.02	5/18/18 7:45	7.450600	-52.510333	275	35.33	17.75
C	020.02	5/18/18 7:45	7.450600	-52.510333	150	36.32	17.75
C	020.02	5/18/18 7:45	7.450600	-52.510333	125	36.53	17.86
C	020.03	5/18/18 10:48	7.454800	-52.500250	110	36.45	16.38
C	020.03	5/18/18 10:48	7.454800	-52.500250	95	36.15	14.24
C	020.03	5/18/18 10:48	7.454800	-52.500250	75	36.09	16.91
C	020.03	5/18/18 10:48	7.454800	-52.500250	50	35.91	16.56
C	020.03	5/18/18 10:48	7.454800	-52.500250	20	35.90	17.98

C	020.03	5/18/18 10:48	7.454800	-52.500250	0	35.90	14.42
U	021.01	5/18/18 19:06	7.717400	-52.913350	0	35.10	17.07
U	021.05	5/18/18 23:03	8.098600	-53.516483	0	35.12	17.09
U	021.17	5/19/18 11:00	9.234067	-55.354983	0	35.14	17.80
C	022.01	5/19/18 19:12	9.897217	-56.211300	150	36.31	18.82
C	022.01	5/19/18 19:12	9.897217	-56.211300	75	36.10	17.75
C	022.01	5/19/18 19:12	9.897217	-56.211300	60	36.00	18.11
C	022.01	5/19/18 19:12	9.897217	-56.211300	50	35.99	17.45
C	022.01	5/19/18 19:12	9.897217	-56.211300	25	34.05	17.80
C	022.01	5/19/18 19:12	9.897217	-56.211300	0	33.90	18.34
C	022.06	5/20/18 8:34	10.006833	-56.243317	70	36.17	14.42
C	022.06	5/20/18 8:34	10.006833	-56.243317	45	36.00	16.73
C	022.06	5/20/18 8:34	10.006833	-56.243317	30	34.55	16.73
C	022.06	5/20/18 8:34	10.006833	-56.243317	15	34.16	12.46
C	022.06	5/20/18 8:34	10.006833	-56.243317	0	34.15	15.49
C	022.08	5/20/18 11:20	10.039450	-56.237350	0	33.77	18.34
C	022.08	5/20/18 11:20	10.039450	-56.237350	15	33.87	17.09
C	022.08	5/20/18 11:20	10.039450	-56.237350	30	34.46	17.80
U	023.01	5/19/18 16:09	10.175850	-56.318783	0	33.20	17.60
U	023.02	5/19/18 17:09	10.240417	-56.477500	0	32.35	17.25
U	023.03	5/19/18 17:36	10.266750	-56.538467	0	31.22	17.25
U	023.04	5/19/18 18:07	10.303533	-56.629283	0	30.16	17.42
U	023.05	5/19/18 19:22	10.369400	-56.801983	0	30.16	17.45
U	023.06	5/19/18 19:58	10.431567	-56.958550	0	29.62	17.45
U	023.07	5/19/18 20:28	10.464450	-57.032400	0	29.12	17.25
U	023.08	5/19/18 21:33	10.540500	-57.203950	0	28.81	17.45
C	024.04	5/21/18 8:14	10.576983	-57.256700	35	36.02	15.31
C	024.04	5/21/18 8:14	10.576983	-57.256700	18	32.33	11.75
C	024.04	5/21/18 8:14	10.576983	-57.256700	10	29.66	13.53
C	024.04	5/21/18 8:14	10.576983	-57.256700	0	29.60	13.53
C*	024.04	5/21/18 8:14	10.576983	-57.256700	0	29.60	18.16
C	025.01	5/24/18 12:35	13.003583	-55.914067	50	36.19	16.02
C	025.01	5/24/18 12:35	13.003583	-55.914067	34	35.76	16.91
C	025.01	5/24/18 12:35	13.003583	-55.914067	20	32.58	13.88
C	025.01	5/24/18 12:35	13.003583	-55.914067	10	32.55	14.60
C	025.01	5/24/18 12:35	13.003583	-55.914067	0	32.55	15.31
C	025.03	5/24/18 15:09	13.024133	-55.906383	75	36.23	17.09
C	025.03	5/24/18 15:09	13.024133	-55.906383	50	36.15	11.75
C	025.03	5/24/18 15:09	13.024133	-55.906383	24	32.70	34.89
C	025.03	5/24/18 15:09	13.024133	-55.906383	0	32.57	34.54
C	025.06	5/24/18 17:40	13.052750	-55.884150	250	35.82	35.56
U	026.01	5/22/18 20:37	13.060383	-55.708033	0	32.55	17.60
U	026.04	5/22/18 23:34	13.033017	-55.238350	0	31.21	18.16

U	026.05	5/23/18 0:38	13.028050	-55.056450	0	30.75	16.89
U	026.06	5/23/18 0:58	13.028317	-54.997400	0	31.91	17.25
U	026.07	5/23/18 1:33	13.027950	-54.893400	0	32.65	17.07
U	026.10	5/23/18 3:47	13.029000	-54.576550	0	32.95	17.25
U	026.11	5/23/18 4:09	13.028017	-54.484333	0	33.99	17.60
U	026.12	5/23/18 4:26	13.027917	-54.445500	0	34.97	17.60
U	026.13	5/23/18 5:07	13.030117	-54.308367	0	35.95	35.41
C	027.03	5/25/18 11:12	13.000783	-53.840067	90	36.29	35.61
C	027.03	5/25/18 11:12	13.000783	-53.840067	0	36.28	34.89
U	028.02	5/23/18 18:49	13.198683	-54.048250	0	35.97	17.96
U	028.11	5/24/18 2:34	14.010300	-55.092650	0	31.86	17.27
C	031.02	5/26/18 8:35	14.591517	-55.329000	0	30.78	16.56
C	031.02	5/26/18 8:35	14.591517	-55.329000	10	30.78	13.71
C	031.02	5/26/18 8:35	14.591517	-55.329000	25	33.54	16.56
C	031.03	5/26/18 11:10	14.588283	-55.333250	27	33.53	35.96
C	031.03	5/26/18 11:10	14.588283	-55.333250	0	30.83	35.25
C	031.08	5/26/18 19:05	14.612117	-55.296400	250	36.30	26.24
C	031.08	5/26/18 19:05	14.612117	-55.296400	150	36.96	28.74
C	031.08	5/26/18 19:05	14.612117	-55.296400	125	36.74	18.77
C	031.08	5/26/18 19:05	14.612117	-55.296400	100	36.52	28.92
C	031.08	5/26/18 19:05	14.612117	-55.296400	75	36.21	18.77
C	031.11	5/27/18 6:57	14.646783	-55.291250	39	35.88	35.61
C	031.11	5/27/18 6:57	14.646783	-55.291250	0	31.13	34.71
C	031.12	5/27/18 8:40	14.646633	-55.300300	65	36.14	16.73
C	031.12	5/27/18 8:40	14.646633	-55.300300	45	36.02	14.95
C	031.12	5/27/18 8:40	14.646633	-55.300300	15	31.14	13.53
C	031.16	5/27/18 18:09	14.682283	-55.295917	75	NaN	29.91
C	031.20	5/28/18 8:35	14.752267	-55.281783	65	36.16	15.67
C	031.20	5/28/18 8:35	14.752267	-55.281783	46	36.04	15.67
C	031.20	5/28/18 8:35	14.752267	-55.281783	25	33.73	14.24
C	031.20	5/28/18 8:35	14.752267	-55.281783	0	31.10	14.60
C	031.21	5/28/18 10:50	14.751717	-55.281967	12	31.09	17.80
U	032.03	5/26/18 23:28	15.115917	-55.563717	0	30.90	18.16
U	032.09	5/27/18 5:35	15.908033	-56.388950	0	31.19	17.80
C	033.01	5/29/18 8:57	16.292350	-56.775300	100	36.96	14.24
C	033.01	5/29/18 8:57	16.292350	-56.775300	75	36.56	14.24
C	033.01	5/29/18 8:57	16.292350	-56.775300	50	36.12	16.73
C	033.01	5/29/18 8:57	16.292350	-56.775300	25	35.33	15.31
C	033.01	5/29/18 8:57	16.292350	-56.775300	10	32.02	13.17
C	033.01	5/29/18 8:57	16.292350	-56.775300	0	32.00	15.67
C	033.02	5/29/18 11:00	16.284667	-56.783283	0	31.89	35.25
C	033.02	5/29/18 11:00	16.284667	-56.783283	50	36.09	34.18

Appendix A2: EN640 Metadata.

U/C	Event Code	Collection Date Time EST	Latitude decimal	Longitude decimal	Depth m	Salinity	Volume L
U	001.16	6/14/19 6:26	12.116050	57.211867	0	31.56	17.80
U	001.17	6/14/19 7:28	12.057133	57.061850	0	31.56	17.80
U	001.18	6/14/19 8:29	11.994750	56.908050	0	31.50	17.45
U	001.19	6/14/19 9:31	11.939067	56.754283	0	31.96	17.45
U	001.20	6/14/19 10:31	11.893283	56.589917	0	33.67	17.80
U	001.21	6/14/19 11:24	11.843867	56.433817	0	33.27	18.52
U	001.22	6/14/19 12:23	11.798633	56.287083	0	33.36	17.80
U	001.23	6/14/19 13:27	11.743200	56.131000	0	31.51	18.52
U	001.24	6/14/19 14:36	11.683000	55.968350	0	30.40	18.34
U	001.25	6/14/19 15:50	11.637767	55.836500	0	29.79	18.52
U	001.26	6/14/19 16:47	11.578867	55.670317	0	29.06	18.16
U	001.27	6/14/19 17:55	11.531183	55.536200	0	28.56	18.87
U	001.28	6/14/19 18:38	11.476767	55.380083	0	28.32	17.62
U	001.29	6/14/19 19:34	11.425667	55.223867	0	28.23	17.80
U	001.30	6/14/19 20:33	11.371400	55.068250	0	28.11	18.34
U	001.31	6/14/19 21:31	11.307150	54.910700	0	27.72	17.27
C	002.01	6/14/19 0:24	11.287433	54.817383	500	34.89	16.73
C	002.01	6/14/19 0:34	11.287433	54.817383	250	35.63	18.52
C	002.01	6/14/19 0:22	11.287433	54.817383	150	36.78	15.31
C	002.01	6/14/19 0:34	11.287433	54.817383	115	37.06	18.52
C	002.01	6/14/19 0:04	11.287433	54.817383	97	36.42	7.47
C	002.01	6/14/19 2:25	11.287433	54.817383	80	36.40	17.80
C	002.01	6/14/19 2:25	11.287433	54.817383	55	36.02	18.16
C	002.01	6/14/19 1:36	11.287433	54.817383	35	34.89	17.45
C	002.01	6/14/19 0:23	11.287433	54.817383	15	29.33	11.03
C	002.01	6/14/19 0:34	11.287433	54.817383	10	27.53	14.24
C	002.01	6/14/19 0:45	11.287433	54.817383	0	27.50	17.80
U	003.01	6/15/19 1:53	11.129067	54.668783	0	27.32	17.80
U	003.02	6/15/19 2:42	11.006367	54.554233	0	26.96	17.80
U	003.03	6/15/19 3:36	10.883117	54.440750	0	26.82	18.52
U	003.04	6/15/19 4:42	10.756033	54.321583	0	27.12	18.16
U	003.05	6/15/19 5:56	10.633850	54.205683	0	27.72	16.73
U	003.06	6/15/19 6:44	10.641667	54.092000	0	27.94	17.80
U	003.07	6/15/19 7:30	10.379617	53.979750	0	28.56	17.80
U	003.08	6/15/19 8:27	10.246467	53.874717	0	28.47	18.87
U	003.09	6/15/19 9:31	10.108000	53.767000	0	28.47	18.16
U	003.10	6/15/19 10:39	9.974317	53.652317	0	29.34	18.69
U	003.11	6/15/19 11:28	9.857383	53.549917	0	30.58	17.45

U	003.12	6/15/19 12:33	9.725517	53.412417	0	31.31	17.45
U	003.13	6/15/19 13:34	9.595617	53.287800	0	31.68	17.80
U	003.14	6/15/19 14:34	9.465917	53.157800	0	31.68	17.09
U	003.15	6/15/19 15:30	9.338550	53.034233	0	31.74	18.16
U	003.16	6/15/19 16:30	9.199200	52.909467	0	31.28	18.52
U	003.17	6/15/19 17:30	9.062650	52.789300	0	30.98	18.16
U	003.18	6/15/19 18:34	8.919233	52.658333	0	32.55	18.52
U	003.19	6/15/19 19:30	8.788933	52.541133	0	34.62	18.16
U	003.20	6/15/19 20:34	8.664167	52.426050	0	34.99	18.16
U	003.21	6/15/19 21:33	8.530033	52.316183	0	35.61	18.52
U	003.22	6/15/19 22:43	8.391150	52.200683	0	35.64	17.80
U	003.23	6/15/19 23:35	8.255183	52.087267	0	35.73	17.80
U	003.24	6/15/19 0:38	8.117517	51.970600	0	35.72	18.16
U	003.25	6/16/19 1:40	7.990933	51.853067	0	35.71	17.45
U	003.26	6/16/19 2:45	7.864083	51.720067	0	35.69	17.45
U	003.27	6/16/19 3:41	7.745417	51.621433	0	35.62	17.80
U	003.28	6/16/19 4:38	7.617217	51.490333	0	35.30	17.45
U	003.29	6/16/19 5:34	7.493550	51.390667	0	35.22	17.45
U	003.30	6/16/19 6:27	7.355417	51.261517	0	34.14	18.16
U	003.31	6/16/19 7:34	7.252350	51.157333	0	33.80	18.52
U	003.32	6/16/19 8:28	7.125717	51.051283	0	32.82	18.16
U	003.33	6/16/19 9:26	7.011283	50.950100	0	32.36	17.80
U	003.34	6/16/19 10:29	7.874617	50.827133	0	32.14	18.52
U	003.35	6/16/19 11:24	6.759683	50.728883	0	33.50	18.16
U	003.36	6/16/19 12:29	6.626417	50.615183	0	34.69	17.80
U	003.37	6/16/19 13:30	6.494683	50.497767	0	34.53	17.80
C	004.01	6/16/19 16:52	6.385050	50.398317	500	34.66	11.61
C	004.01	6/16/19 17:02	6.385050	50.398317	250	35.07	7.72
C	004.01	6/16/19 17:26	6.385050	50.398317	75	36.02	18.52
C	004.01	6/16/19 17:35	6.385050	50.398317	53	35.99	17.80
C	004.01	6/16/19 17:35	6.385050	50.398317	40	35.80	16.73
C	004.01	6/16/19 17:28	6.385050	50.398317	30	35.68	12.10
C	004.01	6/16/19 17:33	6.385050	50.398317	15	35.65	18.16
C	004.01	6/16/19 17:00	6.385050	50.398317	0	35.65	8.90
C	004.03	6/16/19 19:25	6.389517	50.393717	150	36.25	19.23
C	004.03	6/16/19 19:23	6.389517	50.393717	100	36.05	18.52
C	004.03	6/16/19 19:36	6.389517	50.393717	65	35.99	18.16
C	004.03	6/16/19 20:17	6.389517	50.393717	30	35.68	19.23
C	004.03	6/16/19 20:02	6.389517	50.393717	15	35.68	18.52
C	004.03	6/16/19 20:17	6.389517	50.393717	0	35.68	18.69
U	005.01	6/16/19 21:50	6.288583	50.489200	0	35.59	18.16
U	005.02	6/16/19 22:42	6.163417	50.599633	0	34.94	18.87
U	005.03	6/16/19 23:35	6.043417	50.717117	0	32.00	18.87

U	005.04	6/17/19 0:37	5.925867	50.829233	0	31.72	18.16
U	005.05	6/17/19 1:46	5.812750	50.919450	0	23.88	18.87
U	005.06	6/17/19 2:58	5.691867	51.011733	0	15.49	18.16
U	005.07	6/17/19 3:56	5.583833	51.100050	0	13.00	18.16
U	005.08	6/17/19 4:40	5.469217	51.193367	0	12.62	19.58
U	005.09	6/17/19 5:36	5.360917	51.287817	0	13.20	18.34
U	005.10	6/17/19 6:52	5.255067	51.393567	0	14.50	18.52
U	005.11	6/17/19 8:45	5.141767	51.483033	0	17.94	18.16
U	005.12	6/17/19 11:40	4.995050	51.595417	0	23.11	18.87
C	006.01	6/17/19 12:47	4.876733	51.702683	35	36.22	37.72
C	006.01	6/17/19 12:07	4.876733	51.702683	13	36.07	38.13
C	006.01	6/17/19 13:18	4.876733	51.702683	0	15.66	38.48
C	006.03	6/17/19 16:00	5.112000	51.508800	58	36.49	18.87
C	006.03	6/17/19 14:41	5.112000	51.508800	35	36.27	18.52
C	006.03	6/17/19 15:25	5.112000	51.508800	15	36.00	18.87
C	006.04	6/17/19 17:43	5.222367	51.392450	60	36.49	17.98
C	006.04	6/17/19 19:11	5.222367	51.392450	30	36.10	18.69
C	006.04	6/17/19 18:26	5.222367	51.392450	10	34.72	18.87
C	006.04	6/17/19 18:06	5.222367	51.392450	0	17.27	17.80
C	006.05	6/17/19 19:00	5.326250	51.301117	74	36.51	18.87
C	006.05	6/17/19 18:25	5.326250	51.301117	35	36.07	18.69
C	006.05	6/17/19 18:32	5.326250	51.301117	10	35.56	18.16
C	006.05	6/17/19 19:04	5.326250	51.301117	0	16.43	18.16
C	006.06	6/17/19 19:36	5.430300	51.213583	85	36.46	18.87
C	006.06	6/17/19 19:36	5.430300	51.213583	40	36.09	18.87
C	006.06	6/17/19 19:48	5.430300	51.213583	9	35.03	18.87
C	006.06	6/17/19 19:55	5.430300	51.213583	0	16.46	18.87
C	006.07	6/17/19 23:39	5.518333	51.110383	102	36.47	18.87
C	006.07	6/17/19 23:27	5.518333	51.110383	50	36.12	18.52
C	006.07	6/17/19 23:44	5.518333	51.110383	10	35.79	18.87
C	006.07	6/17/19 23:44	5.518333	51.110383	0	15.66	17.80
C	007.02	6/18/19 10:56	5.716167	50.985633	100	36.28	17.80
C	007.02	6/18/19 11:01	5.716167	50.985633	50	36.10	18.52
C	007.02	6/18/19 10:59	5.716167	50.985633	30	36.06	14.24
C	007.02	6/18/19 11:01	5.716167	50.985633	15	35.85	16.38
C	007.02	6/18/19 11:05	5.716167	50.985633	8	35.57	18.16
C	007.02	6/18/19 11:05	5.716167	50.985633	0	17.18	13.17
C	007.03	6/18/19 13:12	5.763383	50.984683	23	35.94	18.16
C	007.03	6/18/19 14:02	5.763383	50.984683	5	21.64	32.36
C	007.06	6/18/19 21:20	5.906600	51.043000	110	36.47	18.16
C	007.06	6/18/19 21:30	5.906600	51.043000	100	36.35	18.52
C	007.06	6/18/19 21:32	5.906600	51.043000	90	36.12	18.87
C	007.06	6/18/19 21:25	5.906600	51.043000	70	36.11	13.53

C	007.06	6/18/19 21:34	5.906600	51.043000	50	36.10	18.52
C	007.09	6/19/19 10:58	6.210183	51.179867	100	36.26	18.52
C	007.09	6/19/19 11:00	6.210183	51.179867	50	36.06	18.16
C	007.09	6/19/19 10:56	6.210183	51.179867	30	35.98	18.16
C	007.09	6/19/19 11:06	6.210183	51.179867	15	35.61	18.16
C	007.09	6/19/19 11:00	6.210183	51.179867	8	30.12	18.16
C	007.09	6/19/19 11:11	6.210183	51.179867	0	19.79	16.73
C	007.10	6/19/19 13:23	6.224200	51.200867	5	20.13	37.02
U	008.01	6/19/19 16:48	6.384700	51.404000	0	18.94	18.52
U	008.02	6/19/19 17:40	6.504067	51.579700	0	19.48	18.87
U	008.03	6/19/19 18:42	6.623550	51.761350	0	21.09	18.52
U	008.04	6/19/19 19:47	6.739583	51.947733	0	22.09	17.45
U	008.05	6/19/19 20:44	6.857033	52.138817	0	21.38	18.87
U	008.06	6/19/19 21:45	6.972867	52.316383	0	19.95	18.87
U	008.07	6/19/19 23:09	7.078083	52.494417	0	18.21	18.16
U	008.08	6/19/19 23:55	7.191350	52.661250	0	17.89	18.16
U	008.09	6/20/19 1:03	7.312083	52.833450	0	18.90	18.87
U	008.10	6/20/19 1:45	7.431500	52.997233	0	22.06	18.52
U	008.11	6/20/19 2:43	7.564667	53.164083	0	24.77	18.52
U	008.12	6/20/19 3:33	7.692600	53.324017	0	27.67	18.16
U	008.13	6/20/19 4:39	7.820333	53.506217	0	31.67	18.87
U	008.14	6/20/19 5:35	7.946033	53.685833	0	31.84	18.16
C	009.02	6/20/19 10:57	7.971400	53.644867	100	36.53	18.16
C	009.02	6/20/19 10:49	7.971400	53.644867	50	35.93	13.88
C	009.02	6/20/19 11:03	7.971400	53.644867	40	35.70	16.38
C	009.02	6/20/19 10:45	7.971400	53.644867	25	35.43	16.02
C	009.02	6/20/19 10:53	7.971400	53.644867	15	33.84	13.88
C	009.02	6/20/19 10:51	7.971400	53.644867	0	31.84	12.46
C	009.06	6/20/19 19:41	8.037867	53.715217	150	36.34	18.16
C	009.06	6/20/19 20:05	8.037867	53.715217	125	36.49	18.52
C	009.06	6/20/19 20:19	8.037867	53.715217	100	36.54	17.80
C	009.06	6/20/19 19:47	8.037867	53.715217	75	36.30	17.45
C	009.06	6/20/19 19:47	8.037867	53.715217	40	35.98	19.23
C	009.06	6/20/19 19:30	8.037867	53.715217	20	35.57	16.38
C	009.06	6/20/19 19:57	8.037867	53.715217	0	29.83	18.52
U	010.01	6/21/19 0:58	7.977367	53.690767	0	25.08	18.52
U	010.02	6/21/19 1:40	7.982050	53.915733	0	24.93	18.52
U	010.03	6/21/19 2:43	7.987900	54.128483	0	26.40	18.52
U	010.04	6/21/19 3:31	7.987717	54.331650	0	30.33	18.87
U	010.05	6/21/19 4:32	7.991650	54.535967	0	31.21	18.52
U	010.06	6/21/19 5:27	7.993083	54.731167	0	33.57	18.16
U	010.07	6/21/19 6:38	7.993733	54.917833	0	33.61	18.52
C	011.02	6/21/19 11:18	7.979333	54.988417	100	36.65	19.58

C	011.02	6/21/19 11:17	7.979333	54.988417	60	36.33	18.87
C	011.02	6/21/19 11:18	7.979333	54.988417	35	35.36	14.60
C	011.02	6/21/19 11:18	7.979333	54.988417	25	34.52	14.95
C	011.02	6/21/19 11:20	7.979333	54.988417	14	33.46	14.60
C	011.02	6/21/19 11:11	7.979333	54.988417	0	33.34	9.97
C	011.03	6/21/19 13:26	7.990067	54.974867	27	35.34	18.52
C	011.03	6/21/19 13:27	7.990067	54.974867	0	33.60	18.87
C	011.06	6/21/19 21:19	8.002367	54.993117	500	34.69	17.66
C	011.06	6/21/19 21:19	8.002367	54.993117	250	35.12	18.02
C	011.06	6/21/19 21:19	8.002367	54.993117	200	35.41	17.30
C	011.06	6/21/19 21:11	8.002367	54.993117	150	36.10	17.52
C	011.06	6/21/19 21:20	8.002367	54.993117	125	36.52	18.87
C	011.06	6/21/19 21:16	8.002367	54.993117	100	36.71	18.16
C	011.06	6/21/19 21:19	8.002367	54.993117	75	36.50	15.67
C	011.06	6/21/19 21:19	8.002367	54.993117	43	35.40	17.80
C	011.06	6/21/19 21:23	8.002367	54.993117	25	33.93	18.16
C	011.06	6/21/19 21:28	8.002367	54.993117	0	33.23	18.52
C	011.08	6/22/19 10:25	7.987733	54.975083	100	36.76	18.52
C	011.08	6/22/19 10:25	7.987733	54.975083	55	36.28	18.87
C	011.08	6/22/19 10:32	7.987733	54.975083	35	35.86	18.87
C	011.08	6/22/19 10:32	7.987733	54.975083	21	34.08	19.23
C	011.08	6/22/19 10:25	7.987733	54.975083	11	32.67	12.82
C	011.09	6/22/19 12:20	8.000883	54.996033	0	32.27	18.69
U	012.01	6/22/19 13:25	8.093483	55.042167	0	32.06	18.34
U	012.02	6/22/19 14:24	8.255550	55.144250	0	31.71	18.16
U	012.03	6/22/19 15:25	8.408517	55.241233	0	31.75	17.80
U	012.04	6/22/19 16:30	8.578500	55.353717	0	31.78	17.62
U	012.05	6/22/19 17:27	8.741583	55.459933	0	31.42	17.27
U	012.06	6/22/19 18:26	8.904567	55.567867	0	31.78	18.16
U	012.07	6/22/19 19:24	9.060033	55.673483	0	32.07	18.16
U	012.08	6/22/19 20:31	9.210517	55.780150	0	31.32	18.16
U	012.09	6/22/19 23:35	9.681750	55.999633	0	31.07	18.16
U	012.10	6/23/19 0:38	9.841750	56.035150	0	31.80	18.52
U	012.11	6/23/19 1:30	10.008733	56.125933	0	30.22	18.87
U	012.12	6/23/19 2:31	10.163550	56.198567	0	29.57	18.52
U	012.13	6/23/19 3:24	10.336833	56.277750	0	29.49	18.52
U	012.16	6/23/19 6:35	10.799017	56.497183	0	NaN	17.80
C	013.02	6/23/19 10:21	10.802633	56.500283	150	36.58	17.80
C	013.02	6/23/19 10:23	10.802633	56.500283	125	36.82	18.52
C	013.02	6/23/19 10:22	10.802633	56.500283	100	37.07	18.52
C	013.02	6/23/19 10:21	10.802633	56.500283	75	36.47	18.52
C	013.02	6/23/19 10:27	10.802633	56.500283	43	35.65	17.80
C	013.02	6/23/19 10:23	10.802633	56.500283	30	33.49	17.80

C	013.02	6/23/19 10:36	10.802633	56.500283	18	31.45	18.52
C	013.02	6/23/19 10:36	10.802633	56.500283	0	28.99	17.45
C	013.03	6/23/19 12:17	10.820567	56.513300	100	37.09	17.45
C	013.03	6/23/19 12:22	10.820567	56.513300	60	36.19	19.23
C	013.03	6/23/19 12:22	10.820567	56.513300	45	35.30	18.87
C	013.03	6/23/19 12:17	10.820567	56.513300	24	31.79	17.45
C	013.03	6/23/19 12:26	10.820567	56.513300	15	29.83	15.31
C	013.03	6/23/19 12:22	10.820567	56.513300	0	29.00	10.32
U	014.01	6/23/19 14:30	10.978250	56.598017	0	NaN	18.52
U	014.02	6/23/19 15:29	11.126400	56.699933	0	NaN	18.52
U	014.03	6/23/19 16:25	11.270567	56.809817	0	NaN	18.52
U	014.04	6/23/19 17:26	11.418483	56.921583	0	31.22	19.23
U	014.05	6/23/19 18:30	11.569017	57.026667	0	31.77	18.52
U	014.06	6/23/19 19:26	11.723317	57.145400	0	31.68	17.80
U	014.07	6/23/19 20:32	11.880767	57.253733	0	31.54	17.62
U	014.08	6/23/19 21:28	12.042850	57.368000	0	31.38	17.27
U	014.09	6/23/19 22:27	12.198700	57.476117	0	31.66	17.27
U	014.10	6/23/19 23:24	12.355850	57.582767	0	32.05	17.45
C	015.02	6/24/19 2:28	12.394333	57.597633	47	35.50	18.16
C	015.02	6/24/19 2:30	12.394333	57.597633	20	32.64	18.16
C	015.02	6/24/19 2:30	12.394333	57.597633	0	32.17	18.87
U	016.01	6/24/19 2:47	12.431417	57.706000	0	32.78	18.16
U	016.02	6/24/19 3:46	12.479583	57.890200	0	33.46	18.16
U	016.03	6/24/19 4:21	12.520900	58.065550	0	33.42	18.52
U	016.04	6/24/19 5:34	12.562633	58.258500	0	33.04	18.87
U	016.05	6/24/19 6:27	12.611633	58.444717	0	31.61	18.16
U	016.06	6/24/19 7:27	12.668800	58.628117	0	31.36	18.52
U	016.07	6/24/19 8:31	12.728517	58.831383	0	31.37	18.52
U	016.08	6/24/19 9:35	12.780450	59.022167	0	30.91	18.87
U	016.09	6/24/19 10:42	12.826300	59.207417	0	30.73	18.87
U	016.10	6/24/19 11:27	12.871417	59.373533	0	NaN	18.52
U	016.11	6/24/19 12:25	12.930867	59.542833	0	NaN	17.80
U	016.12	6/24/19 13:23	13.016650	59.638017	0	NaN	18.52
U	016.13	6/24/19 14:25	13.082733	59.674233	0	NaN	18.52
U	017.01	6/26/19 13:31	13.391067	59.635600	0	31.50	18.16
U	017.02	6/26/19 14:22	13.436133	59.473283	0	31.36	18.16
U	017.03	6/26/19 15:23	13.481150	59.305667	0	31.56	18.52
U	017.04	6/26/19 16:25	13.524167	59.140500	0	32.25	18.52
U	017.05	6/26/19 17:25	13.571200	58.980200	0	33.07	18.52
U	017.06	6/26/19 18:30	13.610083	58.815300	0	33.27	18.16
U	017.07	6/26/19 19:35	13.653933	58.655600	0	33.60	18.87
U	017.08	6/26/19 20:34	13.701867	58.499650	0	32.63	18.52
U	017.09	6/26/19 21:27	13.750333	58.342233	0	31.84	18.52

U	017.10	6/26/19 22:31	13.793333	58.191417	0	31.75	18.52
U	017.11	6/26/19 23:31	13.844917	58.032000	0	31.84	18.87
U	017.12	6/27/19 0:29	13.893967	57.870900	0	31.66	18.16
U	017.13	6/27/19 1:29	13.935800	57.712267	0	31.79	18.52
U	017.14	6/27/19 2:28	13.971550	57.557767	0	31.62	18.52
U	017.15	6/27/19 3:32	14.007167	57.393633	0	31.51	18.52
U	017.16	6/27/19 4:25	14.043083	57.250850	0	31.67	18.52
U	017.17	6/27/19 5:31	14.103400	57.092417	0	30.57	18.52
U	017.18	6/27/19 6:24	14.137900	57.955317	0	30.18	18.87
U	017.19	6/27/19 7:23	14.174633	56.841133	0	30.04	18.87
U	017.20	6/27/19 8:24	14.210533	56.707683	0	29.94	17.80
C	018.02	6/27/19 11:52	14.255017	56.565550	100	37.08	18.52
C	018.02	6/27/19 11:58	14.255017	56.565550	70	36.49	19.94
C	018.02	6/27/19 11:45	14.255017	56.565550	50	36.05	14.24
C	018.02	6/27/19 12:07	14.255017	56.565550	28	35.71	17.80
C	018.02	6/27/19 12:03	14.255017	56.565550	13	29.93	16.73
C	018.02	6/27/19 11:50	14.255017	56.565550	0	29.92	17.09
C	018.03	6/27/19 13:27	14.295550	56.540883	50	36.13	10.32
C	018.03	6/27/19 13:46	14.295550	56.540883	25	35.77	19.58
C	018.03	6/27/19 13:47	14.295550	56.540883	13	30.14	19.23
C	018.03	6/27/19 13:44	14.295550	56.540883	0	29.93	18.87
C	018.08	6/28/19 10:42	14.605200	56.566750	100	37.23	18.87
C	018.08	6/28/19 10:42	14.605200	56.566750	65	36.99	19.94
C	018.08	6/28/19 10:42	14.605200	56.566750	50	36.79	18.16
C	018.08	6/28/19 11:22	14.605200	56.566750	35	36.25	18.87
C	018.08	6/28/19 10:46	14.605200	56.566750	20	31.13	18.52
C	018.08	6/28/19 10:42	14.605200	56.566750	0	30.77	14.95
C	018.09	6/28/19 1:03	14.613650	56.537717	5	30.74	29.53
C	018.09	6/28/19 14:46	14.613650	56.537717	0	30.74	37.43
C	018.09	6/28/19 1:54	14.613650	56.537717	0	30.74	37.02
U	019.01	6/28/19 13:30	14.612667	56.446067	0	30.68	18.87
U	019.02	6/28/19 14:35	14.613033	56.311733	0	30.59	18.52
U	019.03	6/28/19 15:36	14.619083	56.150533	0	30.53	18.87
U	019.04	6/28/19 16:33	14.619517	56.021917	0	30.55	18.87
U	019.05	6/28/19 17:30	14.618867	55.881950	0	30.80	18.52
U	019.06	6/28/19 18:33	14.617000	55.741750	0	30.55	18.87
U	019.07	6/28/19 19:34	14.618750	55.602300	0	30.70	18.87
U	019.08	6/28/19 20:29	14.620867	55.460500	0	30.61	18.87
U	019.09	6/28/19 21:31	14.621800	55.333017	0	30.93	18.87
U	019.10	6/28/19 22:32	14.619233	55.202983	0	31.23	18.87
U	019.11	6/28/19 23:27	14.621017	55.085933	0	31.68	18.87
U	019.12	6/29/19 0:30	14.617150	54.938783	0	31.74	18.52
C	020.02	6/29/19 3:22	14.622017	54.930783	300	35.96	18.02

C	020.02	6/29/19 4:13	14.622017	54.930783	250	36.26	17.52
C	020.02	6/29/19 3:17	14.622017	54.930783	200	36.68	18.52
C	020.02	6/29/19 3:17	14.622017	54.930783	150	37.15	18.69
C	020.02	6/29/19 3:57	14.622017	54.930783	50	36.86	17.80
C	020.02	6/29/19 3:43	14.622017	54.930783	30	36.17	18.16
C	020.02	6/29/19 3:29	14.622017	54.930783	18	31.93	18.52
C	020.02	6/29/19 4:47	14.622017	54.930783	0	31.92	30.93
U	021.01	6/29/19 3:57	14.697717	54.972400	0	31.85	18.16
U	021.02	6/29/19 4:42	14.776783	55.092650	0	31.78	18.52
U	021.03	6/29/19 5:29	14.833500	55.221583	0	31.33	17.80
U	021.04	6/29/19 6:27	14.927617	55.341783	0	31.29	18.16
U	021.05	6/29/19 7:27	15.002700	55.465050	0	31.49	18.16
U	021.06	6/29/19 8:21	15.082400	55.589850	0	31.52	18.16
U	021.07	6/29/19 9:25	15.168817	55.711450	0	31.22	17.80
U	021.08	6/29/19 10:23	15.261567	55.844150	0	31.22	17.62
U	021.09	6/29/19 11:24	15.356883	55.986850	0	31.23	18.16
U	021.10	6/29/19 12:25	15.446183	56.133033	0	31.56	18.52
U	021.11	6/29/19 13:25	15.535750	56.286200	0	31.17	18.52
U	021.12	6/29/19 14:25	15.632350	56.433333	0	31.22	18.87
U	021.13	6/29/19 15:25	15.729750	56.581683	0	31.25	18.87
U	021.14	6/29/19 16:33	15.827883	56.728083	0	30.98	18.52
U	021.15	6/29/19 17:32	15.908033	56.861933	0	31.38	18.52
C	022.02	6/29/19 20:53	16.002783	56.997333	300	36.23	17.66
C	022.02	6/29/19 22:22	16.002783	56.997333	250	36.47	15.02
C	022.02	6/29/19 20:51	16.002783	56.997333	200	36.86	18.52
C	022.02	6/29/19 20:56	16.002783	56.997333	150	37.21	18.52
C	022.02	6/29/19 20:48	16.002783	56.997333	80	37.18	18.16
C	022.02	6/29/19 21:06	16.002783	56.997333	50	36.93	18.52
C	022.02	6/29/19 21:40	16.002783	56.997333	30	36.39	17.45
C	022.02	6/29/19 21:13	16.002783	56.997333	18	31.86	18.87
C	022.02	6/29/19 22:01	16.002783	56.997333	0	31.86	37.37
C	022.05	6/30/19 10:42	16.010983	56.995700	100	37.33	18.87
C	022.05	6/30/19 10:39	16.010983	56.995700	75	37.16	18.52
C	022.05	6/30/19 10:51	16.010983	56.995700	35	36.66	19.58
C	022.05	6/30/19 10:45	16.010983	56.995700	18	31.90	18.87
C	022.05	6/30/19 10:56	16.010983	56.995700	10	31.89	19.58
C	022.05	6/30/19 10:58	16.010983	56.995700	0	31.89	19.23
C	022.06	6/30/19 12:24	16.018200	56.987367	25	35.28	18.87
C	022.06	6/30/19 12:24	16.018200	56.987367	0	31.88	18.87
U	023.01	6/30/19 18:26	15.961383	56.907867	0	31.24	18.87
U	023.02	6/30/19 19:27	15.814483	56.957033	0	31.43	18.52
U	023.03	6/30/19 20:25	15.676083	57.004233	0	31.82	18.87
U	023.04	6/30/19 21:28	15.529217	57.046717	0	31.99	18.52

U	023.05	6/30/19 22:29	15.394533	57.087250	0	32.03	18.87
U	023.06	6/30/19 23:28	15.236533	57.130617	0	32.13	18.52
U	023.07	7/1/19 0:31	15.065033	57.173367	0	32.57	19.23
U	023.08	7/1/19 1:30	14.922817	57.213117	0	32.49	18.87
U	023.09	7/1/19 2:27	14.783367	57.255967	0	32.33	18.52
U	023.10	7/1/19 3:29	14.661267	57.292933	0	32.28	18.52
U	023.11	7/1/19 4:27	14.535583	57.331417	0	31.19	18.52
U	023.12	7/1/19 5:26	14.411517	57.369967	0	30.55	18.87
U	023.13	7/1/19 6:27	14.116450	57.409367	0	30.21	18.16
U	023.14	7/1/19 7:30	14.149033	57.450383	0	29.86	18.87
U	023.15	7/1/19 8:26	14.021183	57.491283	0	29.59	18.16
C	024.02	7/1/19 10:46	14.014433	57.488183	100	36.92	18.87
C	024.02	7/1/19 10:44	14.014433	57.488183	75	36.54	18.16
C	024.02	7/1/19 10:46	14.014433	57.488183	50	36.23	18.16
C	024.02	7/1/19 11:02	14.014433	57.488183	30	33.86	19.58
C	024.02	7/1/19 10:54	14.014433	57.488183	18	29.65	18.52
C	024.02	7/1/19 11:00	14.014433	57.488183	0	29.59	19.23
U	025.01	7/1/19 14:37	14.000783	57.475283	0	29.46	19.23
U	025.02	7/1/19 14:35	13.879350	57.554583	0	29.61	18.52
U	025.03	7/1/19 16:37	13.757450	57.642133	0	29.81	18.87
U	025.04	7/1/19 17:34	13.636233	57.740350	0	30.41	18.87
U	025.05	7/1/19 18:41	13.514517	57.830250	0	29.56	18.52
U	025.06	7/1/19 19:35	13.388400	57.920883	0	29.83	18.52
U	025.07	7/1/19 20:28	13.246767	58.018750	0	30.18	18.52
U	025.08	7/1/19 21:27	13.122233	58.110167	0	30.26	18.87
U	025.09	7/1/19 22:30	12.997767	58.202067	0	30.92	18.87
U	025.10	7/1/19 23:26	12.865917	58.291667	0	31.16	18.87
U	025.11	7/2/19 0:30	12.734067	58.387150	0	31.28	18.52
U	025.12	7/2/19 1:24	12.623583	58.479183	0	31.54	18.69
U	025.13	7/2/19 2:33	12.505667	58.574267	0	31.87	18.52
U	025.14	7/2/19 3:27	12.368417	58.676417	0	32.37	19.23
U	025.15	7/2/19 4:29	12.239883	58.770567	0	32.64	18.52
U	025.16	7/2/19 5:29	12.113150	58.870783	0	32.97	18.87
C	026.03	7/2/19 11:14	11.990550	58.961517	100	36.66	19.23
C	026.03	7/2/19 11:12	11.990550	58.961517	75	36.26	18.87
C	026.03	7/2/19 11:06	11.990550	58.961517	58	36.03	19.23
C	026.03	7/2/19 11:17	11.990550	58.961517	35	34.66	19.58
C	026.03	7/2/19 11:17	11.990550	58.961517	20	33.36	18.52
C	026.03	7/2/19 11:22	11.990550	58.961517	0	33.31	19.23
C	026.08	7/2/19 20:55	11.987333	58.984450	500	36.15	17.52
C	026.08	7/2/19 21:02	11.987333	58.984450	300	36.15	17.52
C	026.08	7/2/19 20:55	11.987333	58.984450	250	36.15	18.87
C	026.08	7/2/19 20:55	11.987333	58.984450	200	36.53	19.23

C	026.08	7/2/19 21:10	11.987333	58.984450	150	36.75	17.09
C	026.08	7/2/19 21:09	11.987333	58.984450	100	36.68	18.52
C	026.08	7/2/19 20:56	11.987333	58.984450	60	35.89	18.87
C	026.08	7/2/19 21:17	11.987333	58.984450	35	34.67	18.52
C	026.08	7/2/19 21:09	11.987333	58.984450	18	33.28	18.16
C	026.08	7/2/19 21:30	11.987333	58.984450	0	33.22	18.87
C	026.10	7/3/19 10:37	11.983967	58.964650	100	36.42	18.87
C	026.10	7/3/19 10:54	11.983967	58.964650	60	35.48	19.23
C	026.10	7/3/19 11:00	11.983967	58.964650	40	34.62	18.87
C	026.10	7/3/19 11:02	11.983967	58.964650	25	32.97	19.23
C	026.10	7/3/19 10:59	11.983967	58.964650	15	32.62	19.58
C	026.10	7/3/19 10:39	11.983967	58.964650	0	32.58	13.53
U	027.01	7/3/19 13:32	12.095517	58.995617	0	32.35	19.23
U	027.02	7/3/19 14:31	12.255433	58.995917	0	32.58	18.87
U	027.03	7/3/19 15:31	12.415333	58.996283	0	32.47	18.52
U	027.04	7/3/19 16:26	12.574267	58.997733	0	32.04	18.52
U	027.05	7/3/19 17:23	12.736933	58.997500	0	31.82	18.87
U	027.06	7/3/19 18:23	12.899833	58.996650	0	31.91	18.52
U	027.07	7/3/19 19:27	13.032050	59.001100	0	32.00	19.58
U	027.08	7/3/19 20:24	13.149650	59.000083	0	32.02	18.87
U	027.09	7/3/19 21:25	13.283067	59.002033	0	31.96	18.87
U	027.10	7/3/19 22:26	13.417950	59.004500	0	31.85	18.52
U	027.11	7/3/19 23:24	13.539083	59.004200	0	31.69	18.16
U	027.12	7/4/19 0:26	13.662900	59.004833	0	31.90	18.16
U	027.13	7/4/19 1:33	13.769483	59.050117	0	32.69	18.16
U	027.14	7/4/19 2:31	13.837333	59.074583	0	32.75	18.52
U	027.15	7/4/19 3:27	13.889650	59.292767	0	32.96	18.52
U	027.16	7/4/19 4:32	13.935233	59.386233	0	32.92	18.52
U	027.17	7/4/19 5:28	13.978183	59.475000	0	32.97	18.52
U	027.18	7/4/19 6:30	14.025183	59.565033	0	33.14	18.87
U	029.01	7/4/19 7:29	14.042867	59.592783	0	33.15	19.23
U	029.03	7/4/19 9:28	14.197250	59.398967	0	32.84	18.52
U	029.05	7/4/19 11:30	14.379033	59.174883	0	32.99	19.23
U	029.07	7/4/19 13:25	14.555517	59.944983	0	33.34	18.87
U	029.09	7/4/19 15:29	14.730800	58.718533	0	34.03	18.52
U	029.10	7/4/19 16:37	14.815367	58.611917	0	33.22	18.16
U	029.12	7/4/19 18:36	15.087467	58.529483	0	33.23	18.16
C	030.05	7/5/19 10:52	15.168383	58.490733	100	36.25	18.52
C	030.05	7/5/19 10:54	15.168383	58.490733	83	36.17	19.23
C	030.05	7/5/19 11:04	15.168383	58.490733	60	36.15	19.58
C	030.05	7/5/19 10:54	15.168383	58.490733	35	36.06	19.23
C	030.05	7/5/19 11:21	15.168383	58.490733	20	33.48	19.23
C	030.05	7/5/19 11:21	15.168383	58.490733	0	33.43	19.41

C	030.06	7/5/19 12:29	15.181200	58.476000	100	36.26	18.16
C	030.06	7/5/19 12:33	15.181200	58.476000	83	36.17	18.52
C	030.06	7/5/19 12:39	15.181200	58.476000	20	33.45	19.23
C	030.06	7/5/19 12:45	15.181200	58.476000	0	33.42	19.58
C	030.10	7/5/19 20:57	15.165400	58.499567	500	34.96	18.16
C	030.10	7/5/19 20:47	15.165400	58.499567	300	35.77	16.45
C	030.10	7/5/19 21:10	15.165400	58.499567	250	36.24	18.52
C	030.10	7/5/19 20:55	15.165400	58.499567	200	36.71	17.52
C	030.10	7/5/19 21:05	15.165400	58.499567	150	37.24	17.80
C	030.10	7/5/19 21:16	15.165400	58.499567	100	36.30	18.16
C	030.10	7/5/19 21:51	15.165400	58.499567	67	36.17	19.23
C	030.10	7/5/19 21:18	15.165400	58.499567	35	36.11	18.52
C	030.10	7/5/19 21:47	15.165400	58.499567	20	33.98	18.16
C	030.10	7/5/19 21:44	15.165400	58.499567	0	33.41	19.23
U	031.01	7/5/19 21:47	15.060517	58.597783	0	33.35	18.87
U	031.02	7/5/19 22:30	14.921700	58.724367	0	33.41	18.87
U	031.03	7/5/19 23:34	14.782500	58.843050	0	33.32	18.16
U	031.04	7/6/19 0:31	14.647017	58.949550	0	33.19	18.87
U	031.05	7/6/19 1:31	14.536733	59.061483	0	33.14	19.23
U	031.06	7/6/19 2:39	14.439867	59.163217	0	33.19	18.52
U	031.07	7/6/19 3:38	14.340267	59.274100	0	33.39	19.23
U	031.08	7/6/19 4:39	14.247633	59.374667	0	33.45	19.23
U	031.09	7/6/19 5:39	14.149267	59.471067	0	33.28	19.58
U	031.10	7/6/19 6:32	14.047433	59.566950	0	33.04	18.87
U	031.11	7/6/19 7:27	13.938400	59.673317	0	33.01	18.87
U	031.12	7/6/19 8:30	13.844567	59.765050	0	33.19	18.87
C	032.02	7/6/19 11:03	13.822667	59.787250	100	36.36	18.87
C	032.02	7/6/19 11:06	13.822667	59.787250	65	36.18	18.52
C	032.02	7/6/19 11:28	13.822667	59.787250	40	36.16	19.58
C	032.02	7/6/19 11:08	13.822667	59.787250	20	36.10	18.16
C	032.02	7/6/19 11:20	13.822667	59.787250	10	33.24	18.16
C	032.02	7/6/19 10:59	13.822667	59.787250	0	33.22	12.10
C	032.03	7/6/19 14:41	13.821933	59.783583	0	33.20	56.57
C	032.03	7/6/19 15:35	13.821933	59.783583	5	33.20	57.33
C	032.03	7/6/19 18:29	13.821933	59.783583	0	33.20	57.28
U	033.01	7/6/19 15:35	13.819133	59.805850	0	32.98	18.52
U	033.02	7/6/19 16:30	13.673283	59.845533	0	32.77	18.87
U	033.03	7/6/19 17:40	13.511983	59.894700	0	33.57	18.87
U	033.04	7/6/19 18:33	13.350417	59.942717	0	32.72	18.87
U	033.05	7/6/19 19:33	13.216233	59.994900	0	32.21	18.87
C	034.03	7/7/19 10:28	13.170400	60.003000	150	36.65	19.23
C	034.03	7/7/19 10:34	13.170400	60.003000	100	36.17	18.87
C	034.03	7/7/19 10:38	13.170400	60.003000	70	36.12	19.23

C	034.03	7/7/19 11:09	13.170400	60.003000	37	35.12	19.23
C	034.03	7/7/19 11:09	13.170400	60.003000	10	32.35	18.52
C	034.03	7/7/19 10:21	13.170400	60.003000	0	32.36	10.32
C	034.05	7/7/19 11:58	13.205300	60.019800	18	34.03	39.54
C	034.05	7/7/19 11:56	13.205300	60.019800	0	32.37	38.48
C	034.10	7/7/19 22:57	13.165683	60.015317	1000	34.81	18.87
C	034.10	7/7/19 22:31	13.165683	60.015317	800	34.60	18.52
C	034.10	7/7/19 23:26	13.165683	60.015317	600	34.76	18.52
C	034.10	7/7/19 23:27	13.165683	60.015317	400	34.94	18.16
C	034.10	7/7/19 23:16	13.165683	60.015317	200	36.02	18.87
C	034.10	7/7/19 23:27	13.165683	60.015317	150	36.72	17.80
C	034.10	7/7/19 23:23	13.165683	60.015317	100	36.13	17.80
C	034.10	7/7/19 23:25	13.165683	60.015317	75	36.12	17.80
C	034.10	7/7/19 23:41	13.165683	60.015317	50	36.01	19.23
C	034.10	7/7/19 23:39	13.165683	60.015317	35	35.06	17.09
C	034.10	7/7/19 23:36	13.165683	60.015317	20	34.08	18.87
C	034.10	7/7/19 23:36	13.165683	60.015317	0	32.38	19.23
U	035.01	7/7/19 23:44	13.188767	59.969733	0	32.27	18.87
U	035.02	7/8/19 0:32	13.178083	59.929100	0	32.09	18.87
U	035.03	7/8/19 1:32	13.163450	59.892817	0	32.15	19.23
U	035.04	7/8/19 2:26	13.155950	59.855217	0	32.25	18.16
U	035.05	7/8/19 3:28	13.146117	59.820217	0	32.41	19.58
U	035.06	7/8/19 4:25	13.141050	59.783300	0	32.49	19.58
U	035.07	7/8/19 5:22	13.134917	59.746767	0	32.54	19.58

Appendix B: Radium Data. Radium isotope activities: ^{223}Ra, excess ^{224}Ra, ^{226}Ra, and ^{228}Ra, for each sample from EN614 (**B1**) and EN640 (**B2**)shown with their corresponding event code and depth. Uncertainties represent the 1-σ measurement uncertainty. 'BD' values indicate measurements below the Minimum Detectable Activity (MDA). 'nd' values represent samples for which there is no data because they have not yet been counted at the time of this publication.

Appendix B1: EN614 Radium Data.

Event Code	Depth m	^{223}Ra dpm/100L	XS ^{224}Ra dpm/100L	^{226}Ra dpm/100L	^{228}Ra dpm/100L
001.01	250	BD	0.52 ± 0.05	11.64 ± 0.93	1.58 ± 0.17
001.01	200	BD	1.27 ± 0.12	16.22 ± 1.26	1.87 ± 0.22
001.01	150	BD	0.75 ± 0.07	14.14 ± 1.13	0.34 ± 0.03
001.01	98	BD	0.99 ± 0.10	17.16 ± 1.06	BD
001.01	75	BD	1.47 ± 0.14	14.92 ± 0.91	6.49 ± 0.47
001.01	50	BD	1.00 ± 0.10	14.70 ± 1.02	4.70 ± 0.35
001.01	20	0.19 ± 0.05	0.43 ± 0.04	14.10 ± 1.01	10.78 ± 0.60
001.01	10	0.29 ± 0.08	0.40 ± 0.04	17.37 ± 1.07	20.91 ± 0.89
001.01	0	0.10 ± 0.04	0.45 ± 0.05	15.24 ± 0.99	9.04 ± 0.55
002.01	0	BD	3.01 ± 0.29	14.43 ± 1.08	0.84 ± 0.08
002.02	0	0.12 ± 0.05	2.18 ± 0.22	19.47 ± 1.21	BD
002.04	0	BD	1.72 ± 0.16	17.20 ± 1.08	4.64 ± 0.41
002.06	0	BD	2.49 ± 0.25	15.77 ± 0.99	6.59 ± 0.53
002.08	0	BD	4.66 ± 0.44	15.89 ± 1.27	8.19 ± 0.55
002.09	0	0.32 ± 0.10	2.14 ± 0.22	19.21 ± 1.14	11.99 ± 0.66
002.10	0	0.41 ± 0.10	1.51 ± 0.15	17.73 ± 1.04	9.34 ± 0.53
003.03	250	BD	1.25 ± 0.16	15.49 ± 0.95	0.91 ± 0.11
003.03	200	BD	1.03 ± 0.28	15.98 ± 1.04	0.22 ± 0.03
003.03	75	BD	1.34 ± 0.77	17.60 ± 1.18	2.97 ± 0.27
003.03	100	0.07 ± 0.03	0.74 ± 0.07	16.18 ± 1.16	4.26 ± 0.38
003.03	75	0.12 ± 0.04	0.63 ± 0.06	14.10 ± 0.95	6.07 ± 0.46
003.03	50	BD	0.81 ± 0.08	16.21 ± 1.10	6.34 ± 0.46
003.03	25	0.36 ± 0.09	1.42 ± 0.14	19.12 ± 1.22	13.69 ± 0.77
003.03	10	0.43 ± 0.10	1.41 ± 0.14	17.46 ± 1.32	3.14 ± 0.44
003.03	0	0.37 ± 0.12	1.66 ± 0.20	17.74 ± 1.75	11.13 ± 1.15
003.07	75	BD	0.52 ± 0.05	16.93 ± 1.21	0.05 ± 0.01
003.07	50	0.13 ± 0.06	0.83 ± 0.12	18.56 ± 1.44	6.95 ± 0.90
003.07	33	BD	0.30 ± 0.03	19.70 ± 1.44	7.53 ± 1.05
003.07	10	0.29 ± 0.09	1.66 ± 0.18	19.73 ± 1.30	17.09 ± 1.60

003.07	0	0.24	±	0.06	0.96	±	0.09	18.37	±	1.41	8.69	±	0.97
003.09	28	0.24	±	0.06	0.52	±	0.05	16.69	±	1.15	5.62	±	0.55
003.09	10	0.37	±	0.09	1.74	±	0.17	17.89	±	1.46	18.26	±	0.89
003.13	110	BD			0.38	±	0.04	19.49	±	1.65	6.17	±	0.46
003.13	29	0.15	±	0.05	0.69	±	0.07	21.45	±	1.41	2.89	±	0.34
003.13	0	BD			0.44	±	0.04	12.40	±	0.65	6.06	±	0.50
004.01	0	0.60	±	0.17	3.72	±	0.37	16.68	±	1.29	2.16	±	0.23
004.02	0	0.30	±	0.09	3.51	±	0.31	20.83	±	1.45	17.61	±	1.43
004.03	0	0.18	±	0.06	4.46	±	0.36	19.01	±	1.32	6.10	±	0.52
004.04	0	0.50	±	0.15	3.69	±	0.37	18.06	±	1.18	13.04	±	0.85
004.05	0	0.63	±	0.18	4.19	±	0.41	19.01	±	1.33	8.29	±	0.58
004.06	0	0.90	±	0.27	9.14	±	0.91	20.96	±	1.47	10.50	±	0.64
004.07	0	0.76	±	0.23	7.77	±	0.73	20.80	±	1.37	9.42	±	0.60
004.08	0	1.07	±	0.30	7.34	±	0.72	16.44	±	1.17	20.95	±	0.97
004.09	0	0.59	±	0.19	6.42	±	0.60	19.73	±	1.52	3.03	±	0.24
004.10	0	0.54	±	0.17	8.39	±	0.71	19.81	±	1.37	8.59	±	0.55
004.11	0	0.98	±	0.31	9.84	±	0.97	17.66	±	1.39	4.88	±	0.39
004.12	0	0.72	±	0.19	10.41	±	0.77	17.82	±	1.16	17.42	±	0.95
004.13	0	1.10	±	0.26	9.01	±	0.72	16.14	±	1.31	17.46	±	1.03
004.14	0	0.83	±	0.25	13.03	±	1.05	21.93	±	1.44	22.97	±	1.12
004.15	0	1.29	±	0.41	16.89	±	1.54	19.04	±	1.30	21.01	±	1.02
004.16	0	1.34	±	0.37	9.45	±	0.94	15.34	±	1.21	19.56	±	0.97
006.01	110	BD			0.50	±	0.05	18.68	±	1.51	BD		
006.01	85	0.16	±	0.05	1.49	±	0.13	18.46	±	1.40	4.17	±	0.44
006.01	50	0.33	±	0.08	2.89	±	0.22	19.30	±	1.69	BD		
006.01	27	BD			0.63	±	0.07	16.06	±	1.63	1.96	±	0.19
006.01	10	0.84	±	0.26	9.91	±	0.94	20.10	±	1.84	BD		
006.01	0	1.72	±	0.39	10.28	±	0.90	20.30	±	1.47	24.85	±	1.95
007.01	0	1.28	±	0.18	11.66	±	0.54	19.30	±	1.24	12.57	±	0.83
007.02	0	1.71	±	0.24	13.80	±	0.66	18.86	±	1.20	30.25	±	1.48
007.03	0	1.16	±	0.37	12.24	±	1.22	19.92	±	1.33	5.44	±	0.34
007.04	0	2.07	±	0.53	12.87	±	1.29	21.22	±	1.47	40.45	±	3.43
007.05	0	1.83	±	0.53	17.55	±	1.74	17.95	±	1.29	12.00	±	0.65
007.06	0	0.99	±	0.31	15.73	±	1.41	20.22	±	1.60	36.18	±	3.37
007.07	0	1.30	±	0.39	12.18	±	1.20	21.23	±	1.25	36.15	±	3.60
007.08	0	1.99	±	0.51	12.29	±	1.21	22.76	±	1.30	31.50	±	1.34
007.09	0	0.93	±	0.23	11.41	±	0.85	19.08	±	1.19	31.18	±	1.43
007.10	0	1.19	±	0.29	8.75	±	0.75	18.37	±	1.32	19.19	±	2.28
007.11	0	0.72	±	0.22	7.44	±	0.68	22.65	±	1.39	30.25	±	2.83
007.12	0	0.98	±	0.25	9.88	±	0.79	19.61	±	1.36	16.11	±	1.95
007.13	0	0.61	±	0.18	8.95	±	0.73	17.42	±	1.20	37.00	±	3.44
008.01	100	0.02	±	0.01	0.02	±	0.00	17.28	±	1.21	BD		
008.01	70	0.04	±	0.01	0.50	±	0.04	19.45	±	1.38	BD		

008.01	45	0.15	±	0.05	0.99	±	0.10	20.31	±	1.67	0.12	± 0.02
008.01	19	0.38	±	0.11	2.78	±	0.28	17.83	±	1.58	12.95	± 0.97
008.01	10	1.41	±	0.36	9.13	±	0.86	18.00	±	1.50	4.60	± 0.31
008.01	0	0.74	±	0.22	7.14	±	0.68	18.58	±	1.18	BD	
008.02	203	0.37	±	0.10	4.87	±	0.37	15.27	±	1.02	10.52	± 0.59
008.02	193	0.35	±	0.10	3.37	±	0.31	15.40	±	0.97	3.30	± 0.26
008.02	150	0.04	±	0.02	0.26	±	0.02	15.78	±	0.99	BD	
008.02	125	BD			0.59	±	0.06	17.28	±	1.12	1.69	± 0.19
009.01	0	0.56	±	0.18	8.74	±	0.74	17.97	±	1.06	10.97	± 1.28
009.02	0	0.90	±	0.27	11.07	±	0.98	17.18	±	0.95	32.39	± 2.67
009.03	0	0.87	±	0.18	8.72	±	0.57	16.57	±	1.02	5.37	± 0.44
009.04	0	0.94	±	0.20	10.68	±	0.69	18.78	±	1.18	19.62	± 1.13
009.05	0	0.37	±	0.11	7.89	±	0.58	18.36	±	1.06	3.94	± 0.50
009.06	0	0.85	±	0.23	6.60	±	0.62	18.03	±	1.29	9.68	± 1.00
009.07	0	0.36	±	0.11	5.37	±	0.46	18.05	±	1.37	2.12	± 0.30
009.08	0	0.41	±	0.12	4.55	±	0.41	21.40	±	1.42	14.35	± 1.36
009.09	0	0.10	±	0.04	2.06	±	0.20	19.24	±	1.32	5.63	± 0.56
009.10	0	0.08	±	0.03	2.04	±	0.15	15.59	±	1.15	BD	
009.11	0	BD			2.07	±	0.14	16.87	±	1.35	BD	
009.12	0	0.08	±	0.03	1.07	±	0.09	17.97	±	1.40	BD	
009.13	0	BD			1.81	±	0.18	12.10	±	1.00	3.24	± 0.28
009.14	0	BD			0.93	±	0.11	15.60	±	1.21	0.79	± 0.07
009.15	0	BD			0.68	±	0.14	17.79	±	1.11	3.30	± 0.26
009.16	0	BD			2.86	±	0.38	15.04	±	1.02	0.99	± 0.12
009.17	0	BD			1.78	±	0.28	13.87	±	0.96	2.76	± 0.24
009.18	0	BD			2.75	±	0.38	14.22	±	0.98	4.74	± 0.37
009.19	0	BD			2.47	±	0.36	14.78	±	1.07	1.64	± 0.14
009.20	0	BD			1.85	±	0.27	14.63	±	1.02	3.87	± 0.29
010.04	77	BD			0.25	±	0.02	9.91	±	0.39	0.12	± 0.01
010.04	0	BD			BD			10.36	±	0.37	3.77	± 0.20
011.01	0	BD			0.85	±	0.05	17.47	±	1.05	2.05	± 0.18
011.02	0	0.13	±	0.04	2.41	±	0.18	15.09	±	1.02	4.48	± 0.37
011.03	0	0.07	±	0.02	1.54	±	0.11	16.74	±	1.34	BD	
011.06	0	0.54	±	0.13	2.36	±	0.23	16.85	±	1.33	6.66	± 0.54
011.07	0	0.83	±	0.22	6.11	±	0.57	21.47	±	1.40	16.75	± 0.89
011.08	0	0.90	±	0.27	9.28	±	0.86	19.60	±	1.31	32.79	± 1.28
011.09	0	2.49	±	0.69	22.93	±	2.08	21.60	±	1.21	48.92	± 1.62
012.01	35	0.85	±	0.24	21.66	±	1.47	17.46	±	1.58	6.76	± 0.90
012.01	20	0.42	±	0.11	6.22	±	0.46	18.81	±	1.41	1.56	± 0.30
012.01	7	7.58	±	1.84	49.67	±	4.46	19.07	±	1.27	24.48	± 1.75
012.01	0	3.88	±	1.04	25.16	±	2.52	18.44	±	1.52	21.78	± 1.70
017.01	12	0.47	±	0.14	3.49	±	0.35	16.74	±	1.41	BD	
017.01	0	3.10	±	0.78	16.87	±	1.69	24.79	±	1.29	24.09	± 1.12

017.03	50	0.31	±	0.15	2.40	±	0.40	16.18	±	1.17	BD	±	BD	
017.03	30	0.32	±	0.10	3.37	±	0.32	16.53	±	1.34	2.35	±	0.28	
017.03	9	1.17	±	0.37	11.73	±	1.16	20.13	±	1.43	24.06	±	1.18	
017.03	0	1.06	±	0.34	14.91	±	1.31	24.39	±	1.57	52.80	±	2.01	
017.90	40	0.30	±	0.09	3.13	±	0.29	15.59	±	1.27	0.08	±	0.02	
017.90	20	0.53	±	0.12	4.45	±	0.32	14.06	±	0.72	4.20	±	0.56	
017.90	7.5	0.60	±	0.17	6.82	±	0.57	18.06	±	0.93	4.68	±	0.62	
017.90	0	2.12	±	0.39	16.64	±	1.06	18.56	±	0.77	27.84	±	2.35	
018.01	0	1.38	±	0.25	7.36	±	0.51	19.17	±	1.24	20.86	±	2.74	
018.02	0	0.41	±	0.12	3.07	±	0.30	14.86	±	1.38	12.24	±	1.42	
018.03	0	1.02	±	0.21	3.20	±	0.31	20.13	±	1.47	19.83	±	1.80	
018.04	0	0.29	±	0.09	2.42	±	0.24	20.87	±	1.29	BD			
018.05	0	0.09	±	0.03	0.75	±	0.07	11.73	±	0.61	7.13	±	0.42	
018.06	0	0.89	±	0.21	4.09	±	0.39	18.93	±	1.28	8.48	±	0.63	
018.07	0	0.70	±	0.20	6.00	±	0.57	18.55	±	1.15	32.77	±	1.45	
018.08	0	1.23	±	0.26	13.08	±	0.83	16.59	±	0.66	36.49	±	1.03	
018.09	0	2.53	±	0.55	25.93	±	1.72	18.42	±	0.78	51.45	±	1.30	
019.01	0	1.95	±	0.59	29.87	±	2.49	24.54	±	1.33	14.33	±	1.37	
019.02	0	2.10	±	0.63	19.84	±	1.90	22.31	±	1.38	39.74	±	2.73	
019.03	0	1.42	±	0.39	11.78	±	1.10	18.20	±	1.17	11.58	±	1.26	
019.04	0	2.13	±	0.49	10.45	±	1.01	18.30	±	1.31	30.27	±	2.51	
019.05	0	0.93	±	0.20	7.09	±	0.53	21.42	±	1.40	25.37	±	2.18	
019.06	0	0.71	±	0.15	7.97	±	0.51	20.17	±	1.29	29.26	±	2.24	
019.07	0	0.48	±	0.12	5.23	±	0.39	19.12	±	1.12	1.36	±	0.10	
019.08	0	0.67	±	0.16	4.38	±	0.36	20.40	±	1.31	8.33	±	0.49	
019.09	0	0.27	±	0.08	2.50	±	0.24	22.70	±	1.45	5.17	±	0.40	
019.10	0	0.18	±	0.06	2.90	±	0.23	20.06	±	1.37	10.54	±	0.63	
019.11	0	0.25	±	0.08	2.36	±	0.23	16.62	±	1.23	7.58	±	0.50	
019.12	0	0.31	±	0.09	2.74	±	0.27	17.65	±	1.51	6.86	±	0.48	
019.13	0	BD			2.10	±	0.19	18.65	±	1.40	0.80	±	0.09	
019.15	0	0.17	±	0.06	2.21	±	0.21	17.44	±	1.34	0.25	±	0.04	
020.02	275	0.03	±	0.01	0.24	±	0.03	18.19	±	1.15	1.06	±	0.13	
020.02	150	0.03	±	0.01	0.83	±	0.06	16.77	±	1.28	2.06	±	0.21	
020.02	125	0.05	±	0.02	0.22	±	0.02	16.99	±	1.38	2.54	±	0.25	
020.03	110	BD			0.18	±	0.02	14.46	±	1.57	BD			
020.03	95	BD			BD			16.51	±	1.50	BD			
020.03	75	BD			1.10	±	0.10	17.21	±	1.36	0.02	±	0.00	
020.03	50	BD			0.53	±	0.05	18.94	±	1.53	2.35	±	0.23	
020.03	20	0.06	±	0.02	0.38	±	0.04	16.98	±	1.32	4.83	±	0.35	
020.03	0	BD			0.14	±	0.01	18.25	±	1.55	2.78	±	0.22	
021.01	0	BD			1.93	±	0.14	16.14	±	1.49	BD			
021.05	0	BD			1.58	±	0.12	17.63	±	1.51	1.02	±	0.11	
021.17	0	0.11	±	0.03	1.68	±	0.13	17.47	±	1.28	2.13	±	0.20	

022.01	150	0.05	±	0.02	0.24	±	0.02	14.61	±	1.12	BD			
022.01	75	0.05	±	0.02	0.68	±	0.06	17.85	±	1.30	3.31	±	0.26	
022.01	60	0.04	±	0.02	BD			18.99	±	1.37	4.49	±	0.36	
022.01	50	0.08	±	0.03	0.60	±	0.05	16.07	±	1.26	BD			
022.01	25	0.23	±	0.06	0.94	±	0.09	17.74	±	1.53	14.92	±	1.49	
022.01	0	0.14	±	0.04	0.83	±	0.08	17.17	±	1.44	9.65	±	0.75	
022.06	70	BD			0.63	±	0.07	19.91	±	1.71	6.20	±	0.49	
022.06	45	0.05	±	0.02	0.77	±	0.06	15.50	±	1.28	2.55	±	0.24	
022.06	30	0.13	±	0.04	0.45	±	0.05	17.53	±	1.38	3.97	±	0.67	
022.06	15	0.14	±	0.05	0.45	±	0.06	25.19	±	2.01	14.07	±	1.83	
022.06	0	0.23	±	0.05	0.41	±	0.04	19.45	±	1.48	9.50	±	1.29	
022.08	0	0.28	±	0.06	0.87	±	0.09	17.14	±	1.27	4.01	±	0.44	
022.08	15	0.12	±	0.04	0.79	±	0.07	19.32	±	1.30	4.31	±	0.48	
022.08	30	0.17	±	0.05	0.57	±	0.06	18.97	±	1.46	9.93	±	0.85	
023.01	0	0.33	±	0.09	1.91	±	0.19	19.06	±	1.41	15.12	±	1.50	
023.02	0	0.16	±	0.05	2.78	±	0.22	14.31	±	1.41	18.17	±	1.62	
023.03	0	0.78	±	0.15	4.40	±	0.35	18.43	±	1.60	17.64	±	1.76	
023.04	0	0.37	±	0.09	4.14	±	0.32	22.25	±	1.34	13.06	±	1.25	
023.05	0	0.48	±	0.13	3.71	±	0.36	20.68	±	1.32	10.98	±	1.07	
023.06	0	0.55	±	0.14	3.44	±	0.34	17.07	±	1.23	29.89	±	3.02	
023.07	0	0.73	±	0.10	3.39	±	0.21	22.46	±	1.29	35.33	±	3.14	
023.08	0	1.15	±	0.24	3.96	±	0.38	20.42	±	1.50	27.93	±	2.64	
024.04	35	BD			0.84	±	0.07	20.29	±	1.54	1.61	±	0.18	
024.04	18	0.43	±	0.09	1.14	±	0.10	25.90	±	1.75	44.09	±	3.01	
024.04	10	0.36	±	0.08	0.68	±	0.07	20.28	±	1.77	14.95	±	1.49	
024.04	0	0.46	±	0.11	1.95	±	0.19	24.85	±	1.83	15.57	±	1.61	
024.04	0	0.52	±	0.11	1.02	±	0.10	21.06	±	1.29	9.34	±	0.97	
025.01	50	0.04	±	0.01	1.14	±	0.08	18.51	±	1.29	14.74	±	1.50	
025.01	34	0.23	±	0.07	0.71	±	0.07	19.65	±	1.57	15.61	±	1.53	
025.01	20	0.16	±	0.05	0.70	±	0.07	20.10	±	1.88	20.58	±	1.90	
025.01	10	0.14	±	0.04	0.97	±	0.08	20.60	±	1.66	15.62	±	1.50	
025.01	0	BD			0.88	±	0.07	19.59	±	1.34	8.24	±	0.65	
025.03	75	BD			0.37	±	0.03	14.30	±	1.53	1.14	±	0.11	
025.03	50	0.05	±	0.02	1.07	±	0.08	24.46	±	2.19	1.74	±	0.19	
025.03	24	0.15	±	0.04	0.34	±	0.03	11.83	±	0.65	17.28	±	1.63	
025.03	0	0.08	±	0.03	0.73	±	0.06	15.69	±	0.79	17.30	±	1.72	
025.06	250	BD			1.17	±	0.07	14.62	±	0.78	1.68	±	0.16	
026.01	0	0.21	±	0.06	0.99	±	0.10	19.14	±	1.38	19.04	±	1.89	
026.04	0	0.17	±	0.05	1.45	±	0.13	17.61	±	1.16	24.49	±	2.41	
026.05	0	0.12	±	0.04	1.59	±	0.12	20.82	±	1.37	26.20	±	1.78	
026.06	0	0.08	±	0.03	0.24	±	0.02	22.64	±	1.53	24.05	±	1.72	
026.07	0	BD			2.01	±	0.14	18.21	±	1.47	19.56	±	1.50	
026.10	0	0.22	±	0.07	1.45	±	0.13	16.86	±	1.20	18.17	±	1.46	

026.11	0	0.07	±	0.02	1.24	±	0.08	17.65	±	1.32	12.10	±	1.21
026.12	0	0.03	±	0.01	1.63	±	0.11	18.79	±	1.41	16.79	±	1.62
026.13	0	0.08	±	0.03	2.00	±	0.15	11.97	±	0.70	10.04	±	1.00
027.03	90	0.02	±	0.00	0.41	±	0.02	12.39	±	0.63	7.97	±	0.76
027.03	0	BD			0.53	±	0.04	12.67	±	0.74	8.08	±	0.74
028.02	0	BD			1.65	±	0.11	17.43	±	1.39	2.79	±	0.27
028.11	0	0.31	±	0.08	1.58	±	0.15	22.30	±	1.35	26.36	±	2.06
031.02	0	0.08	±	0.02	BD			19.47	±	1.26	12.25	±	1.21
031.02	10	0.18	±	0.05	0.15	±	0.01	22.90	±	1.68	6.89	±	0.60
031.02	25	0.10	±	0.03	0.46	±	0.04	21.35	±	1.56	21.98	±	2.20
031.03	27	0.11	±	0.03	0.20	±	0.02	14.25	±	0.69	29.68	±	2.91
031.03	0	0.09	±	0.03	0.25	±	0.02	12.79	±	0.62	18.56	±	1.81
031.08	250	0.03	±	0.01	0.82	±	0.06	13.86	±	0.83	2.11	±	0.21
031.08	150	BD			0.62	±	0.04	13.88	±	0.88	0.47	±	0.05
031.08	125	0.02	±	0.01	BD			17.46	±	1.28	2.20	±	0.22
031.08	100	BD			0.12	±	0.01	13.21	±	0.77	3.45	±	0.33
031.08	75	0.04	±	0.01	0.45	±	0.03	13.59	±	1.51	7.90	±	0.79
031.11	39	0.01	±	0.01	0.29	±	0.02	14.64	±	0.74	2.67	±	0.27
031.11	0	0.07	±	0.02	0.01	±	0.00	13.06	±	0.69	14.29	±	1.19
031.12	65	BD			1.51	±	0.10	16.49	±	1.32	9.52	±	0.93
031.12	45	0.02	±	0.01	1.08	±	0.07	19.46	±	1.58	6.72	±	0.66
031.12	15	0.16	±	0.05	BD			22.16	±	2.03	5.71	±	0.57
031.16	75	BD			0.49	±	0.03	13.06	±	0.76	4.26	±	0.44
031.20	65	0.06	±	0.02	0.46	±	0.04	17.65	±	1.88	10.17	±	1.01
031.20	46	0.07	±	0.02	0.56	±	0.05	14.89	±	2.00	10.44	±	1.00
031.20	25	0.07	±	0.03	0.14	±	0.01	22.20	±	1.71	32.07	±	2.99
031.20	0	0.15	±	0.05	1.16	±	0.11	19.06	±	1.54	25.20	±	2.47
031.21	12	0.14	±	0.03	BD			18.32	±	1.32	12.31	±	1.21
032.03	0	0.08	±	0.03	1.01	±	0.08	15.02	±	1.63	22.65	±	2.26
032.09	0	0.20	±	0.06	1.68	±	0.15	19.78	±	1.36	28.34	±	2.83
033.01	100	BD			BD			17.96	±	1.52	3.08	±	0.24
033.01	75	0.04	±	0.01	0.69	±	0.05	20.24	±	1.64	6.98	±	0.49
033.01	50	BD			BD			20.06	±	1.58	BD		
033.01	25	BD			0.56	±	0.04	20.82	±	1.65	9.01	±	0.57
033.01	10	0.20	±	0.06	0.89	±	0.09	18.70	±	1.79	34.61	±	3.41
033.01	0	0.20	±	0.06	1.02	±	0.10	17.91	±	1.62	27.82	±	2.64
033.02	0	0.10	±	0.03	0.07	±	0.01	13.63	±	0.76	24.25	±	2.19
033.02	50	0.03	±	0.01	0.95	±	0.07	13.83	±	0.71	7.93	±	0.47

Appendix B2: EN640 Radium Data.

Event Code	Depth m	^{223}Ra dpm/100L	XS ^{224}Ra dpm/100L	^{226}Ra dpm/100L	^{228}Ra dpm/100L
001.16	0	0.13 ± 0.05	1.65 ± 0.16	16.80 ± 1.24	nd
001.17	0	BD	1.42 ± 0.14	18.40 ± 1.53	nd
001.18	0	BD	0.24 ± 0.03	17.22 ± 1.68	nd
001.19	0	0.18 ± 0.07	1.12 ± 0.11	20.14 ± 1.34	nd
001.20	0	BD	1.64 ± 0.16	16.83 ± 1.20	nd
001.21	0	0.25 ± 0.08	1.82 ± 0.18	17.91 ± 1.25	nd
001.22	0	0.13 ± 0.05	1.47 ± 0.15	18.84 ± 1.50	nd
001.23	0	0.14 ± 0.06	1.81 ± 0.18	18.65 ± 1.25	nd
001.24	0	BD	1.71 ± 0.17	17.14 ± 1.13	nd
001.25	0	0.16 ± 0.06	1.94 ± 0.19	18.70 ± 1.19	nd
001.26	0	0.65 ± 0.15	2.44 ± 0.23	16.77 ± 1.29	nd
001.27	0	0.23 ± 0.09	2.41 ± 0.23	19.44 ± 1.17	nd
001.28	0	0.28 ± 0.09	2.00 ± 0.19	19.13 ± 1.50	nd
001.29	0	0.23 ± 0.07	0.11 ± 0.01	18.80 ± 1.49	nd
001.30	0	0.59 ± 0.13	1.70 ± 0.17	18.77 ± 1.28	nd
001.31	0	0.37 ± 0.09	1.58 ± 0.14	18.90 ± 1.27	nd
002.01	500	BD	0.95 ± 0.13	25.23 ± 2.29	nd
002.01	250	BD	1.44 ± 0.16	15.69 ± 1.35	nd
002.01	150	BD	1.90 ± 0.23	19.51 ± 1.35	nd
002.01	115	BD	1.32 ± 0.18	15.41 ± 1.25	nd
002.01	97	BD	1.13 ± 0.16	BD	nd
002.01	80	BD	1.50 ± 0.21	15.74 ± 1.68	nd
002.01	55	BD	0.32 ± 0.05	15.50 ± 1.32	nd
002.01	35	BD	0.68 ± 0.09	14.40 ± 1.20	nd
002.01	15	0.17 ± 0.09	0.88 ± 0.13	23.41 ± 2.12	nd
002.01	10	0.49 ± 0.14	BD	29.12 ± 2.57	nd
002.01	0	0.43 ± 0.14	1.01 ± 0.14	20.36 ± 1.33	nd
003.01	0	0.30 ± 0.09	1.97 ± 0.19	18.00 ± 1.32	nd
003.02	0	0.48 ± 0.13	2.33 ± 0.23	26.55 ± 1.55	nd
003.03	0	0.33 ± 0.10	1.99 ± 0.20	17.86 ± 1.28	nd
003.04	0	0.32 ± 0.11	2.75 ± 0.27	18.69 ± 1.18	nd
003.05	0	0.38 ± 0.10	0.49 ± 0.07	12.74 ± 1.71	nd
003.06	0	0.16 ± 0.06	1.39 ± 0.14	20.50 ± 1.35	nd
003.07	0	0.38 ± 0.11	1.47 ± 0.15	17.85 ± 1.27	nd
003.08	0	0.40 ± 0.12	2.05 ± 0.21	18.52 ± 1.38	nd
003.09	0	0.19 ± 0.06	0.54 ± 0.06	16.09 ± 1.58	nd
003.10	0	BD	2.33 ± 0.23	18.69 ± 1.27	nd
003.11	0	0.29 ± 0.09	1.73 ± 0.17	19.77 ± 1.23	nd
003.12	0	BD	2.47 ± 0.25	18.32 ± 1.31	nd

003.13	0	0.30	±	0.09	1.62	±	0.17	16.41	±	1.73	nd
003.14	0	0.13	±	0.05	2.64	±	0.25	18.10	±	1.35	nd
003.15	0	BD			1.87	±	0.19	17.39	±	1.11	nd
003.16	0	0.28	±	0.09	1.70	±	0.18	17.20	±	1.23	nd
003.17	0	0.28	±	0.10	2.46	±	0.26	15.69	±	1.85	nd
003.18	0	BD			1.65	±	0.19	19.12	±	1.27	nd
003.19	0	0.11	±	0.05	0.60	±	0.08	15.58	±	1.25	nd
003.20	0	0.16	±	0.06	2.26	±	0.23	16.33	±	1.60	nd
003.21	0	BD			1.46	±	0.16	14.09	±	2.10	nd
003.22	0	BD			1.68	±	0.17	18.43	±	1.29	nd
003.23	0	0.10	±	0.05	1.35	±	0.14	16.68	±	1.17	nd
003.24	0	BD			2.20	±	0.22	17.77	±	1.24	nd
003.25	0	0.11	±	0.05	1.65	±	0.16	18.60	±	1.87	nd
003.26	0	BD			1.67	±	0.17	18.23	±	1.32	nd
003.27	0	BD			2.49	±	0.26	15.61	±	1.20	nd
003.28	0	BD			0.69	±	0.09	16.49	±	1.25	nd
003.29	0	BD			1.34	±	0.13	17.07	±	1.40	nd
003.30	0	BD			9.52	±	0.95	18.15	±	1.45	nd
003.31	0	0.18	±	0.06	1.55	±	0.15	21.49	±	1.67	nd
003.32	0	BD			2.41	±	0.24	17.02	±	1.23	nd
003.33	0	0.52	±	0.14	2.81	±	0.28	16.68	±	1.22	nd
003.34	0	0.38	±	0.11	3.20	±	0.29	15.90	±	1.21	nd
003.35	0	BD			3.35	±	0.33	21.64	±	1.70	nd
003.36	0	0.49	±	0.12	0.49	±	0.08	17.91	±	1.31	nd
003.37	0	0.15	±	0.06	1.42	±	0.15	15.63	±	1.13	nd
004.01	500	BD			0.16	±	0.03	23.77	±	1.89	nd
004.01	250	BD			3.22	±	0.38	BD			nd
004.01	75	0.10	±	0.05	0.88	±	0.13	BD			nd
004.01	53	BD			0.51	±	0.08	18.65	±	1.28	nd
004.01	40	BD			0.45	±	0.07	17.03	±	1.27	nd
004.01	30	BD			1.52	±	0.21	21.52	±	1.85	nd
004.01	15	BD			0.53	±	0.09	16.96	±	1.22	nd
004.01	0	BD			1.35	±	0.22	24.19	±	2.76	nd
004.03	150	BD			0.61	±	0.10	15.03	±	1.46	nd
004.03	100	BD			BD			15.31	±	1.36	nd
004.03	65	BD			BD			16.30	±	1.17	nd
004.03	30	BD			1.39	±	0.19	15.63	±	1.40	nd
004.03	15	BD			0.42	±	0.08	19.10	±	1.68	nd
004.03	0	BD			0.68	±	0.11	15.05	±	1.18	nd
005.01	0	BD			1.57	±	0.18	16.40	±	1.22	nd
005.02	0	BD			3.53	±	0.35	16.67	±	1.16	nd
005.03	0	BD			3.77	±	0.37	19.99	±	1.61	nd
005.04	0	0.34	±	0.11	2.62	±	0.25	18.23	±	1.30	nd

005.05	0	1.04	±	0.29	6.27	±	0.63	21.41	±	1.15	nd
005.06	0	1.85	±	0.51	12.99	±	1.24	21.74	±	1.23	nd
005.07	0	0.73	±	0.20	3.86	±	0.39	22.94	±	1.81	nd
005.08	0	2.83	±	0.65	13.12	±	1.24	18.48	±	1.24	nd
005.09	0	6.09	±	1.44	25.45	±	2.58	20.18	±	1.18	nd
005.10	0	3.76	±	1.09	35.34	±	3.19	18.27	±	1.48	nd
005.11	0	2.77	±	0.92	35.20	±	3.28	17.80	±	1.32	nd
005.12	0	2.40	±	0.76	37.32	±	3.04	21.28	±	1.17	nd
006.01	35	1.50	±	0.42	9.77	±	0.98	11.32	±	0.60	nd
006.01	13	0.20	±	0.08	3.72	±	0.37	10.61	±	0.60	nd
006.01	0	3.88	±	1.29	43.10	±	4.02	16.55	±	0.79	nd
006.03	58	0.41	±	0.15	6.09	±	0.60	18.84	±	2.25	nd
006.03	35	0.17	±	0.06	0.88	±	0.10	14.71	±	1.30	nd
006.03	15	BD			1.18	±	0.16	16.91	±	1.24	nd
006.04	60	0.33	±	0.12	4.63	±	0.46	17.33	±	1.16	nd
006.04	30	BD			2.94	±	0.29	14.40	±	1.22	nd
006.04	10	0.16	±	0.06	1.77	±	0.18	15.36	±	1.12	nd
006.04	0	2.06	±	0.62	26.14	±	2.19	21.33	±	1.26	nd
006.05	74	0.55	±	0.18	5.61	±	0.56	21.56	±	2.38	nd
006.05	35	0.10	±	0.04	0.65	±	0.08	17.94	±	1.32	nd
006.05	10	0.14	±	0.05	0.83	±	0.10	9.46	±	3.88	nd
006.05	0	1.34	±	0.47	29.22	±	2.43	20.76	±	1.26	nd
006.06	85	0.24	±	0.08	2.21	±	0.22	14.00	±	1.17	nd
006.06	40	BD			8.78	±	1.25	17.19	±	1.38	nd
006.06	9	0.07	±	0.03	0.52	±	0.06	14.32	±	0.89	nd
006.06	0	0.88	±	0.23	14.52	±	0.98	16.80	±	1.08	nd
006.07	102	BD			0.61	±	0.07	26.71	±	1.96	nd
006.07	50	0.09	±	0.04	0.56	±	0.07	15.70	±	1.32	nd
006.07	10	BD			0.51	±	0.08	13.63	±	0.96	nd
006.07	0	3.01	±	0.84	21.47	±	2.07	15.85	±	0.92	nd
007.02	100	BD			0.62	±	0.06	15.76	±	1.20	nd
007.02	50	0.09	±	0.03	0.17	±	0.02	16.25	±	1.20	nd
007.02	30	BD			0.12	±	0.02	BD			nd
007.02	15	BD			0.22	±	0.02	13.80	±	1.10	nd
007.02	8	BD			0.87	±	0.08	20.02	±	1.21	nd
007.02	0	0.49	±	0.20	9.11	±	0.90	19.42	±	1.39	nd
007.03	23	BD			0.13	±	0.02	13.44	±	0.91	nd
007.03	5	0.94	±	0.11	6.95	±	0.26	12.95	±	0.56	nd
007.06	110	0.06	±	0.03	0.79	±	0.09	19.12	±	1.23	nd
007.06	100	BD			BD			16.11	±	1.10	nd
007.06	90	BD			1.10	±	0.13	14.88	±	1.24	nd
007.06	70	BD			0.55	±	0.09	18.33	±	1.64	nd
007.06	50	0.08	±	0.04	0.64	±	0.09	15.57	±	0.97	nd

007.09	100	BD		BD		19.69	±	2.40	nd
007.09	50	BD		0.60	± 0.08	16.84	±	1.31	nd
007.09	30	BD		0.51	± 0.07	15.63	±	1.23	nd
007.09	15	0.08	± 0.04	0.09	± 0.02	15.27	±	1.10	nd
007.09	8	0.17	± 0.05	1.82	± 0.14	11.65	±	1.83	nd
007.09	0	1.35	± 0.48	16.25	± 1.62	17.85	±	1.08	nd
007.10	5	0.79	± 0.23	13.42	± 0.99	13.03	±	0.51	nd
008.01	0	1.69	± 0.26	17.07	± 0.80	16.54	±	0.93	nd
008.02	0	1.42	± 0.23	14.97	± 0.70	16.59	±	0.92	nd
008.03	0	1.97	± 0.35	20.53	± 1.10	19.44	±	1.79	nd
008.04	0	2.46	± 0.39	19.25	± 1.02	18.07	±	1.07	nd
008.05	0	1.76	± 0.40	26.46	± 1.62	20.63	±	1.16	nd
008.06	0	1.67	± 0.38	18.76	± 1.25	15.76	±	1.51	nd
008.07	0	1.68	± 0.40	13.42	± 1.01	20.20	±	1.28	nd
008.08	0	1.52	± 0.32	13.48	± 0.89	19.48	±	1.14	nd
008.09	0	1.12	± 0.24	13.16	± 0.81	20.63	±	1.16	nd
008.10	0	1.12	± 0.24	9.76	± 0.67	BD			nd
008.11	0	1.08	± 0.25	6.05	± 0.49	18.08	±	1.27	nd
008.12	0	0.47	± 0.17	5.30	± 0.51	15.60	±	1.19	nd
008.13	0	0.30	± 0.11	3.99	± 0.40	17.95	±	1.13	nd
008.14	0	BD		1.28	± 0.13	18.44	±	2.28	nd
009.02	100	BD		0.01	± 0.00	15.55	±	1.62	nd
009.02	50	0.10	± 0.04	1.29	± 0.12	17.39	±	1.85	nd
009.02	40	0.12	± 0.05	0.96	± 0.12	18.13	±	1.28	nd
009.02	25	BD		0.64	± 0.08	16.07	±	1.40	nd
009.02	15	0.20	± 0.07	2.27	± 0.22	17.99	±	2.08	nd
009.02	0	0.28	± 0.09	1.94	± 0.19	19.51	±	2.08	nd
009.06	150	BD		0.75	± 0.08	16.22	±	1.18	nd
009.06	125	0.38	± 0.10	1.20	± 0.12	15.09	±	1.22	nd
009.06	100	0.39	± 0.12	2.45	± 0.25	11.34	±	4.50	nd
009.06	75	0.18	± 0.06	1.43	± 0.14	17.10	±	1.41	nd
009.06	40	BD		0.65	± 0.09	15.16	±	1.15	nd
009.06	20	BD		0.26	± 0.03	17.29	±	1.77	nd
009.06	0	0.20	± 0.07	0.66	± 0.07	17.43	±	1.29	nd
010.01	0	0.88	± 0.25	6.01	± 0.58	19.14	±	1.23	nd
010.02	0	1.31	± 0.31	5.62	± 0.55	17.43	±	1.17	nd
010.03	0	1.15	± 0.28	3.30	± 0.32	19.38	±	1.38	nd
010.04	0	BD		4.24	± 0.39	20.88	±	2.15	nd
010.05	0	0.53	± 0.17	4.05	± 0.41	17.77	±	1.30	nd
010.06	0	0.22	± 0.09	3.90	± 0.39	16.49	±	1.18	nd
010.07	0	0.74	± 0.19	3.81	± 0.38	16.02	±	1.21	nd
011.02	100	BD		0.43	± 0.04	15.92	±	1.06	nd
011.02	60	BD		BD		15.60	±	1.24	nd

011.02	35		BD		0.41	±	0.05	18.59	±	3.25	nd
011.02	25	0.07	±	0.03		BD		19.26	±	1.61	nd
011.02	14	0.11	±	0.04	1.59	±	0.13	19.23	±	1.47	nd
011.02	0	0.19	±	0.08	0.12	±	0.02	22.59	±	2.54	nd
011.03	27		BD			BD		21.89	±	2.22	nd
011.03	0	0.15	±	0.05	0.85	±	0.09	16.94	±	1.20	nd
011.06	500		BD		0.04	±	0.01	18.08	±	1.41	nd
011.06	250		BD		0.56	±	0.08	17.41	±	1.75	nd
011.06	200		BD			BD		24.47	±	2.86	nd
011.06	150		BD		0.84	±	0.10	16.99	±	1.46	nd
011.06	125		BD		0.74	±	0.09	15.87	±	1.23	nd
011.06	100		BD		0.52	±	0.07	16.00	±	1.41	nd
011.06	75		BD		0.89	±	0.10	21.97	±	3.58	nd
011.06	43		BD		0.08	±	0.01	18.07	±	1.67	nd
011.06	25	0.27	±	0.08	1.52	±	0.15	15.60	±	1.23	nd
011.06	0	0.08	±	0.04	0.56	±	0.06	18.95	±	1.33	nd
011.08	100		BD		1.17	±	0.11	22.98	±	2.86	nd
011.08	55		BD		0.70	±	0.08	17.26	±	1.44	nd
011.08	35		BD		0.35	±	0.05	14.59	±	1.16	nd
011.08	21	0.29	±	0.08	0.59	±	0.06	14.25	±	1.56	nd
011.08	11		BD		0.20	±	0.03	21.02	±	1.90	nd
011.09	0		BD		0.09	±	0.01	16.39	±	1.18	nd
012.01	0		BD		1.47	±	0.15	17.03	±	1.26	nd
012.02	0	0.20	±	0.07	1.97	±	0.19	21.22	±	2.69	nd
012.03	0		BD		1.63	±	0.16	19.63	±	1.28	nd
012.04	0	0.08	±	0.04	0.99	±	0.10	16.94	±	1.27	nd
012.05	0	0.23	±	0.08	1.63	±	0.16	17.54	±	1.29	nd
012.06	0	0.16	±	0.06	1.43	±	0.14	17.68	±	3.24	nd
012.07	0	0.08	±	0.04	0.50	±	0.06	19.39	±	1.29	nd
012.08	0	0.14	±	0.05	1.59	±	0.16	15.39	±	1.16	nd
012.09	0	0.24	±	0.07	1.16	±	0.11	17.90	±	1.37	nd
012.10	0	0.25	±	0.08	1.96	±	0.20	17.44	±	1.28	nd
012.11	0	0.34	±	0.10	1.43	±	0.14	16.65	±	1.05	nd
012.12	0	0.19	±	0.06	0.58	±	0.06	18.67	±	1.12	nd
012.13	0		BD		1.07	±	0.11	26.66	±	2.41	nd
012.16	0	0.28	±	0.08	0.94	±	0.09	18.58	±	1.23	nd
013.02	150		BD		0.64	±	0.06	16.48	±	1.14	nd
013.02	125		BD		0.18	±	0.03	14.75	±	1.16	nd
013.02	100		BD		1.19	±	0.12	26.63	±	2.47	nd
013.02	75		BD		0.19	±	0.02	17.39	±	1.16	nd
013.02	43		BD			BD		14.00	±	1.00	nd
013.02	30		BD		0.13	±	0.02	14.05	±	1.27	nd
013.02	18	0.12	±	0.05	0.15	±	0.02	17.85	±	2.39	nd

013.02	0	0.11	±	0.05	0.46	±	0.05	16.56	±	1.10	nd
013.03	100	BD			0.05	±	0.01	14.51	±	1.00	nd
013.03	60	0.07	±	0.03	1.05	±	0.12	14.42	±	1.00	nd
013.03	45	BD			1.21	±	0.13	17.29	±	2.22	nd
013.03	24	0.18	±	0.07	BD			16.15	±	1.10	nd
013.03	15	0.16	±	0.07	BD			16.10	±	1.17	nd
013.03	0	0.23	±	0.10	BD			22.81	±	1.77	nd
014.01	0	0.22	±	0.07	1.26	±	0.12	19.03	±	2.36	nd
014.02	0	0.26	±	0.07	1.26	±	0.12	16.46	±	1.07	nd
014.03	0	0.11	±	0.04	0.62	±	0.06	14.16	±	0.98	nd
014.04	0	0.06	±	0.02	1.55	±	0.12	13.45	±	1.12	nd
014.05	0	0.07	±	0.02	2.34	±	0.17	14.23	±	1.04	nd
014.06	0	0.16	±	0.06	1.19	±	0.12	16.55	±	0.96	nd
014.07	0	BD			1.00	±	0.09	15.38	±	1.06	nd
014.08	0	0.15	±	0.06	0.32	±	0.03	15.37	±	2.33	nd
014.09	0	0.15	±	0.06	0.77	±	0.08	17.71	±	1.14	nd
014.10	0	0.16	±	0.06	1.61	±	0.16	16.32	±	1.06	nd
015.02	47	BD			BD			15.50	±	1.01	nd
015.02	20	BD			0.65	±	0.08	13.15	±	2.39	nd
015.02	0	0.14	±	0.05	0.49	±	0.06	17.46	±	1.03	nd
016.01	0	BD			2.45	±	0.21	15.99	±	1.00	nd
016.02	0	BD			1.39	±	0.13	15.81	±	1.18	nd
016.03	0	0.08	±	0.03	0.76	±	0.07	14.64	±	1.06	nd
016.04	0	0.24	±	0.07	1.33	±	0.12	14.20	±	0.94	nd
016.05	0	0.14	±	0.05	0.64	±	0.06	17.08	±	1.03	nd
016.06	0	0.08	±	0.03	0.75	±	0.08	14.82	±	2.73	nd
016.07	0	BD			1.98	±	0.19	15.90	±	1.08	nd
016.08	0	BD			1.55	±	0.16	15.02	±	0.95	nd
016.09	0	BD			2.38	±	0.21	15.76	±	0.95	nd
016.10	0	BD			1.12	±	0.11	20.09	±	2.22	nd
016.11	0	0.15	±	0.06	0.88	±	0.09	14.90	±	1.10	nd
016.12	0	BD			1.12	±	0.11	16.15	±	1.16	nd
016.13	0	0.22	±	0.09	5.75	±	0.53	17.87	±	1.46	nd
017.01	0	0.21	±	0.09	4.40	±	0.41	19.48	±	2.96	nd
017.02	0	0.17	±	0.07	2.90	±	0.28	18.17	±	1.26	nd
017.03	0	BD			2.30	±	0.22	16.14	±	1.07	nd
017.04	0	BD			3.10	±	0.30	15.81	±	1.21	nd
017.05	0	0.27	±	0.09	1.65	±	0.16	17.20	±	2.95	nd
017.06	0	0.37	±	0.11	1.17	±	0.12	18.79	±	1.26	nd
017.07	0	BD			1.59	±	0.16	15.90	±	1.10	nd
017.08	0	0.08	±	0.03	1.59	±	0.12	18.13	±	1.22	nd
017.09	0	0.16	±	0.05	1.27	±	0.11	21.33	±	3.04	nd
017.10	0	BD			2.09	±	0.17	19.31	±	1.26	nd

017.11	0	0.09	±	0.04	2.09	±	0.18	16.79	±	1.16	nd
017.12	0	BD			1.50	±	0.14	18.68	±	1.43	nd
017.13	0	BD			2.25	±	0.22	19.77	±	1.37	nd
017.14	0	BD			1.39	±	0.14	17.38	±	1.13	nd
017.15	0	0.13	±	0.05	0.87	±	0.09	18.08	±	1.26	nd
017.16	0	BD			1.49	±	0.15	27.27	±	2.14	nd
017.17	0	0.18	±	0.06	1.16	±	0.12	18.78	±	1.29	nd
017.18	0	BD			1.78	±	0.17	18.23	±	1.13	nd
017.19	0	0.14	±	0.06	2.29	±	0.23	17.08	±	1.16	nd
017.20	0	0.13	±	0.05	2.27	±	0.22	26.79	±	2.50	nd
018.02	100	BD			1.18	±	0.12	17.11	±	1.25	nd
018.02	70	0.11	±	0.04	0.37	±	0.04	15.03	±	1.10	nd
018.02	50	BD			0.96	±	0.10	20.15	±	1.94	nd
018.02	28	BD			0.91	±	0.09	28.92	±	2.21	nd
018.02	13	BD			1.34	±	0.13	21.55	±	1.42	nd
018.02	0	0.11	±	0.04	0.60	±	0.05	14.68	±	1.26	nd
018.03	50	BD	±	BD	0.54	±	0.05	27.31	±	2.23	nd
018.03	25	BD	±	BD	0.40	±	0.04	15.40	±	1.11	nd
018.03	13	0.14	±	0.05	0.57	±	0.07	15.17	±	0.86	nd
018.03	0	0.16	±	0.05	0.46	±	0.05	24.22	±	2.36	nd
018.08	100	BD	±	BD	0.64	±	0.06	16.53	±	1.24	nd
018.08	65	0.13	±	0.04	BD			14.42	±	1.06	nd
018.08	50	BD			BD			15.98	±	1.54	nd
018.08	35	BD			1.04	±	0.08	15.51	±	3.30	nd
018.08	20	0.09	±	0.04	0.37	±	0.04	19.45	±	1.22	nd
018.08	0	0.12	±	0.05	0.76	±	0.08	17.12	±	1.49	nd
018.09	5	0.09	±	0.03	BD			13.59	±	0.96	nd
018.09	0	0.06	±	0.02	0.40	±	0.04	13.96	±	0.55	nd
018.09	0	0.78	±	0.14	1.33	±	0.13	12.11	±	0.50	nd
019.01	0	0.10	±	0.04	1.32	±	0.12	18.63	±	1.40	nd
019.02	0	BD			1.73	±	0.14	21.01	±	2.79	nd
019.03	0	0.12	±	0.04	1.52	±	0.12	17.64	±	1.22	nd
019.04	0	0.15	±	0.05	1.75	±	0.14	16.48	±	1.13	nd
019.05	0	BD			1.31	±	0.11	17.85	±	1.23	nd
019.06	0	0.11	±	0.04	0.96	±	0.09	23.04	±	2.49	nd
019.07	0	0.16	±	0.05	1.90	±	0.15	17.85	±	1.24	nd
019.08	0	0.18	±	0.06	1.65	±	0.16	18.62	±	1.08	nd
019.09	0	BD			2.37	±	0.23	18.59	±	1.17	nd
019.10	0	BD			1.45	±	0.14	20.72	±	2.76	nd
019.11	0	0.14	±	0.06	1.57	±	0.15	19.17	±	2.80	nd
019.12	0	BD			2.04	±	0.20	17.77	±	1.26	nd
020.02	300	0.09	±	0.04	0.38	±	0.05	17.48	±	1.39	nd
020.02	250	0.09	±	0.04	0.30	±	0.04	15.19	±	1.27	nd

020.02	200	0.52	±	0.10	0.52	±	0.05	15.94	±	1.56	nd
020.02	150	BD			0.67	±	0.07	16.12	±	3.32	nd
020.02	50	BD			1.65	±	0.16	17.54	±	1.32	nd
020.02	30	BD			0.84	±	0.09	14.89	±	1.14	nd
020.02	18	BD			BD			16.35	±	1.29	nd
020.02	0	BD			BD			13.74	±	0.72	nd
021.01	0	BD			0.97	±	0.09	17.71	±	1.14	nd
021.02	0	BD			1.88	±	0.19	17.64	±	1.25	nd
021.03	0	0.26	±	0.09	1.99	±	0.20	19.54	±	3.26	nd
021.04	0	0.11	±	0.04	1.31	±	0.13	18.76	±	1.30	nd
021.05	0	BD	±	BD	1.92	±	0.18	16.42	±	1.21	nd
021.06	0	BD	±	BD	1.72	±	0.17	17.74	±	1.51	nd
021.07	0	BD	±	BD	2.28	±	0.20	27.41	±	2.75	nd
021.08	0	0.10	±	0.04	1.79	±	0.17	21.18	±	1.32	nd
021.09	0	0.82	±	0.16	0.97	±	0.10	15.94	±	1.20	nd
021.10	0	BD			2.70	±	0.27	19.28	±	1.23	nd
021.11	0	0.13	±	0.05	0.73	±	0.07	24.25	±	2.63	nd
021.12	0	BD			1.26	±	0.12	17.74	±	1.26	nd
021.13	0	BD			2.52	±	0.23	17.75	±	1.11	nd
021.14	0	BD			1.25	±	0.13	18.14	±	1.20	nd
021.15	0	BD			1.57	±	0.15	22.10	±	3.07	nd
022.02	300	BD			0.27	±	0.03	18.68	±	1.39	nd
022.02	250	1.72	±	0.22	0.48	±	0.05	17.04	±	1.48	nd
022.02	200	BD			1.11	±	0.11	17.81	±	1.41	nd
022.02	150	BD			0.65	±	0.07	28.49	±	2.82	nd
022.02	80	BD			0.51	±	0.06	16.75	±	1.29	nd
022.02	50	BD			0.49	±	0.06	14.96	±	1.13	nd
022.02	30	BD			1.30	±	0.14	15.98	±	1.31	nd
022.02	18	0.10	±	0.04	1.11	±	0.12	28.62	±	2.69	nd
022.02	0	0.05	±	0.02	0.09	±	0.01	10.85	±	0.55	nd
022.05	100	BD			1.33	±	0.13	16.29	±	1.29	nd
022.05	75	BD			0.68	±	0.07	16.80	±	1.10	nd
022.05	35	BD			0.50	±	0.06	17.37	±	1.15	nd
022.05	18	BD			0.05	±	0.01	29.84	±	2.83	nd
022.05	10	BD			0.27	±	0.03	17.70	±	1.21	nd
022.05	0	0.09	±	0.04	BD			17.09	±	1.16	nd
022.06	25	0.08	±	0.04	BD			17.90	±	1.37	nd
022.06	0	0.08	±	0.04	0.98	±	0.10	BD			nd
023.01	0	BD			1.68	±	0.17	17.54	±	1.21	nd
023.02	0	BD			2.95	±	0.26	17.00	±	1.12	nd
023.03	0	BD			1.35	±	0.13	18.69	±	1.17	nd
023.04	0	0.50	±	0.12	1.05	±	0.10	BD			nd
023.05	0	0.13	±	0.05	1.44	±	0.14	16.98	±	1.28	nd

023.06	0	BD			1.61	±	0.16	18.24	±	1.13	nd
023.07	0	BD			2.20	±	0.20	18.24	±	1.16	nd
023.08	0	BD			1.70	±	0.15	27.59	±	2.47	nd
023.09	0	BD			0.99	±	0.10	17.73	±	1.31	nd
023.10	0	BD			2.27	±	0.23	16.94	±	1.17	nd
023.11	0	0.11	±	0.05	1.72	±	0.18	18.14	±	1.46	nd
023.12	0	0.16	±	0.06	1.21	±	0.12	19.82	±	3.04	nd
023.13	0	0.12	±	0.05	1.35	±	0.14	17.11	±	1.28	nd
023.14	0	BD			0.74	±	0.07	17.68	±	1.11	nd
023.15	0	BD			1.44	±	0.12	18.68	±	1.23	nd
024.02	100	BD			1.00	±	0.08	18.83	±	3.09	nd
024.02	75	BD			1.17	±	0.11	16.76	±	1.32	nd
024.02	50	BD			0.22	±	0.02	16.42	±	1.12	nd
024.02	30	BD			0.52	±	0.05	16.52	±	1.13	nd
024.02	18	0.13	±	0.05	1.03	±	0.11	15.37	±	3.95	nd
024.02	0	1.30	±	0.18	0.87	±	0.10	18.87	±	1.23	nd
025.01	0	0.18	±	0.06	0.74	±	0.08	19.12	±	1.15	nd
025.02	0	0.19	±	0.07	1.16	±	0.12	17.47	±	1.48	nd
025.03	0	BD			0.83	±	0.08	17.17	±	1.29	nd
025.04	0	BD			1.40	±	0.14	17.68	±	1.14	nd
025.05	0	0.19	±	0.07	1.31	±	0.13	17.86	±	1.22	nd
025.06	0	0.27	±	0.08	1.51	±	0.15	19.38	±	1.21	nd
025.07	0	BD			1.32	±	0.13	16.28	±	1.20	nd
025.08	0	BD			1.04	±	0.10	17.26	±	1.23	nd
025.09	0	BD			1.40	±	0.14	16.95	±	1.18	nd
025.10	0	0.16	±	0.06	1.42	±	0.14	17.34	±	1.11	nd
025.11	0	0.20	±	0.06	1.31	±	0.13	20.00	±	1.20	nd
025.12	0	0.11	±	0.05	1.10	±	0.11	17.68	±	1.31	nd
025.13	0	0.16	±	0.06	2.48	±	0.23	18.33	±	1.14	nd
025.14	0	0.17	±	0.06	1.42	±	0.14	16.33	±	1.39	nd
025.15	0	BD			2.02	±	0.20	16.15	±	1.28	nd
025.16	0	BD			1.57	±	0.16	16.71	±	1.10	nd
026.03	100	BD			0.36	±	0.04	15.41	±	1.31	nd
026.03	75	BD			0.76	±	0.09	15.76	±	1.14	nd
026.03	58	0.11	±	0.05	0.72	±	0.09	15.70	±	1.26	nd
026.03	35	0.12	±	0.05	0.80	±	0.09	15.01	±	1.22	nd
026.03	20	0.09	±	0.04	0.68	±	0.08	14.72	±	1.23	nd
026.03	0	BD			BD			17.72	±	1.20	nd
026.08	500	BD			0.09	±	0.01	20.90	±	1.25	nd
026.08	300	BD			0.43	±	0.05	16.46	±	1.28	nd
026.08	250	BD			0.69	±	0.09	14.28	±	1.17	nd
026.08	200	BD			1.73	±	0.14	17.20	±	1.18	nd
026.08	150	BD			0.57	±	0.06	16.88	±	1.31	nd

026.08	100	0.14	±	0.05	1.23	±	0.12	14.13	±	1.15	nd
026.08	60	0.14	±	0.05	0.08	±	0.01	17.11	±	1.19	nd
026.08	35	BD			0.50	±	0.06	19.15	±	1.28	nd
026.08	18	BD			0.36	±	0.04	16.93	±	1.22	nd
026.08	0	0.10	±	0.04	0.90	±	0.10	17.47	±	1.40	nd
026.10	100	BD			0.21	±	0.03	16.50	±	1.20	nd
026.10	60	0.08	±	0.04	0.21	±	0.01	15.85	±	1.15	nd
026.10	40	BD			0.33	±	0.04	17.78	±	1.23	nd
026.10	25	0.08	±	0.04	0.22	±	0.03	18.61	±	1.26	nd
026.10	15	BD			0.59	±	0.07	17.55	±	1.10	nd
026.10	0	0.22	±	0.09	0.75	±	0.11	21.21	±	2.07	nd
027.01	0	0.10	±	0.04	1.30	±	0.13	15.09	±	1.17	nd
027.02	0	BD			1.72	±	0.17	17.95	±	1.20	nd
027.03	0	BD			1.49	±	0.15	16.99	±	1.11	nd
027.04	0	BD			1.72	±	0.17	16.54	±	1.23	nd
027.05	0	0.11	±	0.04	1.28	±	0.13	16.39	±	1.12	nd
027.06	0	BD			1.54	±	0.16	16.94	±	1.27	nd
027.07	0	0.15	±	0.06	1.07	±	0.11	16.21	±	1.07	nd
027.08	0	0.08	±	0.04	1.38	±	0.15	18.12	±	1.18	nd
027.09	0	BD			1.37	±	0.14	16.44	±	1.18	nd
027.10	0	0.20	±	0.07	1.84	±	0.18	18.93	±	1.34	nd
027.11	0	BD			1.18	±	0.13	18.04	±	1.22	nd
027.12	0	BD			1.08	±	0.10	18.95	±	1.47	nd
027.13	0	BD			1.84	±	0.17	15.29	±	1.28	nd
027.14	0	0.12	±	0.05	1.07	±	0.11	17.49	±	1.25	nd
027.15	0	BD			1.17	±	0.12	18.51	±	1.12	nd
027.16	0	BD			1.33	±	0.14	16.83	±	1.22	nd
027.17	0	0.11	±	0.04	2.79	±	0.25	15.14	±	1.25	nd
027.18	0	BD			2.18	±	0.22	18.44	±	1.21	nd
029.01	0	BD			1.17	±	0.12	15.89	±	1.09	nd
029.03	0	BD			1.62	±	0.16	17.54	±	1.22	nd
029.05	0	BD			2.03	±	0.20	16.93	±	1.19	nd
029.07	0	BD			1.79	±	0.18	18.38	±	1.24	nd
029.09	0	0.14	±	0.06	1.44	±	0.16	16.71	±	1.21	nd
029.10	0	0.11	±	0.05	1.17	±	0.12	16.67	±	1.56	nd
029.12	0	0.15	±	0.06	1.08	±	0.11	17.63	±	1.22	nd
030.05	100	BD			1.45	±	0.16	17.65	±	1.25	nd
030.05	83	BD			1.00	±	0.11	15.92	±	1.10	nd
030.05	60	BD			0.76	±	0.07	15.03	±	1.18	nd
030.05	35	0.05	±	0.02	0.65	±	0.06	16.85	±	1.15	nd
030.05	20	BD			0.52	±	0.05	18.69	±	1.22	nd
030.05	0	BD			0.50	±	0.05	14.63	±	1.08	nd
030.06	100	BD			0.71	±	0.08	16.23	±	1.25	nd

030.06	83	BD		1.06	±	0.12	16.89	±	1.16	nd
030.06	20	BD		BD			16.80	±	1.24	nd
030.06	0	BD		BD			17.97	±	1.06	nd
030.10	500	BD		0.51	±	0.08	18.67	±	1.33	nd
030.10	300	BD		0.06	±	0.01	16.50	±	1.24	nd
030.10	250	BD		0.53	±	0.06	19.74	±	1.16	nd
030.10	200	BD		1.11	±	0.12	13.49	±	1.25	nd
030.10	150	BD		0.41	±	0.05	15.72	±	1.21	nd
030.10	100	BD		0.91	±	0.12	14.18	±	1.22	nd
030.10	67	BD		0.99	±	0.13	17.09	±	1.14	nd
030.10	35	BD		0.68	±	0.10	15.02	±	1.02	nd
030.10	20	BD		0.11	±	0.01	17.65	±	1.15	nd
030.10	0	0.09	± 0.04	0.09	±	0.01	17.70	±	1.06	nd
031.01	0	BD		0.69	±	0.07	17.47	±	1.17	nd
031.02	0	BD		1.87	±	0.19	17.63	±	1.16	nd
031.03	0	BD		1.80	±	0.18	17.86	±	1.46	nd
031.04	0	0.11	± 0.05	1.53	±	0.15	14.69	±	1.17	nd
031.05	0	BD		1.47	±	0.17	16.31	±	1.19	nd
031.06	0	BD		1.75	±	0.21	10.63	±	1.48	nd
031.07	0	BD		3.05	±	0.30	16.00	±	1.19	nd
031.08	0	BD		2.48	±	0.24	14.16	±	1.24	nd
031.09	0	0.15	± 0.06	1.49	±	0.16	17.20	±	1.20	nd
031.10	0	BD		2.07	±	0.20	17.62	±	1.08	nd
031.11	0	BD		1.28	±	0.14	17.50	±	1.18	nd
031.12	0	BD		1.17	±	0.13	16.33	±	1.16	nd
032.02	100	0.11	± 0.04	1.85	±	0.18	17.98	±	1.26	nd
032.02	65	BD		0.45	±	0.05	16.41	±	1.18	nd
032.02	40	BD		0.36	±	0.04	14.81	±	1.52	nd
032.02	20	0.04	± 0.02	1.40	±	0.13	16.42	±	1.23	nd
032.02	10	BD		0.79	±	0.08	20.26	±	1.26	nd
032.02	0	0.08	± 0.04	2.17	±	0.22	22.61	±	1.72	nd
032.03	0	BD		1.81	±	0.20	10.17	±	0.37	nd
032.03	5	BD		0.19	±	0.02	12.40	±	0.38	nd
032.03	0	BD		0.39	±	0.04	11.08	±	0.36	nd
033.01	0	BD		1.61	±	0.15	16.81	±	1.19	nd
033.02	0	0.06	± 0.03	1.41	±	0.14	16.84	±	1.22	nd
033.03	0	0.09	± 0.03	3.25	±	0.25	19.25	±	1.27	nd
033.04	0	BD		2.62	±	0.22	16.19	±	1.07	nd
033.05	0	BD		2.31	±	0.21	17.32	±	1.16	nd
034.03	150	BD		1.28	±	0.14	14.95	±	1.19	nd
034.03	100	BD		1.19	±	0.22	18.34	±	1.30	nd
034.03	70	BD		0.27	±	0.03	17.49	±	1.24	nd
034.03	37	0.08	± 0.03	0.87	±	0.08	17.98	±	1.54	nd

034.03	10	0.08	±	0.03	0.73	±	0.08	19.88	±	1.27	nd
034.03	0	BD			2.83	±	0.27	28.42	±	2.43	nd
034.05	18	BD			0.53	±	0.05	7.68	±	0.86	nd
034.05	0	BD			0.08	±	0.01	10.20	±	0.49	nd
034.10	1000	BD			0.67	±	0.08	22.17	±	1.27	nd
034.10	800	BD			11.05	±	1.36	24.24	±	1.31	nd
034.10	600	BD			0.75	±	0.13	20.78	±	1.32	nd
034.10	400	BD			0.88	±	0.13	20.19	±	1.43	nd
034.10	200	BD			0.57	±	0.08	17.59	±	1.17	nd
034.10	150	BD			1.69	±	0.19	18.88	±	1.42	nd
034.10	100	BD			0.80	±	0.12	18.43	±	1.34	nd
034.10	75	0.13	±	0.06	0.92	±	0.12	20.34	±	1.40	nd
034.10	50	BD			0.97	±	0.13	14.58	±	1.15	nd
034.10	35	BD			0.48	±	0.06	19.40	±	1.55	nd
034.10	20	0.08	±	0.04	0.65	±	0.07	15.89	±	1.15	nd
034.10	0	BD			1.46	±	0.15	19.11	±	1.17	nd
035.01	0	BD			1.22	±	0.13	10.75	±	1.27	nd
035.02	0	BD			3.58	±	0.29	16.94	±	1.18	nd
035.03	0	BD			0.54	±	0.06	14.99	±	1.19	nd
035.04	0	0.06	±	0.03	1.39	±	0.13	19.86	±	1.25	nd
035.05	0	BD			1.75	±	0.17	15.89	±	1.04	nd
035.06	0	0.06	±	0.03	1.76	±	0.15	15.96	±	1.18	nd
035.07	0	BD			1.64	±	0.16	17.29	±	1.08	nd

[Intentionally Blank]